University of Alberta

Characterization of Agonist Binding Sites in *Torpedo* Nicotinic Acetylcholine Receptor

By

Ankur Kapur ©

A thesis submitted to the Faculty of Graduate Studies and Research in partial fulfillment of the requirements for the degree of Doctor of Philosophy

Department of Pharmacology
Edmonton, Alberta

Spring 2005

Library and Archives Canada

Published Heritage Branch

395 Wellington Street
Ottawa ON K1A 0N4
Canada

Bibliothèque et Archives Canada

Direction du Patrimoine de l'édition

395, rue Wellington
Ottawa ON K1A 0N4
Canada

0-494-08257-7

Your file *Votre référence*
ISBN
Our file *Notre reference*
ISBN

NOTICE:
The author has granted a non-exclusive license allowing Library and Archives Canada to reproduce, publish, archive, preserve, conserve, communicate to the public by telecommunication or on the Internet, loan, distribute and sell theses worldwide, for commercial or non-commercial purposes, in microform, paper, electronic and/or any other formats.

The author retains copyright ownership and moral rights in this thesis. Neither the thesis nor substantial extracts from it may be printed or otherwise reproduced without the author's permission.

AVIS:
L'auteur a accordé une licence non exclusive permettant à la Bibliothèque et Archives Canada de reproduire, publier, archiver, sauvegarder, conserver, transmettre au public par télécommunication ou par l'Internet, prêter, distribuer et vendre des thèses partout dans le monde, à des fins commerciales ou autres, sur support microforme, papier, électronique et/ou autres formats.

L'auteur conserve la propriété du droit d'auteur et des droits moraux qui protège cette thèse. Ni la thèse ni des extraits substantiels de celle-ci ne doivent être imprimés ou autrement reproduits sans son autorisation.

In compliance with the Canadian Privacy Act some supporting forms may have been removed from this thesis.

While these forms may be included in the document page count, their removal does not represent any loss of content from the thesis.

Conformément à la loi canadienne sur la protection de la vie privée, quelques formulaires secondaires ont été enlevés de cette thèse.

Bien que ces formulaires aient inclus dans la pagination, il n'y aura aucun contenu manquant.

Canada

In dedication to my parents:
Kuldip and Savita Kapur

ABSTRACT

Torpedo nicotinic acetylcholine receptor, a $\alpha_2\beta\gamma\delta$ subunit pentameric complex, carries two high affinity binding sites located at the α-γ and α-δ interfaces. The "multiple loop" model predicts that the α-subunits' amino acids (loops A-C) form the principal component, while loops D-F of the γ- and δ-subunits form the complementary component of the binding sites.

Based on subunit homology considerations, the possibility that binding sites exist at all five subunit interfaces cannot be excluded. The goal of this study was to identify residue(s) involved in forming binding sites distinct from the well-characterized high affinity sites. Arg55 from loop D of the α-subunits lies at the opposite end of the α subunit. The functional consequences of its mutation (to Lys, Glu, Phe and Trp) were studied in *Xenopus* oocytes. Only the αR55F and αR55W mutants result in a modest, but significant decrease in the potency of acetylcholine (~5- and 6-fold respectively). The mutations did not alter the apparent affinity of *d*-tubocurarine (ability to inhibit acetylcholine-induced currents), or acetylcholine (inhibition of initial rate of toxin binding). To assess the contribution of residues from the adjacent γ-subunit, Glu93 from loop A was mutated (γE93R). This results in an increase in acetylcholine potency (8-fold), while the γE93R-αR55F double mutation restores potency to wild-type levels. Thus, at the non-high affinity binding interface (γ-α), γGlu93 and αArg55 modulate channel function by putative ion-pairing interactions.

Previous studies demonstrated that each of the high affinity binding sites is made up of two "subsites". Suberyldicholine, a bisquaternary agonist (interonium distance ~

17Å), displays atypical binding and activation properties. This is attributed to its ability to cross-link these subsites. Acetylcholine binding protein-based molecular modeling suggests that αTrp86 (previously identified by labeling studies) is located ~15Å from the classical high affinity sites. Our results from the αTrp86 mutation (W86F) demonstrate an ~ 500-fold reduction in suberyldicholine potency for channel activation, while acetylcholine potency is unaltered. Suberyldicholine-evoked currents at this mutant fail to desensitize and are insensitive to inhibition by *d*-tubocurarine. We conclude that αTrp86 does not accommodate both ACh and suberyldicholine and specifically contributes to a secondary suberyldicholine binding site.

ACKNOWLEDGEMENTS

The research undertaken for my dissertation would not have come to fruition had it not been for the contributions of many individuals. I am indebted to my supervisor and mentor, Dr. Susan Dunn, for leading me through the confounding labyrinths of science. Her patience, astuteness and ability to inspire me to think beyond the obvious, have helped me become a better researcher and to enjoy my work. It has been a very rewarding experience to study in her laboratory. I would like to express my gratitude to my co-supervisor, Dr. Martin Davies, for his words of wisdom and technical contributions in helping me overcome the challenges of molecular biology.

I am thankful to the members of my supervisory committee, Dr. William Dryden and Dr. James Young, for their intellectual contributions, encouragement and support over the years.

I am also grateful to Brian Tancowny, for his expert technical assistance and to the faculty members of the Department of Pharmacology, for their participation in my graduate training. I thank Judy Deuel and the wonderful administrative staff of the department, for all their help and especially Sharon Kilback, for her prompt aid at bottlenecks.

This long journey through the corridors of the ninth floor of Medical Sciences Building had given me the fortune of meeting some wonderful people, both past and present. I thank Dr. Glen Newell, for showing me the lighter and often brighter side of science. I am also thankful to Dr. Jason Derry, a great colleague, and a cherished friend, for sharing in my joys and dismays, over the years. I thank Reena Hanseen, for her assistance with the preparation of this manuscript.

I especially thank Vandana Shah, for her years of friendship, support and encouragement. She introduced me to the nuances of the Canadian culture and yet kept me in touch with my Indian roots. The successful completion of my degree would not have been possible without the enduring support, love and encouragement of my parents, Kuldip and Savita, of whom I am very proud.

TABLE OF CONTENTS

	Page
CHAPTER 1 – Introduction	1
Nicotinic Acetylcholine Receptors: Overview	2
nAChR Subunit Composition and Stoichiometry	6
Subunit Arrangement of the Nicotinic Acetylcholine Receptor	9
nAChR Subunit Assembly	12
Ligand Binding to the Nicotinic Acetylcholine Receptor	17
Mapping of Agonist/Antagonist Binding Sites by Affinity Labeling Studies	18
Functional Characterization of ACh Binding Site Residues	22
nAChR α-Subunit Mutations Altering Receptor function	23
nAChR γ- and δ-Subunit Mutations Altering Receptor function	25
Model of the Receptor Recognition Site	27
Ligand Recognition Sites on other LGIC Receptors	30
Functional Role of Binding Sites	32
Structure of the *Torpedo* nAChR	37
Crystal Structure of Acetylcholine Binding Protein	40
Aims of the Present Studies	44
Bibliography	60
CHAPTER 2 - The Role of Arginine 55 in the Alpha Subunit of *Torpedo* Nicotinic Acetylcholine Receptor in Channel Function	79
Introduction	80
Materials and Methods	85
Materials	85
Site Directed Mutagenesis	85
In Vitro Transcription	86
Expression in *Xenopus* oocytes and Electrophysiology	87
Binding of [^{125}I]α-BgTx to Intact Oocytes	88
Data and Statistical Analysis	88

Results..... 90
Functional Effects of αR55 Mutations on the Binding of Agonists and Antagonist 90
Desensitization Properties of Wild Type and Mutant nAChR 91
Sensitivity of αR55 Mutant nAChR to Competitive Antagonist 92
Expression Levels and Maximum Currents of Wild Type and Mutant nAChRs 92
Influence of αR55F and αR55W Mutations on the Binding of Acetylcholine 93
Functional Effects of γE93 Mutations on the Potency of Agonist and Antagonist 94
Discussion..... 95
Bibliography..... 141

CHAPTER 3 – Contribution of Tryptophan-86 in the Alpha Subunit of the *Torpedo* Nicotinic Acetylcholine Receptor to Channel Activation by the Bisquaternary Ligand Suberyldicholine 147
Introduction..... 148
Materials and Methods..... 152
Materials 152
Site Directed Mutagenesis 152
In Vitro Transcription 153
Expression in *Xenopus* oocytes and Electrophysiology 153
Binding of [^{125}I]α-BgTx to Intact Oocytes 155
Data and Statistical Analysis 155
Results..... 157
Functional Effects of αW86 Mutations on the Binding of Agonist and Antagonist 157
Altered Sensitivity of αW86F nAChR to Competitive Antagonist 158
Expression Levels and Maximum Currents of Wild Type and Mutant nAChRs 158

Other Mutant nAChR Engineered 159
Discussion..... 160
Bibliography..... 190

CHAPTER 4 – General Discussion and Conclusions 195
General Discussion..... 196
Conclusions and Future Directions 203
Bibliography..... 213

APPENDIX 218

Sequence Alignment of *Torpedo* nAChR subunits with AChBP..... 218

LIST OF TABLES

		Page
Table 1-1	Amino acid residues contributing to ACh binding in *Torpedo* nAChR subunits and homologous residues in AChBP.	59
Table 2-1	Concentration-effect data for ACh, carbamylcholine and PTMA activation of wild type and mutant receptors expressed in *Xenopus* oocytes.	136
Table 2-2	Concentration-effect data for PTMA inhibition of ACh-evoked currents and EC_{50} for ACh-induced channel activation in mutant receptors expressed in *Xenopus* oocytes.	137
Table 2-3	Surface expression and normalized ACh-evoked maximum currents in wild type and mutant receptors expressed in *Xenopus* oocytes.	138
Table 2-4	Data generated from dTC and ACh competition inhibition curves in functional and radioligand binding studies respectively.	139
Table 2-5	Concentration-effect data for ACh activation of γE93 mutant receptors expressed in *Xenopus* oocytes.	140
Table 3-1	Concentration-effect data for ACh and suberyldicholine activation of wild type and mutant receptors expressed in *Xenopus* oocytes.	187
Table 3-2	Apparent K_I values for dTC inhibition of ACh and suberyldicholine evoked currents in wild type and mutant receptors expressed in *Xenopus* oocytes.	188
Table 3-3	Surface expression and normalized maximum currents seen in wild type and mutant receptors expressed in *Xenopus* oocytes.	189
Table 4-1	Concentration-effect data and maximum agonist-induced currents for bisquaternary ligand activation of *Xenopus* oocytes expressing wild type nAChR.	212

LIST OF FIGURES

		Page
Figure 1-1	(A) Schematic of the *Torpedo* nicotinic acetylcholine receptor. (B) Linear representation of the topology of a single subunit.	48
Figure 1-2	Cartoon of the *Torpedo* nicotinic acetylcholine receptor showing the circular subunit arrangement.	50
Figure 1-3	Illustration of key residues identified by labeling and mutagenesis studies in *Torpedo* nAChR.	52
Figure 1-4	Schematic representation of the two subsite high affinity model.	54
Figure 1-5	Depiction of the crystal structure of acetylcholine binding protein. Top view illustrating (A) the AChBP homopentamer parallel to the fivefold axis and (B) the interfacial location of ligand binding sites.	56
Figure 1-6	A single subunit of acetylcholine binding protein. View perpendicular to the fivefold axis illustrating (A) the N- and C-terminals. (B) the structural β-strands, interconnecting loops and α-helix.	58
Figure 2-1	Amino acid sequence alignment of residues from loop D of members of the LGIC family and AChBP.	105
Figure 2-2	Schematic representation of the subunit arrangement of the *Torpedo* nAChR showing the loop model of high-affinity binding domains.	107
Figure 2-3	Chemical structures of the agonists (A) acetylcholine, (B) carbamylcholine and (C) phenyltrimethylammonium, and the competitive antagonist (D) d-tubocurarine.	109
Figure 2-4	ACh activation of wild type and mutant receptors.	111
Figure 2-5	Carbamylcholine activation of wild type and mutant receptors.	113
Figure 2-6	Functional properties of the partial agonist, phenyltrimethylammonium (PTMA). (A) Concentration effect	

curve for PTMA and ACh activation wild type nAChR. (B) Maximal responses for ACh and PTMA. 115

Figure 2-7 PTMA activation of wild type (WT) and inhibition of mutant receptors. (A) Concentration effect curve of PTMA on WT and inhibition (PTMA + ACh coapplication) on αR55F mutant receptors. (B) Concentration effect curve of PTMA on WT and inhibition (PTMA + ACh coapplication) on αR55W mutant receptors. 117

Figure 2-8 Representative traces of currents evoked by EC_{10} concentrations of ACh in *Xenopus* oocytes expressing (A) wild type, (B) αR55F and (C) αR55W mutant receptors. 119

Figure 2-9 Surface nAChR expression in *Xenopus* oocytes. 121

Figure 2-10 Concentration dependent inhibition of ACh-evoked currents by dTC in oocytes expressing wild type and mutant receptors. 123

Figure 2-11 ACh binding to *Torpedo* nAChR expressed on surface of *Xenopus* oocytes. 125

Figure 2-12 Location of Arg55 from loop D of the α-subunit based on the crystal structure of the AChBP. 127

Figure 2-13 Illustration of the subunit arrangement perpendicular to the axes of symmetry based on the crystal structure of AChBP. (A) Representation of the two alpha subunits (yellow) and a gamma subunit (blue) located in between, in an α-γ-α manner. (B). Location of Glu93 from loop A of the γ-subunit relative to Arg55 from loop D of the α-subunit. 129

Figure 2-14 (A) Distance between γGlu93 and αArg55 located at the γ-α subunit interface. (B) Sequence alignment of residues from loop A and loop D of the γ- and α-subunit respectively from various species. 131

Figure 2-15 ACh activation of γE93 mutant receptors. Concentration-effect curves for (A) wild type, γE93 and αR55F nAChR and (B) wild

type and γE93-αR55F nAChR. 133
Figure 2-16 Concentration dependent inhibition of ACh evoked currents by dTC in wild type and γE93 mutant receptors. 135
Figure 3-1 Amino acid sequence alignment of residues from loop A of members of the LGIC family and AChBP. 168
Figure 3-2 Chemical structures of the agonists (A) acetylcholine and (B) suberyldicholine. 170
Figure 3-3 Location of the αTrp86 from loop A of *Torpedo* nAChR. 172
Figure 3-4 (A) Partial structure of α-subunit illustrating location of αTrp86. (B) Approximate distance between αTrp86 and the high affinity ACh-binding pocket. 174
Figure 3-5 Concentration-effect curves for ACh and suberyldicholine in *Xenopus* oocytes expressing wild type and αW86F nAChR. 176
Figure 3-6 Representative current traces showing ACh and suberyldicholine activation of *Xenopus* oocytes expressing wild type and αW86F nAChR. 178
Figure 3-7 (A) Location of conserved proline residues in the vicinity of αTrp86. (B) αP21 and αP88 are both located within 5Å of αW86. 180
Figure 3-8 Concentration dependent inhibition of agonist-evoked currents by dTC in oocytes expressing wild type and αW86F nAChR. 182
Figure 3-9 Surface nAChR expressed in *Xenopus* oocytes labeled with [^{125}I]α-BgTx. 184
Figure 3-10 Suberyldicholine binding to *Torpedo* nAChR expressed on the surface of *Xenopus* oocytes. 186
Figure 4-1 Chemical structure of a generic bisquaternary agonist. (A) Depiction of two quaternary ammonium groups separated by methyl groups of various chain lengths. (B) Methyl chain length and estimated interonium distance. 209
Figure 4-2 Activation of wild type nAChR by bisquaternary agonists. (A)

Concentration-effect curves for bisquaternary agonists. (B) Maximal responses for the bisquaternary ligands. 211

LIST OF ABBREVIATIONS AND SYMBOLS

ACh	acetylcholine
ANOVA	analysis of variance
α-BgTx	alpha bungarotoxin
AChM	acetylcholine mustard
AChBP	acetylcholine binding protein
AdPc	adipyldicholine
ATP	adenosine 5'-triphosphate
AzDc	azelyldicholine
BrACh	bromoacetylcholine
CCh	carbamylcholine
CNBr	cyanogen bromide
cDNA	complementary deoxyribonucleic acid
cRNA	complementary ribonucleic acid
DEPC	diethyl pyrocarbonate
DMT	dimethyl-*d*-tubocurarine
DDF	*p*-dimethylamino benzenediazonium fluoroborate
*d*TC	*d*-tubocurarine
DTT	dithiothreitol
EC_{50}	Half-maximal concentration required for channel activation
ER	endoplasmic reticulum
GABA	γ-aminobutyric acid
GCP	S-(2-glycylaminoethyl)dithio-2-pyridine
Glu	glutaryldicholine
5-HT	5-hydroxytryptamine
HEPES	4-(hydroxyethyl)-1-piperazineethanesulfonic acid
IAS	5-iodoacetamidosalicylic acid
IANBD	4-([iodoacetoxy)ethyl]methylamino)-7-nitro-2,1,3-benzoxadiazole
I_{max}	maximal response

IUPHAR	international union of pharmacology
K_D	equilibrium ligand dissociation constant
K_I	equilibrium inhibitor dissociation constant
LGIC	ligand-gated ion channel
MBTA	4-(N-maleimido)benzyltrimethyl ammonium
MTSEA	N-biotinylaminoethyl methanethiosulfonate
nAChR	nicotinic acetylcholine receptor
NMDA	N-methyl-D-aspartate
n_H	Hill coefficient/slope
PKC	protein kinase C
PTMA	phenyltrimethylammonium
P2X	purinergic or ATP receptor
SCAM	substituted cysteine accessibility method
SEM	standard error of the mean
Scc	succinylcholine
SubDc	suberyldicholine
$T_{1/2}$	half life

CHAPTER 1

Introduction

NICOTINIC ACETYLCHOLINE RECEPTORS: OVERVIEW

The acetylcholine receptors (or cholinergic receptors) are broadly classified as nicotinic (ionotropic) or muscarinic (G protein coupled) receptors based on their transmembrane signaling mechanisms and/or the nature of their selective agonists and antagonists. Nicotinic acetylcholine receptors (nAChR) are neurotransmitter-gated transmembrane ion channels that are responsible for mediating fast excitatory synaptic transmission at the neuromuscular junction and at cholinergic synapses of the central nervous system. The peripheral (muscle-type) nAChR is the prototype of a family of ligand-gated ion channel (LGIC) receptors that includes the neuronal nicotinic, γ-aminobutyric acid type A ($GABA_A$), 5-hydroxytryptamine type 3 ($5HT_3$) and glycine receptors. Although the LGIC receptors have different ligand specificities and functional properties, they are classified as a superfamily based on their structural homology (Schofield *et al.*, 1987). This is indicative of their evolution from a common ancestor gene (Raftery *et al.*, 1980; Ortells and Lunt, 1995). The peripheral nAChR is the best-characterized member of the LGIC superfamily as a consequence of the rich source of this receptor present in the electric organ of *Torpedo* fish, which has permitted its extensive biochemical characterization (Raftery *et al.*, 1983; Dunn, 1993). The marine ray, *Torpedo*, uses its electric organ both defensively and offensively to generate large voltages that stun predators or prey, respectively. Furthermore, the availability of snake neurotoxins (α-neurotoxins) that serve as high affinity labels of the nAChR permitted its early identification, isolation and purification (Conti-Tronconi and Raftery, 1982).

The principal role of the peripheral nAChR is to mediate signal transduction resulting from the action of the endogenous neurotransmitter, acetylcholine (ACh) at the postsynaptic membrane (reviewed by Changeux *et al.*, 1992). ACh released from the motor nerve terminal into the synaptic cleft has been estimated to rise to a local concentration in the order of 100 μM to 1 mM (Kuffler and Yoshikami, 1975; Katz and Miledi, 1977; Land *et al.*, 1980). ACh that diffuses across the synaptic cleft binds to the nAChR in the postsynaptic membrane resulting in a conformational change of the protein that may open its cation-selective ion-channel in a fast (μsec to msec) manner (reviewed by Devillers-Thiéry *et al.*, 1993; Dunn, 1993). The opening of the ion-channel results in a passive transport of cations, predominantly the influx of Na^+ ions, with a channel permeability of 10^6 to 10^7 cations/second (Lester, 1977; Moore and Raftery, 1980). The open state of the ion-channel is very short-lived (less than 1 msec), after which the ion-channel closes and synaptic transmission is terminated as a result of the dissociation of ACh from the receptor (reviewed by Devillers-Thiéry *et al.*, 1993), its diffusion out of the cleft and degradation by acetylcholinesterase to a background level of approximately 1 nM (Katz and Miledi, 1977).

The iontophoretic application of ACh at the frog neuromuscular junction was shown to produce small depolarizing responses as a result of a presumed change in membrane conductance (Katz and Thesleff, 1957). A non-linear, sigmoidal relationship between the ACh concentration and the depolarizing response was observed (Katz and Thesleff, 1957). This set the tone for dose-response relationship studies using voltage-clamp techniques (Dreyer and Peper, 1975; Dreyer *et al.*, 1978; Dionne *et al.*, 1978). Changeux and Podleski (1968) used Hill coefficients from dose-response curves in

isolated monocellular electroplax as an index of cooperativity in the response. The authors reported the activation curve to deviate from that of a simple hyperbola to a sigmoidal shape with a Hill coefficient approaching 2. The cooperative response was attributed to mutual interactions of protomers in the conformational transition at the ACh-receptor complex. At low agonist concentrations, the number of open channels increases approximately as the square of the agonist concentration (Adams, 1981). This suggests that channel activation is a positively cooperative process. Concentration-effect curves thus imply that the receptor is more likely to be activated when more than one molecule of agonist is bound. The EC_{50} for ACh-mediated channel activation is approximately 25 μM (Dreyer and Peper, 1975; Dreyer *et al.*, 1978). For another agonist, carbamylcholine (CCh), the EC_{50} for the conductance response has been reported to lie within the range of 200-400 μM (Dionne *et al.*, 1978; Dreyer *et al.*, 1978). Whereas the above mentioned examples of earlier work on the nAChR came from electrophysiological studies on the frog neuromuscular junction, more recent studies of nAChR kinetics have involved either native or reconstituted *Torpedo* membranes (reviewed by Dunn, 1993; Sine, 2002). Biochemical and biophysical characterization has shown that the *Torpedo* electroplax derived nAChR is structurally and functionally comparable to the muscle nAChR. Similar features include a CCh-induced cation conductance of 7×10^6 ions/second, dose-response curves with half-maximal responses of 90 μM and 960 μM for the agonists ACh and CCh, respectively, and a Hill coefficient for agonist-induced channel activation approaching 2 (Conti-Tronconi and Raftery 1982; Raftery, *et al.*, 1983).

The nAChR, as well as other LGIC receptors, undergo the phenomenon known as desensitization. Katz and colleagues first reported that upon continuous exposure of the receptor to an agonist, the ion channel closes and the receptor becomes "refractory to depolarizing agents" (Katz and Thesleff, 1957). The authors hypothesized that the receptor exists in two forms: an active open state and a "refractory" closed state in which the affinity for the agonist is high. When equilibrium binding assays are used to study radiolabeled ACh binding, the affinity of the receptor-ligand complex is high (ACh K_d ~ 10 nM), consistent with measurement of the binding of ACh to a desensitized state of the receptor (Raftery *et al.*, 1983; Dunn, 1993). In functional studies, the desensitized state of the receptor has been shown to slowly revert to the resting state after complete removal of the agonist. The onset of desensitization (msec) is significantly faster than the recovery (timescale of several minutes). Furthermore, the recovery of the receptor from the desensitized state depends on the duration of agonist exposure, and also on the type of agonist used to induce desensitization (Reitstetter *et al.*, 1999). However, since the action of neurotransmitter at the neuromuscular junction is normally terminated by its dissociation from the receptor and its rapid hydrolysis, desensitization may have little effect on normal synaptic transmission. Nevertheless, under certain conditions, such as congenital myasthenia syndromes and nicotine tolerance in smokers, desensitization of the nAChR may play an important role (Jones and Westbrook, 1996).

Upon binding of the neurotransmitter to these receptors, the ion-channel opens, cation flux ensues and, under appropriate conditions, the receptors undergo desensitization. Despite this straightforward cascade of events, a detailed mechanistic understanding of these processes has not yet been developed. In the absence of detailed

structural information, a number of kinetic models for receptor activation and desensitization have been proposed (reviewed by Adams, 1981; Changeux and Edelstein, 1998). Recent advances in direct structural information of the nAChR using electron microscopy (Unwin, 1995; Miyazawa *et al.*, 2003) and crystallographic studies of the homologous acetylcholine binding protein (AChBP) (Brejc *et al.*, 2001), combined with over three decades of biochemical characterization of these receptors, has considerably enhanced our understanding of the structure-function relationship of the nAChR (discussed later).

nAChR SUBUNIT COMPOSITION AND STOICHIOMETRY

It is now well established that *Torpedo* nAChR is a hetero-oligomer composed of four homologous subunits assembled in a stoichiometry of $(\alpha 1)_2\beta\gamma\delta$. SDS gel electrophoresis of purified *T. californica* nAChR revealed the presence of four polypeptides with apparent molecular weights of 40,000, 50,000, 60,000 and 65,000 daltons, (referred to as the α, β, γ and δ subunits respectively) giving rise to a 270-kDa protein complex (reviewed by Conti-Tronconi and Raftery, 1982). Early investigations focused on establishing the number and ratio of protein subunits constituting the *Torpedo* nAChR and the reports were often conflicting (Reynolds and Karlin, 1978; Sobel *et al.*, 1977). However, the indisputable demonstration of the oligomeric subunit composition of nAChR came from N-terminal partial amino acid sequencing of the isolated subunits, which revealed not only that the structure was $\alpha_2\beta\gamma\delta$ but also that the subunits were homologous in their amino acid sequence (Raftery *et al.*, 1980). This finding not only resolved the dilemma of the receptor subunit composition, but also

paved the way for the subsequent cloning and cDNA sequencing of all four subunits (Noda *et al.*, 1982; 1983; Ballivet *et al.*, 1982). Comparison of the complete primary sequences of the four *Torpedo* muscle-type subunits revealed distinct homology (19% identity and 54% homology), which suggested evolution from a common ancestral gene (Raftery *et al.*, 1980; Noda *et al.*, 1983). Furthermore, hydrophobicity profiles and secondary structure predictions of the subunits suggested that these subunits are organized in a pseudosymmetrical manner that spans the membrane (Noda *et al.*, 1983).

A picture of the overall structure of the receptor began to emerge following the cloning and sequencing of all four subunits forming the nAChR. Each subunit contains a large extracellular N-terminal domain, four homologous, hydrophobic regions that potentially transverse the membrane and a small C-terminus also exposed extracellularly (Noda *et al.*, 1983; Claudio *et al.*, 1983). To date, 17 nAChR subunits have been identified: α1-α10, β1-4, γ, δ, and ε (reviewed by Corringer *et al.*, 2000; Paterson and Nordberg, 2000). According to the IUPHAR subcommittee report, these subunits are represented using a Greek letter followed by an Arabic numeral where necessary (Lukas *et al.*, 1999). The α1 and β1 subunits denote the muscle type nAChR subunits, while α2-10 and β2-4 represent the neuronal nAChR subunits. The γ subunit is present in fetal muscle nAChR (and *Torpedo* nAChR), but this is replaced by the ε-subunit in adult mammalian nAChR, a developmental switch that confers different conductance levels and burst durations in their respective receptors (Mishina *et al.*, 1986; Witzermann *et al.*, 1987). The general consensus of muscle type nicotinic acetylcholine receptor (referred to throughout this thesis as nAChR) structure is that it a heteropentamer (Fig. 1-1A). Each subunit consists of a) a large N-terminal hydrophilic extracellular region comprised

of about 210 amino acids extending approximately 60 Å from the membrane surface towards the synaptic cleft, b) four highly hydrophobic transmembrane domains named M1, M2, M3 and M4, with short hydrophilic stretches separating the M1, M2 and M3 domain and a large intracellular hydrophilic stretch which, in some subunits, contain consensus sequences for phosphorylation separates the M3 and M4 domains and c) a C-terminal that is also oriented towards the synaptic cleft (Fig. 1-1B, reviewed by Changeux *et al.*, 1992; Dunn, 1993; Karlin and Akabas, 1995; Arias, 2000). The nAChR has been shown to be sensitive to phosphorylation by cAMP-dependent protein kinase, protein kinase C and tyrosine-specific protein kinase, and there is evidence to suggest that phosphorylation may increase the rate of receptor desensitization (Huganir *et al.*, 1986; Huganir and Greengard, 1987). The extracellular N-terminal carries the agonist binding sites (discussed later), several glycosylation sites and a signature Cys-Cys loop (2 cysteine residues separated by 13 other residues). This unique 15-residue Cys-loop is common to all members of the LGIC family and therefore these receptors are also called "Cys-loop receptors".

The glutamate receptors (NMDA, AMPA and kainate receptor subtypes) are also ionotropic receptors, which include features such as an extracellular ligand binding domain and a cation-selective ion channel lined with residues from the M2 transmembrane domain (reviewed by Wollmuth and Sobolevsky, 2004). These receptors have global structural similarities to the classical ligand-gated ion channel family. However, in these glutamate receptors, the N- and C- terminal are located on the extracellular and intracellular sides of the membrane respectively. In addition, they have only three transmembrane domains and the M2 pore-forming domain forms a "P-loop"

structure as seen in K^+ channels and other voltage-gated ion channels. This suggests that these glutamate receptors share evolutionary and structural similarity with the K^+ channels (Dingledine *et al.*, 1999). Other neurotransmitter-gated membrane ion-channels include receptors for ATP, i.e., the P2X class of receptors (reviewed by North, 2002). P2X receptors are permeable to monovalent cations and have only two transmembrane domains. The N- and C- terminal for these receptors are suggested to be oriented towards the cytoplasm. The glutamate and P2X receptors, thus, have a significantly different hydrophobicity pattern from that of the Cys-loop receptor superfamily. In addition, glutamate and P2X receptors form tetramer and trimer subunit complexes respectively and consequently are thought to have four and three extracellular agonist binding sites. For simplicity, the reference to LGIC receptors in this thesis does not include the glutamate or P2X class of receptors.

SUBUNIT ARRANGEMENT OF THE NICOTINIC ACETYLCHOLINE RECEPTOR

Having established the subunit composition and stoichiometry of the *Torpedo* nAChR, another challenge faced by researchers was to elucidate the subunit arrangement of these receptors. The observation that two α-subunits could not be covalently cross-linked led to the suggestion that these subunits are not adjacent in the pentameric receptor (Schiebler *et al.*, 1980). Electron microscopy studies of negatively stained *Torpedo* electric organ membranes using avidin-biotin-labeled α-neurotoxin attached to the α-subunit also showed that the two α-subunits were not neighbors, and an α-β-α arrangement was proposed based on artificially generated receptor trimers (Wise *et al.*,

1981). A similar approach using complexes of avidin, biotinyl-toxin and *Torpedo* membrane derived receptors were analyzed by electron microscopy (Holtzman *et al.*, 1982). This study, based on the native δ-δ subunit crosslinked dimer, predicted the location of one of the toxin binding sites (and consequently the α-subunit) to be ~45-85° and the other to be ~100° away from the crosslink between the monomers, suggesting that one α-subunit is located adjacent to the δ-subunit. Based on experimentally generated receptor β-subunit dimers, the two toxin binding alpha subunits were estimated to be separated by 110° (Karlin *et al.*, 1983). This study ruled out the possibility that the β- or δ-subunit was located between the two α subunits, and favored an α-γ-α-δ-β subunit arrangement of the *Torpedo* nAChR. Expression studies in fibroblast cell lines using mouse muscle nAChR subunits demonstrated that the α-subunit co-expressed with the γ- or δ-subunit form pairs, but failed to associate with the β-subunit (Blount and Merlie, 1989). This suggested that the α-subunit is associated with different neighboring subunits, the γ- or δ-subunit, that contribute to two non-equivalent binding sites (discussed later). Subsequent photoaffinity labeling experiments using [^{3}H]dTC demonstrated the covalent incorporation of the photolabel into the α, γ and δ subunit, indicating that these subunits contribute to the ACh binding sites (Pederson and Cohen, 1990). The authors further demonstrated that dTC binds with high affinity (40nM) at the α-γ interface and with much lower affinity (900nM) at the α-δ interface. This led to the suggesting that either the γ- or the δ-subunit is located between the two α subunits. Electron image analysis of tubular crystal from *Torpedo marmorata*, with differently labeled subunits (α-bungarotoxin, Fab35 for the α-subunits,

FabIII for the β-subunit, and wheat germ agglutinin for the δ-subunit), visualized a clockwise subunit arrangement as α-β-α-γ-δ (Kubalek *et al.*, 1987). This arrangement is now thought to be unlikely (discussed later).

Numerous studies using different experimental approaches have suggested that the γ-subunit lies between the two α-subunits, pointing to a circular subunit arrangement of α-γ-α-δ-β or α-γ-α-β-δ (clockwise fashion) when viewed from the synaptic cleft (reviewed by Hucho *et al.*, 1996; Arias, 2000). The former arrangement has been the favored possibility. The arrangement of the subunits has also been investigated using photoactivatable derivatives of the α-neurotoxin II. These studies suggested a clockwise arrangement of α-γ-α-δ-β and ruled out its mirror image (Machold *et al.*, 1995). However, examination of the recent crystal structure of a homologous acetylcholine binding protein (AChBP, discussed later) reveals that binding sites are located at subunit-subunit interfaces, and predicts that the subunit arrangement is in a counter-clockwise α-γ-α-δ-β orientation (Brejc *et al.*, 2001, see Fig. 1-2).

Although the subunit arrangement may still be disputed, it is clear that the presence of all four subunits is required to form a fully functional receptor (Mishina *et al.*, 1985; Kurosaki *et al.*, 1987). A number of groups have omitted specific nAChR subunits and results obtained from using the *Xenopus* oocyte heterologous expression system have suggested that nAChR devoid of the β, γ or δ-subunits (Sumikawa and Miledi, 1989), the γ or δ-subunit (Kurosaki *et al.*, 1987), or even the α-subunit (Buller and White, 1990) is able to respond to ACh application, albeit with significantly smaller currents as compared to the wild type receptor. A criticism of these heterologous expression studies is that the endogenous protein machinery of the oocyte may somehow compensate for

the absence of subunit(s) (Quick and Lester, 1994). In addition, one cannot rule out the possibility that posttranslational folding, processing and oligomerization of these subunit-deficient receptors are quite different from that of the native, wild type nAChR.

nAChR SUBUNIT ASSEMBLY

The formation of a functional nAChR necessitates contacts between individual subunits and their assembly into a pentameric receptor complex. Proper assembly and folding of the nAChR is crucial, and is often considered to be the rate-limiting step in the postsynaptic expression of the receptors at the neuromuscular junction (Wanamaker *et al.*, 2003). The signal sequences at the N-terminals of the subunits guides their insertion to the ER where subsequently subunit synthesis occurs by translation of the mRNAs encoding for the subunits, followed by a series of post-translational modifications (reviewed by Keller and Taylor, 1999; Wanamaker *et al.*, 2003). The ER mediated association with chaperone proteins such as calnexin, immunoglobulin heavy-chain binding protein (BiP) and ERp57 helps to accomplish the correct quaternary structure of the emerging protein (Keller *et al.*, 1996; Wanamaker *et al.*, 2003). Furthermore, key amino acid residues in the extracellular amino-terminal of the subunits modulate correct subunit assembly into the $\alpha_2\beta\gamma\delta$ pentameric complex (Blount and Merlie, 1990; Gu *et al.*, 1991; Kreienkamp *et al.*, 1995; Sugiyama *et al.*, 1996; Green and Wanamaker, 1997). Misfolded or unassembled subunits are prone to rapid degradation in the ER, as a protective mechanism to prevent the appearance of nonfunctional surface receptors (Blount and Merlie, 1990).

The highly conserved cysteine residues, C128 and C142 form the signature disulfide Cys-loop in all four *Torpedo* nAChR subunits. These along with two additional cysteine residues (C192 and C193 found in the α-subunits) have been targeted to identify potential sites involved in posttranslational processing of the receptor. Mutation of the Cys-loop cysteine residues, or deletion of the entire Cys-loop region in the α-subunit, were shown to abolish α-BgTx binding and reduce receptor expression (Mishina *et al.*, 1985; Blount and Merlie, 1990). In contrast, mutation of C192/193 to serines had no effect on α-BgTx binding (Blount and Merlie, 1990). Interestingly, this study showed that the mutated α-subunit retained the ability to assemble with the δ-subunit when coexpressed in fibroblast cells, but the dimers were prone to rapid degradation ($t_{1/2}$ ~ 20min to 2hrs). Green and Wanamaker (1997) have also shown that the conserved Cys-loop in nAChR is crucial to the receptor assembly process. Mutations of the α-subunit cysteines to serines (C128S, C142S) resulted in αβγ trimers, but blocked the subsequent subunit assembly required to form a pentamer. The addition of DTT, which prevents the formation of disulfide bonds, had a similar effect, suggesting that the presence of the Cys-loop is essential for proper subunit assembly.

Other regions of the subunits have also been shown to influence the proper folding and subunit association required for assembly into a pentameric receptor complex. Mutation of the anionic residue Asp152, in the α-subunit, to an asparagine (αD152N) creates a consensus glycosylation sequence (Asn-Gly-Ser) and reduces the ability of the receptor to assemble (Sugiyama *et al.*, 1996). The αD152N mutant receptor displays a reduction in α-bungarotoxin binding, while elimination of the glycosylation sequence by the double mutation αD152N-S154A significantly increases receptor surface expression.

The altered receptor expression level was attributed to a reduction in the association between the α/γ and α/δ subunits during the initial stages of dimer formation, as determined by analysis of sucrose density gradient profiles of transfected α-subunits with the γ- or δ-subunits. In addition, two amino acid residues (S106 and Y115) in the extracellular domain of the mouse ε-subunit were shown to be responsible for the 10-fold higher surface expression than was observed when the rat ε-subunit was coexpressed with other mouse or rat subunits, suggesting that these residues are important for nAChR assembly (Gu *et al.*, 1991). This study would also help explain differences in inter-species nAChR surface expression levels observed. Similarly, cell-surface expression levels of *Torpedo* nAChRs were demonstrated to be 8 to 10-fold lower than those observed with the mouse αβεδ nAChRs in tSA201 cells (Eertmoed *et al.*, 1998). Furthermore, no expression was observed for *Torpedo* nAChR at a subunit ratio of 2:1:1:1 (αβγδ), whereas increasing the ratio of the δ subunit to 7.5 times that of the α-subunit resulted in receptor expression above background levels. It is not clear why or how altering the subunit ratio alters expression levels (personal communication from Dr. William N. Green, Univ. of Chicago).

Chimeric subunit approaches have also been undertaken to identify specific amino acid regions that are crucial for subunit assembly. Studies with subunit chimeras using the N-terminal of the ε-subunit and the carboxy-terminal of the β-subunit (ε_β chimera) demonstrated that this chimera can substitute for the ε-subunit in the pentameric nAChR receptor as determined by toxin binding assays (Yu and Hall, 1991). The β_ε chimera (β-subunit N-terminal), in contrast, was unable to substitute for the ε-subunit, suggesting that the α-subunit recognizes specific residues in the extracellular domain of the ε-

subunit to form an α-ε heterodimer. This may be an intermediate in the assembly process. Similarly, a γ-subunit (N-terminal) and β-subunit (C-terminal) chimera demonstrated that amino acid sequence 71-131 of the γ-subunit are important for association with the α-subunit (Krienekamp *et al.*, 1995). The β-subunit mutation, R117Y resulted in a significant decrease in surface receptor expression, suggesting that this residue contributes to β-subunit association with a neighboring subunit, possibly the δ-subunit. Coexpression of α and δ subunits resulted in α-δ dimer formation while association of γ- with the α-subunit resulted in the formation of both α-γ dimers, and α-γ-α-γ tetramers (Krienekamp *et al.*, 1995). This suggests that the γ- subunit can be inserted between the two α-subunits, further supporting an α-γ-α subunit arrangement (see previous section). Work with γ and δ-subunit chimeras has led to the identification of residues I145 and T150 of the γ-subunit that promote its contact with the α-subunit (Krienekamp *et al.*, 1995). Studies employing truncated N-terminal segments of the α and δ subunits expressed in COS cells have shown that the complete first transmembrane domain (M1) is required for the subunits to assemble into a heterodimer with the acquisition of high affinity toxin binding properties (Wang *et al.*, 1996).

Phosphorylation of the subunits has been proposed to regulate nAChR assembly, since increased intracellular cAMP levels were shown to increase expression levels of surface nAChR (Green *et al.*, 1991a; Ross *et al.*, 1991). Similarly, forskolin treatment resulted in a 2-3 fold increase in *Torpedo* nAChR expression by a mechanism attributed to increased phosphorylation of the unassembled γ-subunit (Green *et al.*, 1991b). Thus, phosphorylation of the nAChR is a key mechanism that, in addition to modulating channel function by accelerating the desensitization process of the assembled cell

surface receptors (Huganir *et al.*, 1986), also plays a role in the assembly process of the receptors.

The assembly of nAChR is a slow ($t_{1/2}$ ~ 2-hrs) and inefficient process, with only approximately 30% of synthesized α-subunits being assembled into pentamers (Merlie and Lindstrom, 1983). The synthesized subunits undergo folding before assembly as shown by the conformational change of the Cys-loop in the α-subunit, which buries the loop to allow exposure of subunit recognition sites and assembly (Green and Wanamaker, 1997). The ER chaperone protein, calnexin, appears to associate with individual unassembled subunits to prevent their degradation. It subsequently dissociates from the assembled complex, thereby assisting in formation of pentameric receptors (Keller *et al.*, 1996; 1998). Additionally, ER-associated degradation processes act in concert with chaperone proteins, which retain unassembled subunits in the ER. These are prone to interaction with the ubiquitin-proteasome pathway through exposed lysine residues on the subunits, which facilitates the degradation of these misfolded/unassembled proteins (Keller *et al.*, 1998; Keller and Taylor, 1999; Wanamaker *et al.*, 2003).

There are currently two schools of thought on the assembly of α, β, γ, and δ subunits in the ER into intermediate complexes that finally assemble into the oligomeric nAChR. One group proposes the association of mature α-subunit with γ or δ subunits to form α-γ and α-δ heterodimers, which subsequently associate with the β-subunit to form $\alpha_2\beta\gamma\delta$ pentamers (Blount and Merlie, 1989; Saedi *et al.*, 1991; Gu *et al.*, 1991; Kreienkamp *et al.*, 1995). An alternative scheme is the "sequential model" of subunit assembly proposed from studies using stably transfected *Torpedo* nAChR subunits in mouse L

fibroblast cells (Green and Wanamaker, 1997; 1998). Here, the α, β and γ subunits rapidly associate to form the first intermediate α-β-γ trimer, followed by addition of the δ-subunit and finally an additional α-subunit is added to the tetramer to make the pentameric complex.

In conclusion, through a variety of checkpoint mechanisms collectively referred to as "ER quality control" (Ellgaard and Helenius, 2001), the ER ensures that only the appropriately folded, assembled and posttranslationally modified proteins are transported out of the ER to the Golgi and subsequently to the cell surface (Gu *et al.*, 1991). The misfolded and unassembled proteins are retained and degraded in the ER.

LIGAND BINDING TO THE NICOTINIC ACETYLCHOLINE RECEPTOR

Ligands known to modulate the function of the nAChR fall under the following broad categories: a) agonists (e.g. ACh, carbamylcholine), b) competitive antagonists (e.g. tubocurarine, α-bungarotoxin), c) noncompetitive blockers (e.g. local anesthetics, histrionicotoxin, and neuroleptics such as chlorpromazine). The noncompetitive blockers act by either blocking the ion-channel or by allosterically altering receptor function by binding to a site distinct from the agonist binding site (reviewed by Devillers-Thiery *et al.*, 1993). Agonist association with the extracellular N-terminal domain of the receptor induces both localized and global conformational changes in the receptor resulting in its activation as a consequence of opening of the ion channel (Unwin, 1995; Miyazawa *et al.*, 2003, discussed later). The nAChR is suggested to exist in several interconvertible states including resting, active and desensitized states (Katz and Thesleff, 1957; see earlier section). Various models of receptor activation have been

proposed in order to explain the transition of the nAChR from a basal resting state to a conducting open state (Katz and Thesleff, 1957; Monod *et al.*, 1965; Adam, 1981; Changeux and Edelstein, 1998). A widely accepted model, the MWC (Monod, Wyman and Changeux) model predicts that allosteric oligomeric proteins exist in equilibrium between at least two pre-existing conformations and cooperativity in binding results from stabilization of a discrete state(s) for which the ligand displays higher affinity. This "two-state" receptor model describes concerted changes in the conformation of the receptor oligomer and incorporates intermediate stages of ligand affinity while the receptor is undergoing transition to a final desensitized state (Changeux and Edelstein, 1998). While the MWC model tries to rationalize kinetic properties of the nAChR, in its original form, it oversimplifies the very complex and dynamic processes that the receptor undergoes during activation. By an elegant series of experiments using extrinsic fluorescent probes covalently attached to *Torpedo* membrane bound nAChR, a model for multiple classes of distinct binding sites present on the same receptor that modulate channel function has been proposed by Dunn and colleagues (Dunn and Raftery, 1982a; 1982b, Dunn *et al.*, 1983; Dunn and Raftery, 1993; Dunn and Raftery, 2000). This model proposes that channel activation is mediated by agonist binding to distinct low affinity binding sites (discussed later).

MAPPING OF AGONIST/ANTAGONIST BINDING SITES BY AFFINITY LABELING STUDIES

Insight into structural details of the receptors in terms of binding site residues have been explored by their covalent labeling with reactive ligands in affinity and

photoaffinity labeling studies. A summary of key residues involved in agonist/antagonist recognition that have been identified by such labeling studies is provided in Fig. 1-3 and Table 1-1. Initial labeling studies using the alkylating antagonist, [^{3}H]MBTA (4-(N-maleimido) benzyltrimethyl ammonium), or the agonist, [^{3}H]bromoacetylcholine suggested that the binding sites are associated with the 40000-dalton polypeptide (or the α-subunits) of the *Torpedo* nAChR. Labeling with these ligands was achieved following DTT reduction of a readily reducible disulphide bond near the binding site(s) (Karlin and Cowburn, 1973; Moore and Raftery, 1979). Subsequently it was verified by CNBr proteolysis of labeled subunits and amino acid sequencing that MBTA exclusively labels the cysteine residues, C192 and C193 of the *Torpedo* nAChR α-subunit, suggesting these residues to be in close proximity to the agonist/antagonist binding site in the extracellular domain (Kao *et al.*, 1984). The photoactive agonist, [^{3}H]acetylcholine mustard (AChM) labeled mainly the nAChR α-subunit residue, Y93 (Cohen *et al.*, 1991). Furthermore, since the photolabel, AChM, is a reactive analog of ACh and contains a positively charged quaternary aziridinium group, the labeled αY93 residue was predicted to emphasize the role of aromatic interaction in the recognition of quaternary ammonium group. In other photoaffinity labeling studies, the agonist, [^{3}H]nicotine principally labeled αY198 (80% incorporation) and to a lesser extent, αY190 (13%) and αC192 (7%) (Middleton and Cohen, 1991).

Competitive antagonists have also been employed as probes to map residues involved in ligand recognition. By using a photoactive ligand, DDF (*p*-(dimethylamino) benzenediazonium fluoroborate), a competitive antagonist for the nAChR binding sites,

various amino acid residues were identified as specific sites of incorporation. [^{3}H]DDF labeling studies demonstrated that the *Torpedo* nAChR α-subunit amino acid residues that were unequivocally labeled (60% photoincorporation) were Y93, Y190, C192 and C193 (Dennis *et al.*, 1988; Galzi *et al.*, 1990). Other α-subunit residues were also labeled in these studies, albeit to a lesser extent (5% photoincorporation). These include, W86, W149, Y151 and Y198. αY190 is sensitive to labeling by the competitive antagonists, lophotoxin analog-I and dTC (Abramson *et al.*, 1989; Pederson and Cohen, 1990). Although dTC labels primarily αY190, it also labels αC192 and αY198 residues with lower efficiency (Chiara and Cohen, 1997). Similarly, [^{3}H]5-HT has been shown to label αY190, αC192 and αC193 in a cholinergic ligand protectable fashion (Blanton *et al.*, 2000). The labeled α-subunit residues (cysteine and aromatic residues) are highly conserved in muscle α-subunits from various species supporting their possible role in forming the ligand recognition sites.

A similar approach has been used to identify residues from the non-α subunits that contribute to the ACh binding site(s). [^{3}H]dTC labels γW55, γY111, γY117, δW57 and δR113 (Chiara and Cohen, 1997; Chiara *et al.*, 1999). When [^{3}H]nicotine was employed as a photoaffinity agonist label, the major site of incorporation was γW55 (Chiara *et al.*, 1998). A novel photoaffinity probe, [^{3}H]TDBzcholine (4-[(3-trifluoromethyl)-3*H*-diazirin-3-yl]benzoylcholine), which behaves as a competitive antagonist, labeled γL109 and δL111 in addition to αC192, αC193 and αP194 residues (Chiara *et al.*, 2003).

Aromatic residues constitute the bulk of the amino acids photolabeled by agonists and competitive antagonists. Thus far, no negatively charged residues have been labeled suggesting that aromatic amino acids may have sufficient electronegativity (through

their π-electrons) to stabilize the positively charged quaternary ammonium group carried by most cholinergic ligands (O'Leary *et al.*, 1994). Czajkowski and colleagues hypothesized (1991; 1995) that acidic residues (aspartates and glutamates) may constitute an additional negative subsite within the ACh binding site. S-(2-glycylaminoethyl)dithio-2-pyridine (GCP), a 9-Å long bisfunctional reagent that specifically forms a disulfide bond with the reduced αC192/193 residues on the α-subunit was demonstrated to cross-link with acidic residues in the δ-subunit, which were later identified by peptide mapping to be δD165, δD180 and δE182 (Czajkowski and Karlin, 1991; 1995).

The above labeling studies showed that key amino acids are labeled by both agonists and antagonists i.e., αY93, αY190, αY198, αC192, αC193, γW55, suggesting a common or overlapping binding site(s) for these classes of ligands. However some residues display ligand selectivity. This suggests that structurally diverse ligands may have several different contact regions within the overall ligand recognition domain(s). In the studies quoted above, labeling of specific residues was inhibited by agonists and competitive antagonists but not by noncompetitive blockers. Labeling studies thus provided the first direct evidence of residues that are important for the agonist/antagonist recognition. However, they could not shed light on the role of these binding sites in receptor function.

FUNCTIONAL CHARACTERIZATION OF THE ACh BINDING SITE RESIDUES

The heterologous expression of cloned nAChR subunit cDNAs and the ability to manipulate these DNAs *in vitro* has provided significant impetus to the pharmacological characterization of the putative binding site residues using biochemical, molecular and biophysical techniques. For biochemical analyses, nAChRs have been expressed in mammalian cell lines such as HEK 293 or tSA 201 cells. However, the transient expression of recombinant *Torpedo* nAChR is problematic since the assembly of these receptors is both inefficient and temperature dependent (Claudio *et al.*, 1987; Paulson and Claudio, 1990). In preliminary experiments, I found only very poor expression of *Torpedo* nAChR subunits in tSA 201 precluding further characterization (unpublished observations). In contrast, mouse nAChRs have been shown to express well in these cell lines (Prince and Sine, 1996; Sine, 1997; Osaka *et al.*, 1998; Akk, 2002). Similarly, I observed that mouse nAChR clones (generous gift from Dr. Gustav Akk, Washington University School of Medicine, St Louis, USA), displayed significant expression above background in tSA201 cells (unpublished observations). Due to the difficulties in expressing *Torpedo* nAChR in tSA201 cells, the electrophysiological characterization of this recombinant nAChR has been undertaken using the *Xenopus* oocyte expression system. The functional significance of the residues that had been identified in labeling studies has been investigated by mutagenesis experiments of recombinant cDNA's encoding for the subunit. The mutant subunit(s) is/are coexpressed with the remaining wild type subunits in a suitable expression system and the expressed mutant receptors are subsequently analyzed by radioligand binding assays and/or electrophysiology.

Examples of amino acid residues that are crucial for modulating agonist and competitive antagonist sensitivity at nAChR are summarized in Table 1-1.

nAChR α-subunit mutations altering receptor function

Wild type *Torpedo* or mouse nAChR expressed in *Xenopus* oocytes and probed using two-electrode voltage clamp techniques have been reported to have an EC_{50} value (agonist concentration that evokes half the maximal current) for ACh-induced activation of ~10 to 30 μM with a Hill coefficient approaching 2 (Tomaselli *et al.*, 1991; O'Leary and White, 1992; Aylwin and White, 1994a,b; Sullivan *et al.*, 2002). Mutation of αC192 and αC193 (to serine) resulted in a reduction in the apparent affinity for the agonist and completely abolished the ACh-evoked response suggesting that these residues are important for both agonist binding and receptor function. The αC128S and αC142S mutations abolished receptor expression as detected by α-bungarotoxin binding and no functional receptors were observed in oocytes, supporting the structural role of these residues (Mishina *et al.*, 1985). The importance of αY93, αY190 and αY198 residues has been demonstrated by their substitution with phenylalanine (Tomaselli *et al.*, 1991; O'Leary and White, 1992; Aylwin and White, 1994a,b). These studies demonstrated that the αY190F mutation resulted in 20-50 fold rightward shift in the EC_{50} for ACh-induced channel activation while the αY198F mutation resulted in lesser reduction in the EC_{50} value (approximately 6-fold reduction). These studies clearly underscore the importance of αY190 in forming a receptor site for ACh. Also, the αY190S mutation abolished agonist sensitivity for channel activation suggesting that an aromatic residue at this position may be required for receptor activation (O'Leary and White, 1992). Similarly, the αY93F substitution caused a ~20-fold shift towards higher

concentrations for ACh-induced channel activation (Aylwin and White, 1994b). Kinetic analyses of single-channel currents in mutant receptors revealed that the shift in dose-response curve for αY93F or αY198F mutants was a consequence of reduction in the apparent affinity for ACh rather than a gating effect (Aylwin and White, 1994a) while both the binding and gating processes were altered for the αY190F mutant (Chen *et al.*, 1995). Sine and colleagues (1994) suggested that the aromatic hydroxyl groups of αY93 and αY190 and the aromaticity of αY198 are all essential for binding of agonists. The αY93F and αY190F mutations also resulted in a reduction of affinity for the competitive antagonist, dTC suggesting that these residues are also important for the binding of these ligands (O'Leary *et al.*, 1994). Surprisingly, the αY198F substitution resulted in an increase in affinity for dTC and it has been suggested that this is a consequence of an aromatic-aromatic interaction between the aromatic ring of curare and aromatic residues within the binding site (O'Leary *et al.*, 1994).

Other residues identified by labeling studies included αW149 (and possibly αW86, αY151). A novel approach of using unnatural amino acids to replace the conserved Trp residues (αW86, αW149), suggested (based on EC_{50} changes of ACh-induced channel activation) that a cation-π interaction at W149 plays an important role in associating with the agonist (Zhong *et al.*, 1998). Moreover, the replacement of αW149 with an unnatural amino acid containing a tethered quaternary ammonium group attached to W149 resulted in a constitutively active receptor (Zhong *et al.*, 1998). In contrast, the αW149C mutant receptor produced no functional ACh-mediated currents. In the αY151F mutant, agonist-evoked channel activation was not altered as compared to wild type nAChR suggesting that αY151 is not critical for nAChR activation (O'Leary and

White, 1992). This finding may also explain its only minor labeling by [^{3}H]DDF (see previous section).

The substituted cysteine accessibility method (SCAM) is another approach that has been utilized to characterize the binding site and ion channel structural requirements. SCAM involves mutating individual residues to cysteine and studying their accessibility to sulfhydryl reactive cholinergic ligands (reviewed by Karlin, 2002). These studies demonstrated that αY93 and αN94 were accessible to ACh while αY198 was accessible to both ACh and dTC (Sullivan and Cohen, 2000; Sullivan *et al.*, 2002) consistent with the pattern of αY198 labeling by dTC (and not of αY93). An additional observation was that dTC bestows protection to only even numbered residues in this region (α196, 198 and 200). This suggests that in this segment of binding sites form a β-strand (Sullivan *et al.*, 2002), which is in accordance with the structure of a related protein, the AChBP (discussed later).

nAChR γ- and δ-subunit mutations altering receptor function

The participation of residues in the non-α subunits in modulating agonist/antagonist sensitivity has also been investigated. The γW55L mutation resulted in an approximate 8-fold reduction in dTC affinity (as determined by its ability to inhibit ACh-evoked currents in *Xenopus* oocytes) consistent with the notion that γW55 contributes to curare binding. The γW55L mutation also increased (by 7-fold) the EC_{50} for ACh-induced channel activation indicating that the agonist recognizes residues in the γ-subunit, a finding supportive of γW55 being labeled by the agonist, nicotine (see previous section). In contrast, the δW57L sensitivity to ACh or curare was unaltered (O'Leary *et al.*, 1994). Xie and Cohen (2001) demonstrated that although neither γW55L nor δW57L

mutations altered the equilibrium binding of dTC, they resulted in a reduction of ACh binding affinity by 7,000- and 20-fold respectively (as determined by inhibition of binding of [^{125}I]α-BgTx). The γW55L mutation was also shown to alter receptor activation by ACh (to a similar extent as demonstrated by O'Leary and colleagues, see above) suggesting that γW55 is crucial for both agonist binding and agonist-induced receptor activation. In contrast to the above results, γY111 (identified by dTC photolabeling) and its equivalent residue in the δ-subunit, R113, were demonstrated to be unimportant for the equilibrium binding of ACh or for channel activation but to be crucial determinants of antagonist binding affinities (Chiara *et al.*, 1999). In additional studies, γY117 (along with αY198) was demonstrated to stabilize the binding of the antagonist, dimethyl-*d*-tubocurarine (DMT) (Fu and Sine, 1994).

Expression of subunit dimers (α-γ and α-δ) or trimers (α-β-γ and α-β-δ) were shown to have significantly different affinities for the antagonist, DMT and the agonist, carbamylcholine depending on whether the γ- or δ- was incorporated (Sine, 1993; Prince and Sine, 1996). γ-δ-Subunit chimeras were first used to identify the regions in each subunit that are determinants of ligand selectivity at the two binding sites. Subsequent mutational analysis showed that γK34/δS36, γF172/δI178, γE57/δD59 and γC115/δY117 affected selectivity for carbamylcholine while γI116/δV118, γY117/δT119 and γS161/δK163 contributed to the higher affinity of DMT at the α-γ interface. Furthermore, under desensitizing conditions (induced by application with proadifen), γE57 was demonstrated to contribute to the binding of agonist in the desensitized receptor state (Prince and Sine, 1996). Using SCAM techniques, it has been demonstrated that γE57 is accessible to both ACh and dTC (Sullivan and Cohen, 2000;

Sullivan *et al.*, 2002) while γL109 is also afforded protection by dTC (Sullivan *et al.*, 2002). A similar approach demonstrated that γL119C (and residues at equivalent position, εI119C and δL121C) contribute to α-bungarotoxin binding (Sine, 1997).

Acidic residues have been postulated to provide a negative subsite to contribute to the ACh binding site (Czajkowski and Karlin, 1991; 1995, see previous section). The δD180N and δE189Q mutations reduced the affinity (and potency) of ACh by ~100- and 10-fold respectively suggesting that the carboxylate group of both δD180 and δE189 may constitute a negative subsite for ACh binding (Czajkowski *et al.*, 1993). Mutation of γD174 (the equivalent position to δD180) significantly decreased the affinity for agonists and to a lesser extent that of competitive antagonists (Martin *et al.*, 1996). Similarly, elimination of the charge on αD152 was shown to reduce both agonist and antagonist affinities (Osaka *et al.*, 1998). These data suggest that anionic residues from the α, γ and δ-subunits also contribute in the stabilization of cholinergic ligands.

The mounting evidence from labeling and mutagenesis experiments is that aromatic groups and charged residues from the α, γ and δ-subunit contribute to the ACh binding sites. Furthermore, the residues involved in ligand recognition lie in discrete domains contributed by different subunits, suggesting a probable location of ligand binding sites lying at the α- and the non-α subunit interfaces (α-γ and α-δ).

MODEL OF THE RECEPTOR RECOGNITION SITE

It is now generally accepted that the binding sites for agonists and competitive antagonists are formed at the interfaces of the α-γ and the α-δ subunit (Blount and Merlie 1989; Pederson and Cohen, 1990). For some ligands, these sites display very

different affinities. Previous studies, for example, demonstrate that α-γ and α-δ pairs represent the high and low affinity-binding sites respectively for dTC. Similarly, expression of subunit triplets, αβγ and αβδ displayed high and low affinity binding respectively for DMT while the reverse was true for the toxin, lophotoxin (Sine and Claudio, 1991). Using the alkylating agent, [^{3}H]bromoacetylcholine, it was demonstrated that in a reduced form of *Torpedo* nAChR, a high affinity binding site is located at the α-γ subunit interface in the vicinity of disulfide bonds (Dunn *et al.*, 1993). Thus far the β-subunit has not been implicated in contributing to the ACh binding site(s). It now appears likely that the β-subunit may be involved in stabilizing the quaternary structure of the pentamer and/or contributing allosterically to the properties of the receptor. However, since all the nAChR subunits share high sequence homology (~40%), it is possible that the β-subunit might also contribute to the binding of ligands.

In labeling studies, the α-subunits residues were more strongly labeled than residues in γ- and δ-subunits (see above). This has led to the terminology that regions from the α-subunits constitute the "principal component" and the non-α subunits (γ and δ) contribute to the "complementary component" of the ACh binding sites (Corringer *et al.*, 1995). Benefiting from over two decades of research, the "multiple loop hypothesis" for the ligand-binding sites was developed (reviewed by Changeux *et al.*, 1992; Corringer *et al.*, 2000; Arias, 2000; Karlin, 2002). This model envisaged that the polypeptide chain of each subunit twists several times like a ribbon and residues in the extracellular N-terminal domain that contribute to ligand binding are located in clusters in discontiguous regions on different polypeptide chains. These localized regions that carry the residues of interest for ligand binding were designated as loops A-C contributed by the α-

subunits and loop D-F from the neighboring γ- or δ-subunits (Fig. 1-2). As described above, important residues in these distinct regions include: αY93 (and possibly αW86) from loop A; αW149 (and possibly αY151) from loop B; αY190, αC192, αC193 and αY198 from loop C; γW55, γE57 and δW57 from loop D; γL109, γY111 and δR113 from loop E; γD174 and δD180 from loop F (Fig. 1-3).

Mutational studies of the majority of the residues implicated in forming the ACh binding site(s) have usually demonstrated a shift of agonist potency towards higher concentrations. A caveat must, however, be placed on interpreting results from mutational studies as the mutation might have affected the tertiary or quaternary structure of the receptor or the mutation may have indirectly altered the affinity for ligand leading to a false identification of binding site residues. Nevertheless, the combination of biochemical, molecular and electrophysiological techniques has greatly aided in our understanding of structure-function relationships of the nAChR. The emerging picture of the receptor's ligand recognition site is that a group of amino acids, primarily aromatic but perhaps also some acidic residues are involved in ligand recognition. Any model must include the stabilization of the positive charge of quaternary ammonium group of cholinergic ligands. The most plausible mechanism for this association has been stated to be a cation-π noncovalent interaction (Dougherty and Stauffer, 1990). However, other forms of interactions between residues close enough to interact may include hydrophobic interactions, hydrogen bonding and ion-pairing, which can result in salt bridge formation.

LIGAND RECOGNITION SITES ON OTHER MEMBERS OF THE LGIC SUPERFAMILY

The extensive characterization of the *Torpedo* nAChR has led to its undisputed role as the prototype of the Cys-loop receptor superfamily. Consequently, information accumulated on the nAChR has been extrapolated to other receptors belonging to this superfamily such as the glycine receptors (reviewed by Casio, 2004), serotonin type 3 receptor (5-HT_3R) (reviewed by Reeves and Lummis, 2002), the γ-aminobutyric acid type A receptor ($GABA_A$R) (reviewed by Kash *et al.*, 2004) and neuronal nicotinic acetylcholine receptors (reviewed by Paterson and Nordberg, 2000). Data generated from studies of these homologous receptors support the notion that ligand binding occurs at subunit-subunit interfaces and supports a multiple loop model akin to that suggested for the nAChR.

Residues in the homomeric α7 neuronal nicotinic receptor, Y92 (loop A), W148 (loop B) and Y187 (loop C) present at homologous position to αY93, α149, α190 from the *Torpedo* nAChR were demonstrated to be crucial in the binding of ACh and nicotine lending further credence to the multiple loop hypothesis (Galzi *et al.*, 1991). Furthermore, substitution of these residues by serine or histidine resulted in total ablation of functional response, reinforcing the importance of aromatic residues in the ligand binding domain. Cysteines 150 and 164 in the α7-nAChR (homologous to *Torpedo* C128 and C142 forming the Cys-loop) were demonstrated to be crucial for receptor assembly and expression (Dunckley *et al.*, 2003). In the $GABA_A$ receptor β2-subunit, homologous residues L99 and Y97 (Boileau *et al.*, 2002), Y157 (loop B) and Y205 (loop C) are important for GABA binding and receptor activation (Amin and Weiss, 1993).

The importance of aromatic amino acids in the ligand-binding domain of $5HT_3$ receptor was investigated by mutating tryptophan residues, W121 (loop A), W183 (loop B) and W90 (loop D) (equivalent positions to *Torpedo* nAChR αW86, αW149 and γW57 residues respectively) (Spier and Lummis, 2000). W121 was shown to be crucial for receptor expression while W90 and W183 were important for mediating agonist sensitivity, possibly via a cation-π association.

Similarly, residues from other members of the LGIC family present at homologous positions to γW55 and δW57 from loop D of the *Torpedo* nAChR have been shown to contribute to the ligand recognition site. A key example includes the mutation of W54 in the α7 neuronal nicotinic receptor, which resulted in a 10-200-fold reduction in sensitivity to agonists (Corringer *et al.*, 1995). In the α1β2γ2 $GABA_AR$, the α1F64L mutation caused a 200-fold reduction in the apparent affinities for agonist and antagonists suggesting the involvement of the α1-subunits in forming an agonist/antagonist binding site (Sigel *et al.*, 1992). Similarly, Y62 in the β2 subunit of the $GABA_A$ R (also lying in loop D) was shown to contribute to high affinity agonist binding (Newell *et al.*, 2000). In addition, γ2F77 of these receptors appears to be important for mediating the effects of allosteric modulators such as benzodiazepines (Buhr *et al.*, 1997). In the homooligomeric $5HT_3$ receptor, W89 was demonstrated to contribute to antagonist binding (Yan *et al.*, 1999). These studies clearly underscore the importance of aromatic residues from loop D of members of the LGIC superfamily in contributing to the sensitivity of ligands.

FUNCTIONAL ROLE OF BINDING SITES

An important conclusion from the preceding sections is that the two well characterized ligand binding sites on the *Torpedo* nAChR lie at subunit interfaces, namely, the α-γ and α-δ subunit interfaces. The non-symmetry of these interfaces also accounts for the differences in binding affinities for competitive antagonists at these two sites. Upon binding of agonists, the *Torpedo* nAChR has been suggested to undergo ligand-mediated conformational changes that lead to an equilibrium high affinity state, which may represent the desensitized state of the receptor (Weber *et al.*, 1975; Quast *et al.*, 1978). Under equilibrium binding conditions, ACh binds to the two high affinity binding sites in *Torpedo* nAChR with identical affinities (dissociation constant of 10-30 nM, Raftery *et al.*, 1983). Most current models for receptor activation assume that binding of agonist to these two sites mediates both channel activation and desensitization. It has been presumed that activation and desensitization are sequential processes. The approximately 3 orders of magnitude difference in agonist concentration required to activate the nAChR (EC_{50} for receptor activation by ACh of 10-100 μM) and the affinity for [^{3}H]ACh measured in equilibrium binding assays (K_d ~ 10 nM) reflects the different receptor states i.e. activated and desensitized state (Raftery *et al.*, 1983). An alternative explanation is that different classes of agonist binding sites are involved in activation and desensitization. The homology between the subunit polypeptide chains originally led to the suggestion that additional binding sites may be present on each subunit (reviewed by Conti-Tronconi and Raftery, 1982). The active state of the nAChR is of intrinsically low affinity (agonist EC_{50} for receptor activation in the μM range), raising the possibility that receptor activation is mediated by binding sites different from

the high affinity sites that are readily measured at equilibrium (Dunn and Raftery, 1982b). While tremendous strides have been achieved in elucidating the structure of the ACh-binding sites and its correlation with receptor function, our knowledge of the coupling mechanisms between these two processes resulting in synaptic transmission is limited at best. In this laboratory, fluorescence techniques have often been used to explore the conformational transitions of the *Torpedo* nAChR that result from agonist binding.

Torpedo membrane-bound nAChRs were covalently labeled with a sulfydryl selective alkylating fluorescent probe, 5-iodoacetamidosalicylic acid (IAS) subsequent to mild reduction (Dunn *et al.*, 1980). This probe was deliberately targeted to the readily reducible disulfide formed between vicinal cysteines, C192 and 193, close to the high affinity site. Carbamylcholine binding to the IAS-labeled receptors under equilibrium conditions resulted in a saturable enhancement of fluorescence that was sensitive to inhibition by the antagonist, α-BgTx and the alkylating agonist, bromoacetylcholine suggesting that changes in the fluorescence of IAS reflects binding to the nearby binding sites. An excellent correlation was observed between the dissociation constant value (K_d) for [^{3}H]carbamylcholine binding to native membranes and to IAS-labeled membranes (~100 nM). Of particular importance is that the kinetics of the carbamylcholine-induced fluorescence changes were too slow to allow its correlation with the receptor activation process.

Evidence for the presence of low affinity sites(s) for agonists on *Torpedo* nAChR under equilibrium conditions that is/are separate from the high affinity binding sites came by monitoring the agonist-induced fluorescent changes of another fluorescent

probe, 4-([(iodoacetoxy)ethyl]methylamino)-7-nitro-2,1,3-benzoxadiazole (IANBD) covalently bound to the receptors (Dunn and Raftery, 1982a,b; Dunn *et al.*, 1983). In equilibrium fluorescence titrations, ACh and carbamylcholine enhanced the fluorescence of this probe in a saturable fashion, and this was abolished by prior incubation with α-BgTx suggesting that the observed fluorescence changes were specific for the receptor (Dunn and Raftery, 1982a,b). However, the fluorescence enhancement was not affected by covalently bound BrACh, dTC and channel blockers such as histrinotoxin or lidocaine. This suggested that IANBD is monitoring binding to sites that are distinct from the high affinity sites. For all agonists studied, the apparent dissociation constants for fluorescence titrations (e.g. for ACh K_d ~ 80 μM) correlated well with their concentration dependencies observed in ion flux studies (ACh EC_{50} ~ 100 μM). Furthermore, the kinetics of the fluorescent enhancement were very rapid and correlated well with the rapid (msec) timescale of channel activation. These studies indicated the presence of a separate class of binding site(s) under equilibrium conditions that may be important in modulating receptor function and are of much lower affinity than those reported in equilibrium binding experiments. This led to the suggestion that there are multiple classes of binding sites for agonists on *Torpedo* nAChR and that these sites play a distinct role in modulating synaptic transmission with channel activation and desensitization occurring in parallel (Dunn *et al.*, 1983).

Although it has been suggested that the discrepancy between equilibrium binding affinities and the concentrations of agonist that induce channel activation can be explained by the two-state receptor model (reviewed by Changeux *et al.*, 1992), the above mentioned studies challenged the dogma that the two high affinity sites on nAChR

identified earlier by biochemical studies are the only sites present and that these mediate both channel activation and desensitization. Further characterization of multiple classes of binding sites present on the same receptor came from studying the properties of *Torpedo* nAChR doubly labeled with both extrinsic fluorescent probes, IAS and IANBD (Dunn and Raftery, 1993). It was shown that although the fluorophores are both sulfhydryl-selective, they did not did not react at the same location. As suggested earlier, binding of agonists to IAS-labeled receptor preparation resulted in a saturable enhancement of fluorescence. A similar enhancement was observed upon the binding of competitive antagonists such as hexamethonium. In contrast, the fluorescence enhancement observed upon agonist binding to IANBD-labeled receptor preparations revealed sites of much lower affinity, and binding to these sites was unaffected by most competitive antagonists but was blocked by α-BgTx.

The unequivocal demonstration of the role of multiple agonist binding sites on *Torpedo* nAChR function was that preequilibration of the high affinity sites with saturating concentrations of carbamylcholine did not attenuate the ion flux response to subsequent challenge with activating concentrations of carbamylcholine. This provided direct evidence that the high affinity sites could not be directly involved in channel activation process, suggesting that distinct low affinity sites (see above) must mediate this process (Dunn and Raftery, 2000). Furthermore, since the nAChR could still be activated even after saturation of all its high affinity sites, these sites cannot be solely involved in mediating the desensitization process. So the obvious question is that, if the high affinity sites mediate neither activation nor desensitization, what is their role?

Recently, in the $GABA_A$ receptor it was demonstrated that the β2 subunit residue, Y62 residue is an important determinant for high affinity agonist binding (Newell *et al.*, 2000). Further characterization of a receptor (α1β2γ2) carrying the β2Y62S mutation revealed altered desensitization properties (Newell and Dunn, 2002). The mutant receptor that displayed no high affinity binding for [^{3}H]muscimol desensitized but rapidly recovered from desensitization even in the continued presence of agonist. This led to the suggestion that although the high affinity binding sites may not be directly involved in inducing desensitization, they may play a role in maintaining the desensitized state subsequent to it entering this phase. By analogy with the $GABA_A$ receptor, a similar mechanism may be present in the nAChR.

Kinetic studies of the association and dissociation of acetylcholine and suberyldicholine to *Torpedo* nAChR membranes have suggested that each of the high affinity binding sites comprise of two subsites that are mutually exclusive at equilibrium (Dunn and Raftery, 1997a,b). The dissociation kinetics of bound [^{3}H]ACh (at concentrations sufficient to saturate all the high affinity sites) were significantly increased upon addition of micromolar concentrations of unlabeled agonists suggesting that that each of the high affinity sites comprises two subsites (arbitrarily named as subsite A and B). When sites A are initially saturated with [^{3}H]ACh, the binding of an additional ACh molecule (to site B with higher concentrations) significantly reduced the affinity of site A, thereby enhancing its dissociation from this site (see Fig. 1-4A). Further evidence in support of this two-subsite hypothesis is that the dissociation of the bisfunctional agent, [^{3}H]suberyldicholine is only marginally affected by the presence of unlabeled agonists such as ACh or suberyldicholine suggesting that suberyldicholine, by

virtue of its bisquaternary character, is able to bridge the two subsites simultaneously or at least occlude the accessibility to subsite B (see Fig. 1-4B). Further characterization of the association kinetics of agonists, ACh and suberyldicholine at these sites using receptor preparations labeled with the fluorescent probe, IAS, that reports agonist binding to the high affinity sites suggested significantly different association kinetics for these two ligands (Dunn and Raftery, 1997b).

The emerging theme from these studies is that there is heterogeneity within the high affinity site. The exact location of the second subsite is not known but the fact that suberyldicholine appears to bridge these two subsites suggests that the second subsite should be close enough to the first subsite for simultaneous association of two quaternary groups of suberyldicholine.

STRUCTURE OF THE *TORPEDO* nAChR

The understanding of the structure of *Torpedo* nAChR has come a long way since the first reports of the primary sequencing of the subunits to its subsequent cloning and suggestions of domains of the receptor to thread across the membrane (Raftery *et al.*, 1980; Noda *et al.*, 1982).

The approximate shape of the receptor was revealed by cryo-electron microscopy of two-dimensional tubular crystals of *Torpedo* nAChR (Unwin, 1993; Unwin, 1995; Unwin, 1998). At 9Å resolution, the shape and dimensions of the receptor were revealed and suggested the receptor to be 80Å in diameter and ~120Å long with about 65Å protruding extracellularly towards the synaptic cleft and about 20Å protruding intracellularly, while the rest is immersed in the membrane. In addition, about 30Å

distal from the membrane towards to the extracellular surface, a cavity surrounded by three density peaks in each subunit was visualized. The peaks were suggested to be a group of three rods presumably α-helices that were angled perpendicular to the lipid bilayer. Two of these α-helix rods were oriented towards the entrance of the channel while the third was facing outwards. The rods of the α-subunits were suggested to constitute the ACh binding site. Furthermore, in the lipid bilayer an additional rod in each subunit, closer to the five-fold axis of symmetry was suggested to be present. The five rods (one from each subunit) that transverses the membrane is suggested to correspond to the M2 transmembrane domain. The outer rim of rod is suggested to be star shaped, presumably composed of β-sheets, while the portion of the rods lining the pore were predicted to be predominantly α-helical, which were visualized to bend as they thread across the bilayer forming a kink toward the middle that forms the gate to regulate the flow of ions through the pore.

In an attempt to visualize the changes in the receptor induced up on ACh binding, a brief exposure (<5ms) of *Torpedo* postsynaptic membranes was undertaken followed by its rapid freezing to capture the resulting structural reorganization (Unwin, 1995). The activated structure suggested significant movements of the rods (~28° anticlockwise rotations) in the α-subunit adjacent to the δ-subunit (α_δ). In contrast, a smaller movement of the α-subunit neighboring the γ-subunit was observed while the β-subunit simply displaced away from the α_δ-subunit. The localized movement of the α_δ subunit was predicted to communicate with the neighboring subunits thereby propagating subunit movements all over. Although in these studies the subunit arrangement was presumed to be α-β-α-γ-δ in a clockwise orientation, the important conclusion is that the

localized changes first initiated in the extracellular domain are communicated through rotations of the subunits eventually to the bilayer associated domain that lines the channel pore resulting in opening of the ion-channel.

Structural information of *Torpedo* nAChR by electron microscopy studies was limited due the low resolution of the technique. The discovery of a related homologous protein, acetylcholine binding protein (AChBP) and its crystallization (discussed later) provided a template for modeling of nAChR structure. The higher resolution (4.6Å) of the images of *Torpedo* membranes (with the subunit arrangement now assumed to be α-γ-α-δ-β) and its comparison to the crystal structure of AChBP further provided a better glimpse of the secondary structures of the subunit and the possible coupling mechanism between the binding and gating processes (Unwin *et al.*, 2002; Miyazawa *et al.*, 2003). The ligand-binding domain is suggested to be formed predominantly by β-sheets while the domains transversing the membrane are α-helical with short interconnecting loops. Agonist binding is suggested to induce a ~ 15° clockwise rotation of the inner β-sheets of both the α-subunits towards its neighboring γ- and δ-subunit. This rotational movement occurs about an axis that transverses the Cys-loop disulfide bond (Loop 7, amino acids 128-142, see below), which is oriented towards the transmembrane domains. This results in a contact between the extracellular N-terminal oriented segment (Loop 2, amino acid 45-48) and the interconnecting loop between the transmembrane domain, M2-M3 and these small rotations are conveyed to the inner M2 helices facing the pore resulting in the removal of the kink forming the gate and the opening of the ion-channel occurs. This study thus provided the first direct evidence of communication between the extracellular agonist binding domains and the gating mechanism and

implicated the L2 region (immediately preceding loop D) as the instigator, L7 (Cys-loop) as the mediator and M2-M3 as the final modulator of the gating mechanism. A similar mechanism was recently validated in the $GABA_A$ receptors, wherein negatively charged residues, α1D57 (from L2) and α1D149 (L7) were shown to interact with the positively charged residue, α1K279 (in the M2-M3 linker) to account for the coupling of agonist association to channel gating (Kash *et al.*, 2003).

Electron microscopy studies helped to better define the structure and more recently a possible gating mechanism of the nAChR protein but the crystal structure of the receptor remains lacking. Recently the most revealing insight into the spatial location of the subunits and the ACh-binding site of the nAChR has come from elucidation of the atomic structure of a related protein, AChBP.

CRYSTAL STRUCTURE OF ACETYLCHOLINE BINDING PROTEIN

In 2001, Sixma and colleagues published a landmark paper wherein they report the crystal structure of an acetylcholine-binding protein (AChBP). This is a soluble protein produced in the glial cells of the snail, *Lymnaea stagnalis* that is a truncated homologue of the nAChR (Brejc *et al.*, 2001). The molluscan glial cells release AChBP into the synaptic cleft in an ACh-dependent manner, where it behaves like a protein mop by buffering ACh and thus regulating synaptic transmission (Smit *et al.*, 2001). Hence, the concentration of the released AChBP acts like a homeostasis regulatory control mechanism that determines whether transmission occurs or not (Sixma and Smit, 2003).

The crystal structure of AChBP was characterized at a resolution of 2.7Å and revealed conspicuous similarities to the extracellular ligand-binding domain of the

nAChR (Brejc *et al.*, 2001). The AChBP is made up of five identical monomers ("Subunits") that assemble into homopentamers along a five-fold axis of symmetry (Fig. 1-5A). These form a soluble protein that is 62Å in height, 80 Å in diameter and with a central "hole" of about 18Å diameter, dimensions that correlate well with the EM images suggested for the *Torpedo* nAChR by Unwin and colleagues (Unwin, 1998; Miyazawa *et al.*, 2003). Each AChBP subunit consists of an α-helix proximal to the N-terminal, two short 3_{10} helices and a curled β-sandwich comprised of ten β-strands (and connecting loops) that are considerably convoluted and the β-sheets turn around against each other forming two distinct hydrophobic cores (Fig. 1-6B). The most notable difference between the structure of nAChR and AChBP is the absence of transmembrane domains in the latter. Consequently, the N-terminal is located on the top while the C-terminal is located at the bottom of this homopentameric protein. An AChBP monomer contains 210 amino acids and displays between 20-25% homology to the aligned sequences from the extracellular amino ligand-binding domain of the nAChR subunits (see Appendix), with the greatest homology to the neuronal α7 nAChR. Furthermore, AChBP exhibits similar pharmacological properties to the nAChR and binds nAChR agonists such as ACh, nicotine and epibatidine and also binds nAChR competitive antagonists such as *d*-tubocurarine and α-bungarotoxin. In addition, AChBP possesses the characteristic Cys-loop, the signature loop seen in all LGIC members. In the case of the AChBP, however, there are 12 intervening residues that are predominantly hydrophilic in nature as compared with the 13 hydrophobic residues seen in nAChR subunits. This Cys-loop is proximal to the C-terminus at the bottom of the protein complex (Fig.1-6 A,B), a finding proposed also for *Torpedo* nAChR (Miyazawa *et al.*,

2003) leading to the suggestion that the Cys-loop in nAChR may interact with the transmembrane domain of the receptor in the gating process. Of particular note is that most of the conserved residues in the putative binding sites of the nAChR are also present in AChBP, with hydrophobic residues constituting the core. In essence, all of the amino acids identified by labeling and mutagenesis studies to be involved in the ACh binding sites formed by the α-, γ- and δ-subunits of nAChR (residues listed in parentheses) are conserved in AChBP. These include, loop A: Y89 (αY93), loop B: W143 (αW149), loop C: Y185 (αY190), C187, C188 (αC192, αC193), Y192 (αY198). Binding site residues contributed by the complementary component of the receptor sites include but are not limited to, are loop D: W53 (γW55, δW57), loop E: R104 (γL109, δL111), V106 (γY111 and δR113), L112 (γY117) and loop F: Y164 (no equivalent residue identified in γ- and δ-subunit, instead cross-linking experiments suggested neighboring γD174 and δD180 to contribute the negative subsite for ligand binding). It should be noted that loop F residues are poorly conserved in members of the LGIC family. In addition, αW86 in loop A of nAChR was predicted to be part of the binding site based on its meager labeling by DDF (Galzi *et al.*, 1991); however its homologue in AChBP, W82 is shown to be located distal to the binding pocket and predicted not to participate in ligand binding (see Table1-1).

The ligand binding pocket in AChBP appears to be a cavity located at the interfaces between subunits (Fig.1-5B) that is flanked by a series of loops between β-strands (loop A-C) from the principal component of one subunit and a string of β-strands (loop D and E) from the complementary face of the neighboring subunit. Access to the AChBP binding site is from the outside of the pentamer complex. Since, the AChBP is made up

of 5 identical subunits, the binding site residues that align with the α-subunit residues are depicted as lying on one side of AChBP (the "+" side) while the residues contributing to the complementary component of the binding site that align with the γ- and δ-subunit residues be on the opposite side, the "-" side. Hence, the ligand binding interface in AChBP is formed between the anticlockwise side of one subunit, the (+)-side and the clockwise side, the (-)-side of the adjacent subunit. This also addressed the issue of the handedness of the subunit arrangement for the nAChR long under debate; showing it to be α-γ-α-δ-β in a counter-clockwise orientation when viewed from the synaptic cleft. Another interesting aspect of the structure of AChBP is that, although it was crystallized in the absence of a ligand specific for the binding site, HEPES derived from the buffer used in crystallization (which like ACh carries a positively charged quaternary nitrogen atom) was found in the putative binding site that was close to W143 (αW149), consistent with a cation-π interaction as predicted in nAChR (Zhong *et al.*, 1998).

The elucidation of the crystal structure of the related AChBP reinforced earlier predictions of the structure of nAChR and this has resulted in a series of attempts to model the extracellular ligand binding domains of the nAChR and other members of the LGIC family (e.g. Le Novère, *et al* 2002; Sine, 2002; Ernst *et al.*, 2003). In these models, the protein sequence (or its predicted binding "loops") of a yet uncrystallized receptor is superimposed on the atomic structure of AChBP. The limitation of such models is the low sequence identity of AChBP with members of the LGIC receptors (such as 15-18% for the $GABA_A$ and 5-HT_3 receptors as compared to a modest similarity of 20-24% with the nicotinic receptor family). Such studies must therefore be

interpreted with caution. Moreover, since the AChBP structure is predominantly formed by alternating β-strands, a miscalculation in sequence alignment of even a single residue could result in its being placed on the wrong side of the β-sheets (Sine, 2002), thus having serious implications on the interpretation of the structural details of the protein under study. In this thesis, I have therefore used a more cautious approach by using the AChBP crystal structure to map the potential distances of specific amino acids from putative binding sites.

AIMS OF THE PRESENT STUDY

The objective of the research described in this thesis is to probe the role of specific amino acid residues in the extracellular amino terminal domains of the recombinant *Torpedo* nAChR subunits in modulating receptor function, with the overall goal of better understanding structure-function relationships of this receptor. To accomplish these goals, a multi-disciplinary approach of molecular, biochemical and biophysical techniques such as site-directed mutagenesis, radioligand binding and two-electrode voltage clamp electrophysiology is employed.

Although the high affinity binding sites have been exhaustively characterized, there are certain aspects of equilibrium ligand binding and receptor activation that are unresolved. A major disparity is the differences between the agonist concentrations that mediate these two processes. Some have argued that such discrepancies may be explained by a two-state model of receptor activation (reviewed by Changeux *et al.*, 1992) and that the high affinity sites simply represent a desensitized conformation of the low affinity sites that mediate channel activation (Baur and Sigel, 2003). In contrast, the

use of covalently labeled fluorescent probes in *Torpedo* nAChR led to the suggestion of multiple classes of agonist binding sites each with a distinct role (Dunn and Raftery, 1982a; 1982b, Dunn *et al.*, 1983; Dunn and Raftery, 1993). In support of a multiple site model is the high sequence homology of individual nAChR subunits, which suggests that all subunits (or subunit-subunit interfaces) may contribute to ligand binding (Raftery *et al.*, 1983; Dunn and Raftery, 1993). Recently, the crystal structure of the homopentameric protein, AChBP revealed ligand-binding interfaces at each subunit with the (+)-face of a subunit contributing the principal component whereas the (-)-face of the adjacent subunit contributing the complementary part to the ligand binding site. This crystal structure has proved to be very important in guiding current studies aimed to elucidate nAChR binding domains.

Based on the above considerations and sequence alignment, it was hypothesized that agonist-recognition sites in *Torpedo* nAChR may also be present at subunit interfaces that are distinct from those that are described as the "classical" high affinity binding interfaces. As is described in Chapter 2, the arginine residue at position 55 of loop D of the α-subunit ((-)-side), a domain that until now has not previously been implicated in ligand binding, is shown to play a role in modulating agonist potency and channel function. We speculate that this residue could be involved in forming additional binding sites by association with residues from the loop A-C of the neighboring γ-subunit (and possibly the β-subunit). As a secondary hypothesis, it is predicted that Glu93 from loop A of the γ-subunit located at its (+)-face (homologous to αTyr93) could provide a subsite for ligand recognition. Furthermore, αArg55 (loop D) and γGlu93 (loop A) by virtue of their opposite charge could form a putative ion-pairing interaction at the γ-α

subunit interface. The characterization of the functional significance of these residues will help in better defining the role of different molecular motifs and their role in forming additional putative ligand interacting domains.

The objective of Chapter 3 is to try to elucidate the mechanism underlying the functional behavior of bisfunctional cholinergic agonists such as suberyldicholine. Previous work in our laboratory has suggested that each of the high affinity binding sites comprise two subsites that are mutually exclusive at equilibrium (Dunn and Raftery, 1997a,b). Furthermore, it was predicted that suberyldicholine by virtue of its bisquaternary character is able to bridge the two subsites. Thus, the basic tenet of Chapter 3 is that, based on the chain length of suberyldicholine, the secondary subsite (lower affinity) is in the vicinity of the primary subsite (high affinity), close enough to be bridged by suberyldicholine. Therefore, the specific aim in this chapter is to demonstrate the significance of putative residue(s) in this region that is crucial for modulating the sensitivity of suberyldicholine.

In conclusion, the purpose of the research undertaken in this study is to identify amino acid residues that are important for modulating the sensitivity of agonists and competitive antagonists and to further validate the previous predictions of additional ligand interacting domains present on other subunits as well as to investigate the role of the putative two subsite high affinity model in channel function.

Figure 1-1

(A). Schematic of the *Torpedo* nicotinic acetylcholine receptor showing the overall arrangement of the five subunits in the postsynaptic membrane bilayer. (B). Linear representation of the topology of a single subunit showing the large extracellular amino terminal, four hydrophobic transmembrane domains (M1-M4) and a carboxy terminal also oriented extracellularly facing the synaptic cleft.

A)

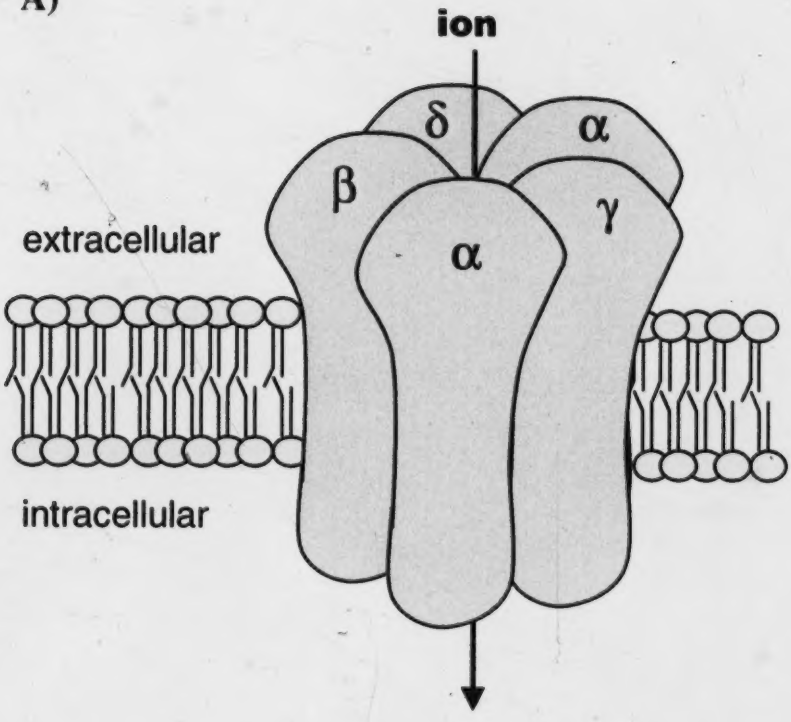

B)

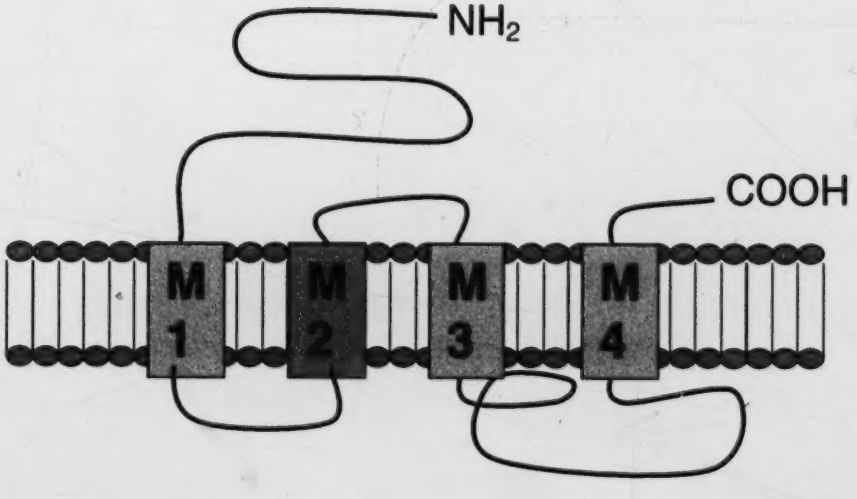

Figure 1-2

Cartoon of the *Torpedo* nicotinic acetylcholine receptor showing the circular subunit arrangement as α-γ-α-δ-β in an anticlockwise manner (see direction of arrows). Also depicted are the two high affinity ACh binding sites flanked by residues from loop A-C of the α-subunits (principal component) along with residues from loop D-F of the neighboring γ- and δ-subunit (complementary component).

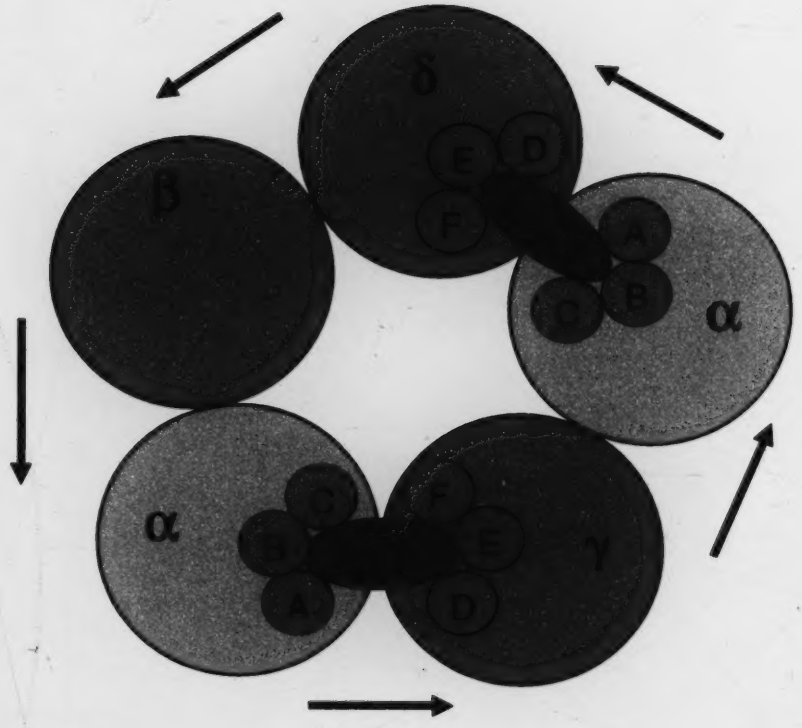
δ
E
D
F
β
A
B
C
α
α
C
B
A
F
E
D
γ

Figure 1-3

Illustration of key residues identified by labeling and mutagenesis studies in *Torpedo* nAChR from the loop A-C (in blue) of the α-subunits (principal component) along with residues from loop D-F (in green) of the neighboring γ- and δ-subunit (complementary component) contributing to the high affinity ACh binding sites (see text for details). The arrangement of the loops is from N-terminal to C-terminal.

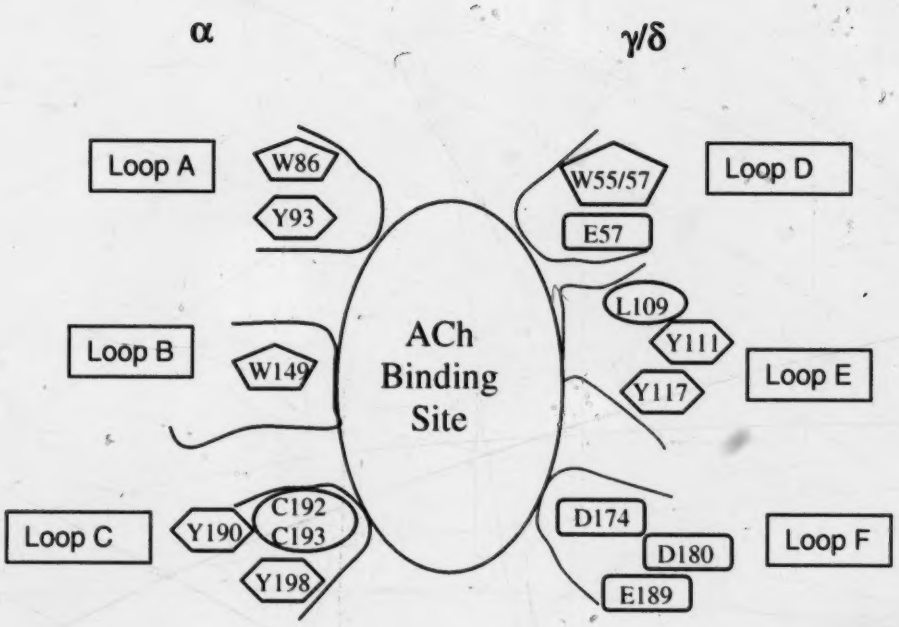
α
γ/δ
Loop A
W86
Y93
W55/57
Loop D
E57
L109
Y111
Loop B
W149
ACh
Binding
Site
Loop E
Y117
C192
C193
Loop C
Y190
D174
Loop F
D180
Y198
E189

Figure 1-4

Schematic representation of the two subsite high affinity model. (A). Micromolar concentrations of unlabeled ACh accelerate the rate of dissociation of [^{3}H]ACh from its high affinity subsite (site A). (B) [^{3}H]SubDc (suberyldicholine) associates with both the subsites simultaneously (site A and B) and consequently no acceleration in its dissociation is observed. Figure modified from Dunn and Raftery, 1997a.

A)

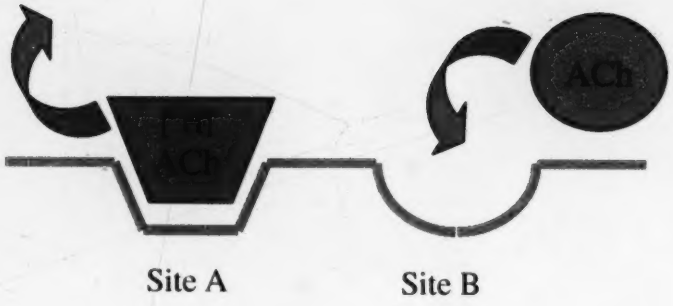

B)

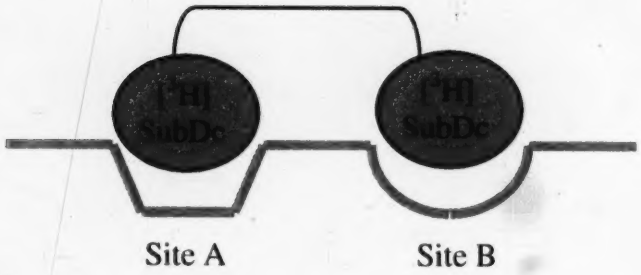

Figure 1-5

Depiction of the crystal structure of acetylcholine-binding protein (AChBP). Top view illustrating (A) the AChBP homopentamer parallel to the fivefold axis (ribbon illustration) and (B) interfacial location of binding sites at each subunit depicted in a line-ribbon illustration for better visualization of the overall structure. Each of the five identical subunits are depicted in a separate color for clarity and labeled A, B, C, D and E. Ligand binding sites are located at each subunit interface in a counter-clockwise orientation, A-B, B-C, C-D, D-E and E-A. Also depicted are some key ligand binding residues (stick-representation in black) at each subunit interface.

A)

B)

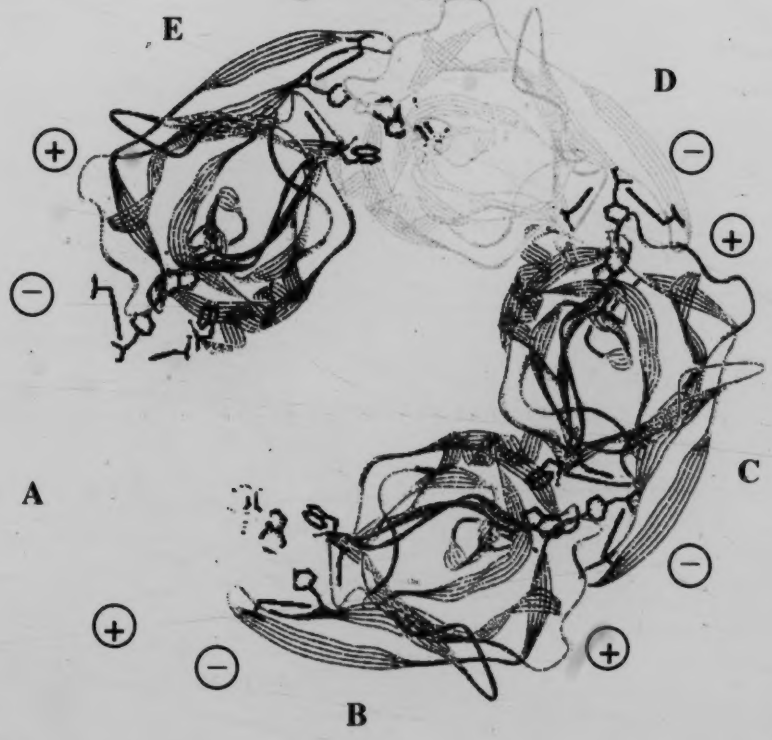

Figure 1-6

A single subunit of acetylcholine-binding protein (AChBP). View perpendicular to the fivefold axis illustrating (A) an α-helix close to the N-terminus, which is oriented towards the synaptic cleft; a C-terminus at the bottom of the structure. Also illustrated is the conserved double cysteine residues (C187/188 homologous to *Torpedo* αC192/193 respectively) that is facing the adjacent subunit (in a counter-clockwise subunit arrangement, not shown) and the signature Cys-loop (C123-136) that is situated at the bottom of the protein, which is predicted to facilitate gating in *Torpedo* nAChR (Miyazawa *et al.*, 2003). The remainder of the subunit is predominantly β-strands. (B) Schematic representation of (A) depicting the ten β-strands and the interconnecting loops. The red cylinder on the top of the subunit depicts the α-helix. The direction of the arrow indicates the folding pattern of the β-strands that turn around each other.

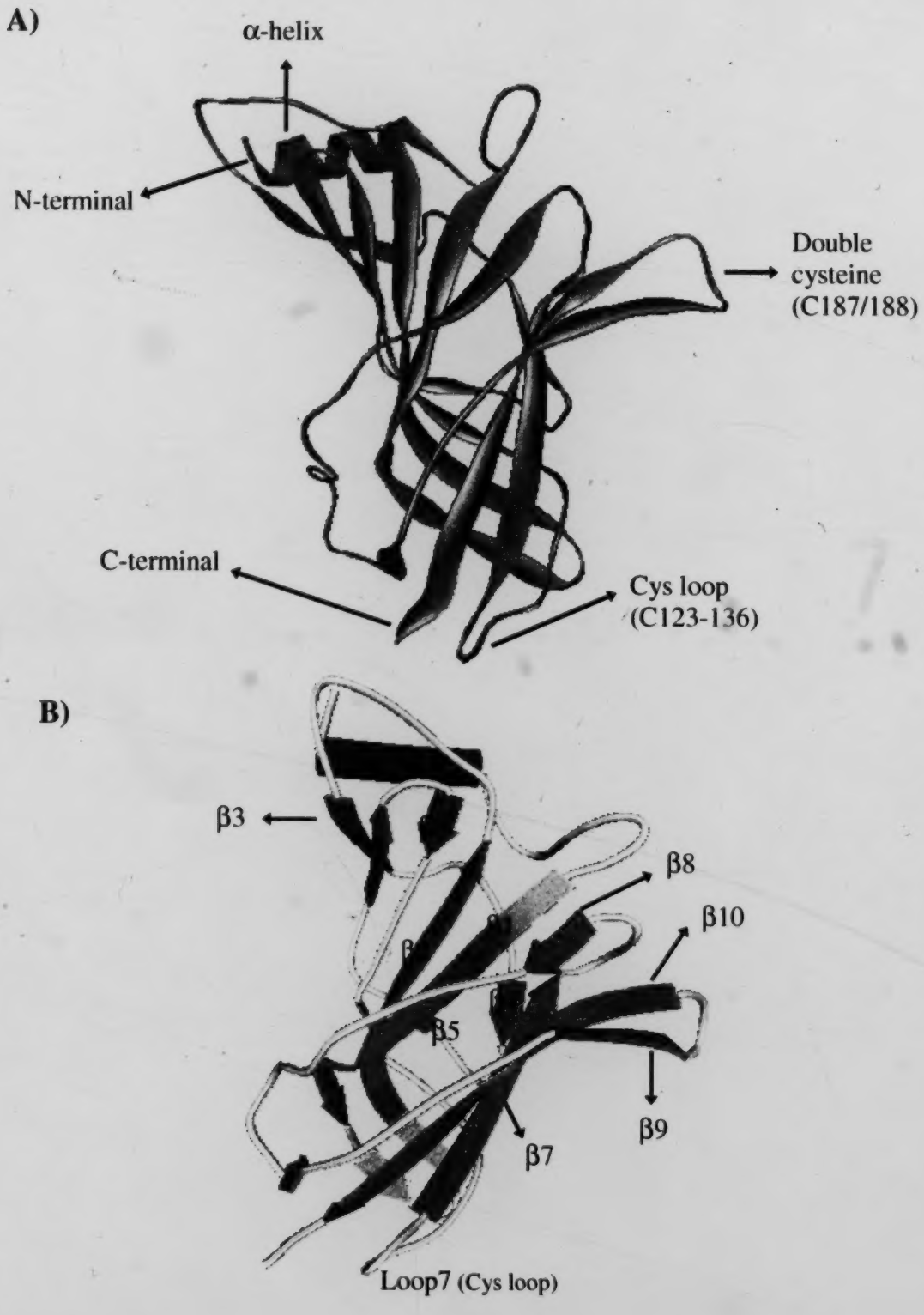
A)
α-helix
N-terminal
Double
cysteine
(C187/188)
C-terminal
Cys loop
(C123-136)
B)
β3
β8
β10
β5
β9
β7
Loop7 (Cys loop)

Table 1-1. Amino acids residues contributing to ACh binding in *Torpedo* nAChR subunits and homologous residues in AChBP (See text for details).

Loop	α	γ	δ	AChBP
A	Y93	E93*	Q95*	Y89
	W86			W82$
B	W149			W143
	Y151@			
C	Y190			Y185
	C192			C187
	C193			C188
	Y198			Y192
D	R55*	W55	W57	W53
	R57*	E57	D59	Q55
E		L109	L111	R104
		Y111	R113	V106
		Y117	T119	L112
F		#	#	Y164
		D174	D180	

* Has not been identified or implicated in ligand binding or modulating agonist/antagonist sensitivity.

$ W82 in AChBP has been suggested not to participate in ligand binding (Brejc *et al.*, 2001)

@ αY151 (loop B) was identified by DDF labeling (Dennis *et al.*, 1990), however functional characterization of this residue demonstrated its lack of role in channel activation (O'leary and White, 1992).

\# Residues equivalent to AChBP Y164 (loop F) in γ- or δ-subunit of nAChR have not been identified to constitute the binding site.

- β-subunit has not been demonstrated till date to contribute to the binding site and hence not represented in the table.
- Table modified from Smit *et al.*, 2003.

BIBLIOGRAPHY

ABRAMSON, S.N., LI, Y., CULVER, P. AND TAYLOR, P. (1989). An analog of lophotoxin reacts covalently with Tyr190 in the α-subunit of the nicotinic acetylcholine receptor. *J. Biol. Chem.*, **264,** 12666-12672.

ADAMS, P.R. (1981). Acetylcholine receptor kinetics. *J. Memb. Biol.*, **58**, 161-174.

AKK, G. (2002). Contributions of the non-α subunit residues (loop D) to agonist binding and channel gating in the muscle nicotinic acetylcholine receptor. *J. Physiol.*, **544.3,** 695-705.

AMIN, J. AND WEISS, D.S. (1993). $GABA_A$ receptor needs two homologous domains of the beta-subunit for activation by GABA but not by pentobarbital. *Nature,* **366,** 565-569.

ARIAS, H.R. (2000). Localization of agonist and competitive antagonist binding sites on nicotinic acetylcholine receptors. *Neurochem. Int.*, **36,** 595-645.

AYLWIN, M.L. AND WHITE, M.M. (1994a). Gating properties of mutant receptors. *Mol. Pharmacol.*, **46,** 1149-1155.

AYLWIN, M.L. AND WHITE, M.M. (1994b). Ligand-receptor interactions in the nicotinic acetylcholine receptor probed using multiple substitutions at conserved tyrosines on the α subunit. *FEBS Lett.*, **349,** 99-103.

BALLIVET, M., PATRICK, J., LEE, J. AND HEINEMANN, S. (1982). Molecular cloning of cDNA coding for the γ subunit of *Torpedo* acetylcholine receptor. *Proc. Natl. Acad. Sci. USA,* **79,** 4466-4470.

BAUR, R. AND SIGEL, E. (2003). On high- and low-affinity agonist sites in $GABA_A$ receptors. *J. Neurochem.*, **87,** 325-332.

BLANTON, M.P., McCARDY, E.A., FRYER, J.D., LIU, M. AND LUKAS, R.J. (2000). 5-Hydroxytryptamine interaction with the nicotinic acetylcholine receptor. *Eur. J. Pharmacol.*, **389,** 155-163.

BLOUNT, P. AND MERLIE, J.P. (1989). Molecular basis of the two nonequivalent ligand binding sites of the muscle nicotinic acetylcholine receptor. *Neuron*, **3,** 349-357.

BLOUNT, P. AND MERLIE, J.P. (1990). Mutational analysis of muscle nicotinic acetylcholine receptor subunit assembly. *J. Cell Biol.*, **111,** 2613-2622.

BOILEAU, A.J., NEWELL, J.G. AND CZAJKOWSKI, C. (2002). $GABA_A$ receptor $\beta2$ Tyr^{97} and Leu^{99} line the GABA-binding site. *J. Biol. Chem.*, **277,** 2931-2937.

BREJC, K., DIJK, W.J.V., KLAASSEN, R.V., SCHUURMANS, M., OOST, J.V.D., SMIT, A.B. AND SIXMA, T.K. (2001). Crystal structure of an ACh-binding protein reveals the ligand-binding domain of nicotinic receptors. *Nature*, **411,** 269-276.

BUHR A., BAUR, R. AND SIGEL, E. (1997). Subtle changes in residue 77 of the γ subunit of the $\alpha1\beta2\gamma2$ $GABA_A$ receptors drastically alter the affinity for ligands of the benzodiazepine binding site. *J. Biol. Chem.*, **272,** 11799-11804.

BULLER, A.L. AND WHITE, M.W. (1990). Functional acetylcholine receptors expressed in *Xenopus* oocytes after injection of *Torpedo* β, γ, and δ subunit RNAs are a consequence of endogenous oocytes gene expression. *Mol. Pharm.*, **37,** 423-428.

CASCIO, M. (2004). Structure and function of the glycine receptor and related nicotinicoid receptors. *J. Biol. Chem.*, **279,** 19383-19386.

CHANGEUX, J.-P AND EDELSTEIN, S.J. (1998). Allosteric receptors after 30 years. *Neuron,* **21,** 959-980.

CHANGEUX, J.-P., GALZI, J.-L., DEVILLERS-THIÉRY, A. AND BERTRAND, D. (1992). The functional architecture of the acetylcholine nicotinic receptor explored by affinity labeling and site-directed mutagenesis. *Quart. Rev. Biophy.*, **25**, 395-432.

CHANGEUX, J.-P AND PODLESKI, T.R. (1968). On the excitability and cooperativity of the electroplax membrane. *Proc. Natl. Acad. Sci. USA,* **59,** 944-950.

CHEN, J., ZHANG, Y., AKK, G., SINE, S. AND AUERBACH, A. (1995). Activation kinetics of recombinant mouse nicotinic acetylcholine receptors: Mutations of α-subunit tyrosine 190 affect both binding and gating. *Biophy. J.,* **69,** 849-859.

CHIARA, D.C. AND COHEN, J.B. (1997). Identification of amino acids contributing to high and low affinity *d*-tubocurarine sites in the *Torpedo* nicotinic acetylcholine receptor. *J. Biol. Chem.,* **272,** 32940-32950.

CHIARA, D.C., MIDDLETON, R.E. AND COHEN, J.B. (1998). Identification of tryptophan 55 as the primary site of [^{3}H]nicotine photoincorporation in the γ-subunit of the *Torpedo* nicotinic acetylcholine receptor. *FEBS Lett.,* **423,** 223-226.

CHIARA, D.C., XIE, Y. AND COHEN, J.B. (1999). Structure of the agonist-binding sites of the *Torpedo* nicotinic acetylcholine receptor: Affinity labeling and mutational analyses identify γTyr-111/δArg-113 as antagonist affinity determinants. *Biochem.,* **38,** 6689-6698.

CHIARA, D.C., TRINIDAD, J.C., WANG, D., ZIEBELL, M.R., SULLIVAN, D. AND COHEN, J.B. (2003). Identification of amino acids in the nicotinic acetylcholine receptor agonist binding site and ion channel photolabeled by 4-[(3-trifluoromethyl)-3*H*-diazirin-3-yl]benzoylcholine, a novel photoaffinity antagonist. *Biochem.,* **42,** 271-283.

CLAUDIO, T., BALLIVET, M., PATRICK, J. AND HIENEMANN, S. (1983). Nucleotide and deduced amino acid sequences of *Torpedo californica* acetylcholine receptor gamma subunit. *Proc. Natl. Acad. Sci. USA.*, **80,** 1111-1115.

CLAUDIO, T., GREEN, W.N., HARTMAN, D.S., HAYDEN, D., PAULSON, H.L., SIGWORTH, F.J., SINE, S. AND SWEDLUND, A. (1987). Genetic reconstitution of functional acetylcholine receptor-channels in mouse fibroblasts. *Science,* **238,** 1688-1694.

COHEN, J.B., SHARP, S.D. AND LIU, W.S. (1991). Structure of the agonist-binding site of the nicotinic acetylcholine receptor. [3H] acetylcholine mustard identifies residues in the cation-binding subsite. *J. Biol. Chem.,* **266,** 23354-23364.

CONTI-TRONCONI, B.M. AND RAFTERY, M.A. (1982). The nicotinic cholinergic receptor: Correlation of molecular structure with functional properties. *Ann. Rev. Biochem.,* **51,** 491-530.

CORRINGER, P.-J., GALZI, J.-L., EISELÉ, J-L., BERTRAND, S., CHANGEUX, J.-P. AND BERTRAND, D. (1995). Identification of a new component of the agonist binding site of the nicotinic α7 homooligomeric receptor. *J. Biol. Chem.,* **270,** 11749-11752.

CORRINGER, P.J., LE NOVERE, N. AND CHANGEUX, J.-P. (2000). Nicotinic receptors at the amino acid level. *Ann. Rev. Pharmacol. Toxicol.*, **40,** 431-58.

CZAJKOWSKI, C. AND KARLIN, A. (1991). Structure of the nicotinic receptor acetylcholine-binding site. Identification of acidic residues in the δ subunit within 0.9 nm of the α subunit binding site disulfide. *J. Biol. Chem.,* **266,** 22603-22612.

CZAJKOWSKI, C. AND KARLIN, A. (1995). Structure of the nicotinic acetylcholine receptor acetylcholine-binding site. Identification of acidic residues in the δ subunit within 0.9 nm of the α subunit-binding site disulfide. *J. Biol. Chem.*, **270,** 3160-3164.

CZAJKOWSKI, C., KAUFMANN, C. AND KARLIN, A. (1993). Negatively charged amino acid residues in the nicotinic receptor δ subunit that contribute to the binding of acetylcholine. *Proc. Natl. Acad. Sci. USA*, **90,** 6285-6289.

DENNIS, M., GIRAUDAT, J., KOTZYBA-HIBERT, F., GOELDNER, M., HIRTH, C., CHANG, J.Y., LAZURE, C., CHRETIEN, M. AND CHANGEUX, J.-P. (1988). Amino acids of the *Torpedo marmorata* acetylcholine receptor alpha subunit labeled by a photoaffinity ligand for the acetylcholine binding site. *Biochem.*, **27,** 2346-2357.

DEVILLERS-THIÉRY, A., GALZI, J.L., EISELÉ, J.L., BERTRAND, S., BERTRAND, D. AND CHANGEUX, J.-P. (1993). Functional architecture of the nicotinic acetylcholine receptor: a prototype of ligand-gated ion channels. *J. Mem. Biol.*, **136,** 97-112.

DINGLEDINE, R., BORGES, K., BOWIE, D. AND TRAYNELIS, S.F. (1999). The glutamate receptor ion channels. *Pharmacol. Rev.*, **51,** 7-61.

DIONNE, V.E., STEINBACH, J.H. AND STEVENS, C.F. (1978). An analysis of the dose-response relationship at voltage-clamped frog neuromuscular junctions. *J. Physiol.*, **281**, 421-444.

DOUGHERTY, D.A. AND STAUFFER, D.A. (1990). Acetylcholine binding by a synthetic receptor: Implications for biological recognition. *Science*, **250,** 1558-1560.

DREYER, F. AND PEPER, K. (1975). Density and dose-response curve of acetylcholine receptors in frog neuromuscular junction. *Nature*, **253,** 641-643.

DREYER, F., PEPER, K. AND STERZ, R. (1978). Determination of dose-response curves by quantitative ionophoresis at the frog neuromuscular junction. *J. Physiol.*, **281,** 395-419.

DUNCKLEY, T., WU, J., ZHAO, L. AND LUKAS, R.J. (2003). Mutational analysis of roles for extracellular cysteine residues in the assembly and function of human α7-nicotinic acetylcholine receptors. *Biochem.*, **42**, 870-876.

DUNN, S.M.J. (1993). Structure and function of the nicotinic acetylcholine receptor. *Adv. Struc. Biol.*, **2**, 225-244.

DUNN, S.M.J., BLANCHARD, S.G. AND RAFTERY, M.A. (1980). Kinetics of carbamylcholine binding to membrane bound acetylcholine receptor monitored by fluorescence changes of a covalently bound probe. *Biochem.*, **19,** 5645-5652.

DUNN, S.M.J., CONTI-TRONCONI, B.M. AND RAFTERY, M.A. (1983). Separate sites of low and high affinity for agonists on *Torpedo californica* acetylcholine receptor. *Biochem.*, **22**, 2512-2518.

DUNN, S.M.J., CONTI-TRONCONI, B.M. AND RAFTERY, M.A. (1993). A high-affinity site for acetylcholine occurs close to the α-γ subunit interface of *Torpedo* nicotinic acetylcholine receptor. *Biochem.*, **32,** 8616-8621.

DUNN, S.M.J. AND RAFTERY, M.A. (1982a). Activation and desensitization of *Torpedo californica* acetylcholine receptor: Evidence for separate binding sites. *Proc. Nat. Acad. Sci. USA.*, **79,** 6757-6761.

DUNN, S.M.J. AND RAFTERY, M.A. (1982b). Multiple binding sites for agonists on *Torpedo californica* acetylcholine receptor. *Biochem.*, **21**, 6264-6272.

DUNN, S.M.J. AND RAFTERY, M.A. (1993). Cholinergic binding sites on the pentameric acetylcholine receptor of *Torpedo californica*. *Biochem.*, **32**, 8608-8615.

DUNN, S.M.J. AND RAFTERY, M.A. (1997a). Agonist binding to the *Torpedo* acetylcholine receptor. 1. Complexities revealed by dissociation kinetics. *Biochem.*, **36,** 3846-3853.

DUNN, S.M.J. AND RAFTERY, M.A. (1997b). Agonist binding to the *Torpedo* acetylcholine receptor. 2. Complexities revealed by association kinetics. *Biochem.*, **36,** 3854-3863.

DUNN, S.M.J. AND RAFTERY, M.A. (2000). Roles of agonist-binding sites in nicotinic acetylcholine receptor function. *Biochem. Biophys. Res. Commun.*, **279,** 358-362.

EERTMOED, A.L., VALLEJO, Y.F. AND GREEN, W.N. (1998). Transient expression of heteromeric ion channels. *Methods Enzymol.*, **293,** 564-585.

ELLGAARD, L. AND HELENIUS, A. (2001). ER quality control: towards an understanding at the molecular level. *Curr. Opin. Cell Biol.*, **13,** 431-437.

ERNST, E., BRAUCHART, D., BORESCH, S. AND SIEGHART, W. (2003). Comparative modeling of the $GABA_A$ receptors: Limits, insights, future developments. *Neurosci.*, **119,** 933-943.

FU, D.-X. AND SINE, S.M. (1994). Competitive antagonists bridge the α-γ subunit interface of the acetylcholine receptor through quaternary ammonium-aromatic interactions. *J. Biol. Chem.*, **269,** 26152-26157.

GALZI, J.-L., REVAH, F., BLACK, D., GOELDNER, M., HIRTH, C. AND CHANGEUX, J.-P. (1990). Identification of a novel amino acid alpha-tyrosine 93 within the cholinergic ligands-binding sites of the acetylcholine receptor by photoaffinity labeling. Additional evidence for a three-loop model of the cholinergic ligands-binding sites. *J. Biol. Chem.*, **265,** 10430-10437.

GALZI, J.-L., BERTRAND, D., DEVILLERS-THIÉRY, A., REVAH, F., BERTRANS, S. AND CHANGEUX, J.-P. (1991). Functional significance of aromatic amino acids from three peptide loops of the α7 neuronal nicotinic receptor site investigated by site-directed mutagenesis. *FEBS Lett.*, **294,** 198-202.

GREEN, W.N., ROSS, A.F. AND CLAUDIO, T. (1991a). cAMP stimulation of acetylcholine receptor expression is mediated through posttranslational modifications. *Proc. Natl. Acad. Sci. USA,* **88,** 854-858.

GREEN, W.N., ROSS, A.F. AND CLAUDIO, T. (1991b). Acetylcholine receptor assembly is stimulated by phosphorylation of its γ subunit. *Neuron,* **7,** 659-666.

GREEN, W.N. AND WANAMAKER, C.P. (1997). The role of the cysteine loop in acetylcholine assembly. *J. Biol. Chem.*, **272,** 20945-20953.

GREEN, W.N. AND WANAMAKER, C.P. (1998). Formation of the nicotinic acetylcholine receptor binding sites. *J. Neurosci.*, **18,** 5555-5564.

GU, Y., CAMACHO. P., GARDNER, P. AND HALL, Z.W. (1991). Identification of two amino acid residues in the ε subunit that promote mammalian muscle acetylcholine receptor assembly in COS cells. *Neuron,* **6,** 879-887.

HOLTZMAN, E., WISE, D., WALL, J. AND KARLIN, A. (1982). Electron microscopy of complexes of isolated acetylcholine receptor, biotinyl-toxin, and avidin. *Proc. Natl. Acad. Sci. USA.*, **79,** 310-314.

HUCHO, F., TSETLIN, V.I. AND MACHOLD, J. (1996). The emerging three-dimensional structure of a receptor. The nicotinic acetylcholine receptor. *Eur. J. Biochem.*, **239,** 539-557.

HUGANIR, R.L., DELCOUR, A.H., GREENGARD, P. AND HESS, G.P. (1986). Phosphorylation of the nicotinic acetylcholine receptor regulates its rate of desensitization. *Nature,* **321,** 774-776.

HUGANIR, R.L. AND GREENGARD, P. (1987). Regulation of receptor function by protein phosphorylation. *Trends Pharmacol. Sci.,* **8,** 472-477.

JONES, M.V. AND WESTBROOK, G.L. (1996). The impact of receptor desensitization on fast synaptic transmission. *Trends Neurosci.,* **19,** 96-101.

KAO, P.N., DWORK, A.J., KALDANY, R.R., SILVER, M.L., WIDEMAN, J., STEIN, S. AND KARLIN, A. (1984) Identification of the alpha subunit half-cysteine specifically labeled by an affinity reagent for the acetylcholine receptor binding site. *J. Biol. Chem.*, **259,** 11662-11665.

KARLIN, A. (2002). Emerging structure of the nicotinic acetylcholine receptors. *Nature Neurosci.,* **3,** 102-114.

KARLIN, A. AND AKABAS, M.H. (1995). Toward a structural basis for the function of nicotinic acetylcholine receptors and their cousins. *Neuron,* **15,** 1231-1244.

KARLIN, A. AND COWBURN, D. (1973). The affinity-labeling of partially purified acetylcholine receptor from electric tissue of Electrophorus. *Proc. Natl. Acad. Sci. USA.,* **70,** 3636-3640.

KARLIN, A., HOLTZMAN, E., YODH, N., LOBEL, P., WALL, J. AND HAINFELD, J. (1983). The arrangement of the subunits of the acetylcholine receptor of *Torpedo californica*. *J. Biol. Chem.,* **258,** 6678-6681.

KASH, T.L., JENKINS, A., KELLY, J.C., TRUDELL, J.R. AND HARRISON, N.L. (2003). Coupling of agonist binding to channel gating in the GABA(A) receptor. *Nature,* **421,** 272-275.

KASH, T.L., TRUDELL, J.R. AND HARRISON, N.L. (2004). Structural elements involved in activation of the γ-aminobutyric acid type A ($GABA_A$) receptor. *Biochem. Soc. Trans.,* **32,** 540-546.

KATZ, B. AND MILEDI, R. (1977). Transmitter leakage from motor nerve endings. *Proc. Royal Soc. Lond. - Series B: Biol. Sci.,* **196**, 59-72.

KATZ, B. AND THESLEFF, S. (1957). A study of the desensitization produced by acetylcholine at the motor end-plate. *J. Physiol.*, **138**, 63-80.

KELLER, S.H., LINDSTROM. J. AND TAYLOR, P. (1996). Involvement of the chaperone protein calnexin and the acetylcholine receptor beta-subunit in the assembly and cell surface expression of the receptor. *J. Biol. Chem.,* **271,** 22871-22877.

KELLER, S.H., LINDSTROM, J. AND TAYLOR, P. (1998). Inhibition of glucose trimming with castanospermine reduces calnexin association and promotes degradation of the α-subunit of the nicotinic acetylcholine receptor. *J. Biol. Chem.,* **273,** 17064-17072.

KELLER, S.H. AND TAYLOR, P. (1999). Determinants responsible for assembly of the nicotinic acetylcholine receptor. *J. Gen. Physiol.,* **113,** 171-176.

KREINEKAMP, H-J., MAEDA, R.K., SINE, S.S. AND TAYLOR, P. (1995). Intersubunit contacts governing assembly of the mammalian nicotinic acetylcholine receptor. *Neuron,* **14,** 635-644.

KUBALEK, E., RALSTON, S., LINDSTROM, J. AND UNWIN, N. (1987). Location of subunits within the acetylcholine receptor by electron image analysis of tubular crystals from *Torpedo marmorata*. *J. Cell Biol.*, **105,** 9-18.

KUROSAKI, T., FUKUDA, K., KONNO, T., MORI, Y., TANAKA, K., MISHINA, M. AND NUMA, S. (1987). Functional properties of nicotinic acetylcholine receptor subunits expressed in various combinations. *FEBS letts.*, **214,** 253-258.

KUFFLER, S.W. AND YOSHIKAMI, D. (1975). The number of transmitter molecules in a quantum: an estimate from iontophoretic application of acetylcholine at the neuromuscular synapse. *J. Physiol.*, **251**, 465-482.

LAND, B.R., SALPETER, E.E. AND SALPETER, M.M. (1980). Acetylcholine receptor site density affects the rising phase of miniature endplate currents. *Proc. Natl. Acad. Sci. USA,* **77,** 3736-3740.

LESTER, H.A. (1977). The response to acetylcholine. *Sci. Am.*, **236**, 106-116.

LE NOVÈRE, N., GRUTTER, T. AND CHANGEUX, J.-P.(2002). Models of the extracellular domains of the nicotinic receptors and of agonist- and Ca^{2+}-binding sites. *Proc. Natl. Acad. Sci. USA,* **99,** 3210-3215.

LUKAS, R.J., CHANGEUX, J.-P., LE NOVÈRE, N., ALBUQUERQUE, E.X., BALFOUR, D.J., BERG, D.K., BERTRAND, D., CHIAPPINELLI, V.A., CLARKE, P.B., COLLINS, A.C., DANI, J.A., GRADY, S.R., KELLAR, K.J., LINDSTROM, J.M., MARKS, M.J., QUIK, M., TAYLOR, P.W. AND WONNACOTT, S. (1999). International Union of Pharmacology. XX. Current status of the nomenclature for nicotinic acetylcholine receptors and their subunits. *Pharmacol. Rev.*, **51,** 397-401.

MACHOLD, J., WEISE, C., UTKIN, Y., TSETLIN, V. AND HUCHO, F. (1995). The handedness of the subunit arrangement of the nicotinic acetylcholine receptor from *Torpedo californica*. *Eur. J. Biochem.*, **234,** 427-430.

MARTIN, M., CZAJKOWSKI, C. AND KARLIN, A. (1996). The contributions of aspartyl residues in the acetylcholine receptor γ and δ subunits to the binding of agonists and competitive antagonists. *J. Biol. Chem.*, **271,** 13497-13503.

MERLIE, J.P. AND LINDSTROM, J. (1983). Assembly in vivo of mouse muscle acetylcholine receptor: identification of an alpha subunit species that may be an assembly intermediate. *Cell*, **34,** 747-757.

MIDDLETON, R.E. AND COHEN, J.B. (1991). Mapping of the acetylcholine binding site of the nicotinic acetylcholine receptor: [3H]nicotine as an agonist photoaffinity label. *Biochem.*, **30,** 6987-6997.

MISHINA, M., TOBIMATSU, T., IMOTO, K., TANAKA, K-I., FUJITA, Y., FUKUDA, K., KURASAKI, M., TAKAHASHI, H., MORIMOTO, Y., HIROSE, T., INAYAMA, S., TAKAHASHI, T., KUNO, M. AND NUMA. S. (1985). Location of functional regions of acetylcholine receptor α-subunit by site-directed mutagenesis. *Nature*, **313**, 364-369.

MISHINA, M., TAKAI, T., IMOTO, K., NODA, M., TAKAHASHI, T., NUMA, S., METHFESSEL, C AND SAKMANN, B. (1986). Molecular distinction between fetal and adult forms of muscle acetylcholine receptor. *Nature*, **321,** 406-410.

MIYAZAWA, A., FUJIYOSHI, F. AND UNWIN, N. (2003). Structure and gating mechanism of the acetylcholine receptor pore. *Nature*, **423**, 949-955.

MONOD, J., WYMAN, J. AND CHANGEUX J.-P. (1965). On the nature of allosteric transitions: a plausible model. *J. Mol. Biol.*, **12,** 88-118.

MOORE, H.P.H. AND RAFTERY, M.A. (1979). Ligand-induced interconversion of affinity states in membrane-bound acetylcholine receptor from *Torpedo californica*. Effects of sulfhydryl and disulfide reagents. *Biochem.*, **18,** 1907-1911.

MOORE, H.P.H. AND RAFTERY, M.A. (1980). Direct spectroscopic studies of cation translocation by *Torpedo* acetylcholine receptor on a time scale of physiological relevance. *Proc. Natl. Acad. Sci. USA*, **77**, 4509-4513.

NEWELL, J.G., DAVIES, M., BATESON, A.N. AND DUNN, S.M.J. (2000). Tyrosine 62 of the γ-aminobutyric acid type A receptor β2 subunit is an important determinant of high affinity agonist binding. *J. Biol. Chem.*, **275**, 14198-14204.

NEWELL, J.G. AND DUNN, S.M.J. (2002). Functional consequences of the loss of high affinity agonist binding to the γ-aminobutyric acid type A receptor. Implications for receptor desensitization. *J. Biol. Chem.*, **277**, 21423-21430.

NODA, M., TAKAHASHI, H., TANABE, T., TOYOSATO, M., FURUTANI, Y., HIROSE, T., ASAI, M., INAYAMA, S., MIYATA, T. AND NUMA, S. (1982). Primary structure of α-subunit precursor of *Torpedo californica* acetylcholine receptor deduced from cDNA sequence. *Nature,* **299,** 793-797.

NODA, M., TAKAHASHI, H., TANABE, T., TOYOSATO, M., KILYOTANI, S., FURUTANI, Y., HIROSE, T., TAKASHIMA, H., INAYAMA, S., MIYATA, T. AND NUMA, S. (1983). Structural homology of *Torpedo californica* acetylcholine receptor subunits. *Nature,* **302,** 528-532.

NORTH, R.A. (2002). Molecular physiology of P2X receptors. *Physiol. Rev.*, **82,** 1013-1067.

O'LEARY, M.E. AND WHITE, M.M. (1992). Mutational analysis of ligand-induced activation of the *Torpedo* acetylcholine receptor. *J. Biol. Chem.*, **267,** 8360-8365.

O'LEARY, M.E., FILATOV, G.N. AND WHITE, M.M. (1994). Characterization of *d*-tubocurarine binding site of *Torpedo* acetylcholine receptor. *Am. J. Physiol.*, **266,** C648-C653.

ORTELLS, M.O. AND LUNT, G.G. (1995). Evolutionary history of the ligand-gated ion-channel superfamily of receptors. *Trends Neurosci.*, **18**, 121-127.

OSAKA, H., SUGIYAMA, N. AND TAYLOR, P. (1998). Distinctions in agonist and antagonist specificity conferred by anionic residues of the nicotinic acetylcholine receptor. *J. Biol. Chem.*, **273,** 12758-12765.

PATERSON, D. AND NORDBERG, A. (2000). Neuronal nicotinic receptors in human brain. *Prog. Neurobiol.*, **61**, 75-111.

PAULSON, H.L. AND CLAUDIO, T. (1990). Temperature-sensitive expression of all-*Torpedo* and *Torpedo*-rat hybrid AChR in mammalian muscle cells. *J. Cell Biol.*, **110,** 1705-1717.

PEDERSON, S.E. AND COHEN, J.B. (1990). *d*-Tubocurarine binding sites are located at α-γ and α-δ subunit interfaces of the nicotinic acetylcholine receptor. *Proc. Nat. Acad. Sci., USA.*, **87**, 2785-2789.

PRINCE, R.J. AND SINE, S.M. (1996). Molecular dissection of subunit interfaces in the acetylcholine receptor. *J. Biol. Chem.*, **271,** 25770-25777.

QUAST, U., SCHIMERLIK, M., LEE, T., WITZERMANN, V., BLANCHARD, S. AND RAFTERY, M.A. (1978). Ligand-induced conformation change in *Torpedo californica* membrane bound acetylcholine receptor. *Biochem.*, **17,** 2405-2413.

QUICK, M. W. AND LESTER, H. A. (1994). Methods for expression of excitability proteins in *Xenopus* oocytes, in: *Methods in Neuroscience*, Academic Press, London, volume 19, pp. 261-279.

RAFTERY, M.A., HUNKAPILLER, M.W., STRADER, C.D. AND HOOD, L.E. (1980). Acetylcholine receptor: Complex of homologous subunits. *Science*, **208,** 1454-1456.

RAFTERY, M.A., DUNN, S.M.J., CONTI-TRONCONI, B.M., MIDDLEMAS, D.S. AND CRAWFIRD, R.D. (1983). The nicotinic acetylcholine receptor: subunit structure, functional binding sites, and ion transport properties. *Cold Spring Harb. Symp. Quant. Biol.*, **48**, 21-33.

REEVES, D.C. AND LUMMIS, S.C.R. (2002). The molecular basis of the structure and function of the 5-HT3 receptor: a model ligand-gated ion channel. *Mol. Memb. Biol.*, **19,** 11-26.

REITSTETTER, R., LUKAS, R.J. AND GRUENER, R. (1999). Dependence of nicotinic acetylcholine receptor recovery from desensitization on the duration of agonist exposure. *J. Pharmacol. Exp. Ther.*, **289,** 656-660.

REYNOLDS, J.A. AND KARLIN, A. (1978). Molecular weight in detergent solution of acetylcholine receptor from *Torpedo californica*. *Biochem.*, **17**, 2035-2038.

ROSS, A.F., GREEN, W.N., HARTMAN. D.S. AND CLAUDIO, T. (1991). Efficiency of acetylcholine receptor subunit assembly and its regulation by cAMP. *J. Cell Biol.*, **113,** 623-636.

SAEDI, M.S., CONROY, W.G. AND LINDSTROM, J. (1991). Assembly of *Torpedo* acetylcholine receptors in *Xenopus* oocytes. *J. Cell Biol.*, **112,** 1007-1015.

SCHIEBLER, W., BANDINI, G. AND HUCHO, F. (1980). Quaternary structure and reconstitution of acetylcholine receptor from *Torpedo californica*. *Neurochem. Int.*, **2**, 281-290.

SCHOFIELD, P.R., DARLISON, M.G., FUJITA, N., BURT, D.R., STEPHENSON, F.A., RODRIGUEZ, H., RHEE, L.M., RAMACHANDRAN, J., REALE, V., GLENCORSE, T.A., SEEBURG, P.H. AND BARNARD, E.A. (1987). Sequence and functional expression of the $GABA_A$ receptor shows a ligand-gated receptor superfamily. *Nature*, **328**, 221-227.

SIGEL, E., BAUR, R., KELLENBERGER, S. AND MALHERBE, P. (1992). Point mutations affecting antagonist affinity and agonist dependent gating of the $GABA_A$ receptor channels. *EMBO J.*, **11**, 2017-2023.

SINE, S.M. (1993). Molecular dissection of subunit interfaces in the acetylcholine receptor: Identification of residues that determine curare selectivity. *Proc. Natl. Acad. Sci. USA*, **90**, 9436-9440.

SINE, S.M. (1997). Identification of equivalent residues in the γ, δ, and ε subunits of the nicotinic receptor that contribute to α-bungarotoxin binding. *J. Biol. Chem.*, **272**, 23521-23527.

SINE, S.M. (2002). The nicotinic receptor ligand binding domain. *J. Neurobiol.*, **53**, 431-446.

SINE, S.M. AND CLAUDIO, T. (1991). γ- and δ-subunits regulate the affinity and the cooperativity of ligand binding to the acetylcholine receptor. *J. Biol. Chem.*, **266**, 19369-19377.

SINE, S.M., QUIRAM, P., PAPANIKOLAOU, F., KREIENKAMP, H-J. AND TAYLOR, P. (1994). Conserved tyrosines in the α subunit of the nicotinic

acetylcholine receptor stabilizes quaternary ammonium groups of agonists and curariform antagonists. *J. Biol. Chem.*, **269,** 8808-8816.

SIXMA, T.K. AND SMIT, A.B. (2003). Acetylcholine Binding protein (AChBP): A secreted glial protein that provides a high-resolution model for the extracellular domain of pentameric ligand-gated ion channels. *Ann. Rev. Biomol. Struct.*, **32,** 311-334.

SMIT, A.B., SYED, N.I., SCHAAP, D., VAN MINNEN, J., KLUMPERMAN, J., KITS, K.S., LODDER, H., VAN DER SCHORS, R.C., VAN ELK, R., SORGEDRAGER, B., BREJC, K., SIXMA, T.K. AND GERAERTS, W.P. (2001). A glial-derived acetylcholine-binding protein that modulates synaptic transmission. *Nature*, **411,** 261-268.

SOBEL, A., WEBER, M., AND CHANGEUX, J.-P. (1977). Large scale purification of the acetylcholine-receptor protein in its membrane-bound and detergent-extracted forms from *Torpedo marmorata* electric organ. *Eur. J. Biochem.*, **80,** 215-224.

SPIER, A.D. AND LUMMIS, S.C.R. (2000). The role of tryptophan residues in the 5-hydroxytryptamine$_3$ receptor ligand binding domain. *J. Biol. Chem.*, **275,** 5620-5625.

SUGIYAMA, N., BOYD, A.E. AND TAYLOR, P. (1996). Anionic residue in the α-subunit of the nicotinic acetylcholine receptor contributing to subunit assembly and ligand binding. *J. Biol. Chem.*, **271,** 26575-26581.

SULLIVAN, D.A. AND COHEN, J.B. (2000). Mapping the agonist binding site of the nicotinic acetylcholine receptor. Orientation requirements for activation by covalent agonist. *J. Biol. Chem.*, **275,** 12651-12660.

SULLIVAN, D.A., CHIARA, D.C. AND COHEN, J.B. (2002). Mapping the agonist binding site of the nicotinic acetylcholine receptor by cysteine scanning mutagenesis: Antagonist footprint and secondary structure prediction. *Mol. Pharmacol.*, **61,** 463-472.

SUMIKAWA, K. AND MILEDI, R. (1989). Assembly and N-glycosylation of all ACh receptor subunits are required for their efficient insertion into plasma membranes. *Mol. Brain Res.*, **5,** 183-192.

TOMASELLI, G.F., McLAUGHLIN, J.T., JURMAN, M.E., HAWROT, E. AND YELLEN, G. (1991). Mutations affecting agonist sensitivity of the nicotinic acetylcholine receptor. *Biophy. J.*, **60,** 721-727.

UNWIN, N. (1993). Nicotinic acetylcholine receptor at 9Å resolution. *J. Mol. Biol.*, **229,** 1101-1124.

UNWIN, N. (1995). Acetylcholine receptor channel imaged in the open state. *Nature,* **373,** 37-43.

UNWIN, N. (1998). The nicotinic acetylcholine receptor of the *Torpedo* electric ray. *J. Struc. Biol.*, **121,** 181-190.

UNWIN, N., MIYAZAWA, A. AND FUJIYOSHI, Y. (2002). Activation of the nicotinic acetylcholine receptor involves a switch in conformation of the α subunits. *J. Mol. Biol.*, **319,** 1165-1176.

YAN, D., SCHULTE, M.K., BLOOM, K.E. AND WHITE, M.M. (1999). Structural features of the ligand-binding domain of the serotonin 5HT3 receptor. *J. Biol. Chem.*, **274,** 5537-5541.

YU, X-M. AND HALL, Z.W. (1991). Extracellular domains mediating ε subunit interactions of muscle acetylcholine receptor. *Nature,* **352,** 64-67.

WANAMAKER, C.P., CHRISTIANSON, J.C. AND GREEN, W.N. (2003). Regulation of nicotinic acetylcholine receptor assembly. *Ann. N.Y. Acad. Sci.*, **998,** 66-80.

WANG, Z-Z., HARDY, S.F. AND HALL, Z.W. (1996). Assembly of the nicotinic acetylcholine receptor. *J. Biol. Chem.*, **271,** 27575-27584.

WEBER, M., DAVID-PFEUTY, T. AND CHANGEUX, J.-P. (1975). Regulation of binding properties of the nicotinic receptor protein by cholinergic ligands in membrane fragments from *Torpedo marmorata*. *Proc. Nat. Acad. Sci. USA,* **72,** 3433-3447.

WISE, D.S., WALL, J. AND KARLIN, A. (1981). Relative locations of the beta and delta chains of the acetylcholine receptor determined by electron microscopy of the isolated trimer. *J. Biol. Chem.*, **256,** 12624-12627.

WITZEMANN, V., BARG, B., NISHIKAWA, Y., SAKMANN, B. AND NUMA, S. (1987). Differential regulation of muscle acetylcholine receptor gamma- and epsilon-subunit mRNAs. *FEBS Letts.*, **223,** 104-112.

WOLLMUTH, L.P. AND SOBOLEVSKY, A.I. (2004). Structure and gating of the glutamate receptor in ion channel. *Trends Neurosci.*, **27,** 321-328.

XIE, Y. AND COHEN, J.B. (2001). Contributions of *Torpedo* nicotinic acetylcholine receptor γTrp-55 and δTrp-57 to agonist and competitive antagonist function. *J. Biol. Chem.*, **276,** 2417-2426.

ZHONG, W., GALLIVAN, J.P., ZHANG, Y., LI, L., LESTER, H.A. AND DOUGHERTY, D.A. (1998). From *ab initio* quantum mechanics to molecular neurobiology: a cation-pi binding site in the nicotinic receptor. *Proc. Natl. Acad. Sci. USA,* **95,** 12088-12093.

CHAPTER 2[1]

The Role of Arginine 55 in the Alpha Subunit of *Torpedo* Nicotinic Acetylcholine Receptor in Channel Function

[1] *A version of this chapter is in preparation for submission.* Kapur, A., Dryden, W.F., Davies, M. and Dunn, S.M.J. (2004). Ankur Kapur carried out all experimental work.

INTRODUCTION

The muscle-type nicotinic acetylcholine receptor (nAChR) is a pentameric transmembrane protein complex composed of four structurally related subunits that exist in a stoichiometry of $(\alpha 1)_2\beta 1\gamma\delta$ arranged pseudosymmetrically around a central cation-selective ion-channel. This receptor is responsible for mediating the fast excitatory effects of the endogenous neurotransmitter, acetylcholine. (Raftery *et al.*, 1980; Dunn, 1993). Ligand binding sites in the nAChR are suggested to be located at the interfaces of subunits (reviewed by Grutter and Changeux, 2001). Equilibrium radioligand binding studies have demonstrated that, under these conditions, the nAChR carries two high affinity binding sites for both agonists and competitive antagonists (reviewed by Dunn, 1993). It has been suggested that these binding sites for the competitive antagonist, *d*-tubocurarine (dTC), are non-equivalent as a result of being formed at non-identical interfaces i.e., those between the α-γ and the α-δ subunits (Blount and Merlie, 1989, Pederson and Cohen, 1990). Biochemical and mutational studies have identified amino acid residues in the α-subunit along with residues from the neighboring γ- and δ- subunit that contribute to the binding of agonists and competitive antagonists (see reviews by Corringer *et al.*, 2000; Arias, 2000; Karlin, 2002). Evidence from these studies led to the suggestion of a "multiple loop model" for the ligand binding sites in which a cluster of electron-rich or aromatic amino acids from discrete non-contiguous regions of the α-subunits (designated as loop A-C, forming the 'primary component'), together with residues from the neighboring γ and δ subunits (loop D-F, 'secondary component') form the high affinity binding pockets.

Insight into the structural details of the nAChR has been provided by electron microscopy studies of the receptor (Unwin, 1995; Miyazawa *et al.*, 2003), and by X-ray crystallographic studies of a related protein, the acetylcholine binding protein (AChBP) (Brejc *et al.*, 2001). The crystal structure of the AChBP, which is secreted by the glial cells of snail, *Lymnaea stagnalis*, shows that it is a truncated homologue of the extracellular amino terminal domains of the nAChR. Inspection of its structure has reinforced earlier findings from biochemical and mutational studies that the residues involved in forming the binding sites occur at subunit interfaces formed by amino acids that are arranged in "loop" like structures.

The processes initiated by agonist binding to the receptor and resulting in the opening of the ion channel, i.e. the fundamental process of receptor activation, has been extensively studied, but remains poorly understood. The approximately thousand-fold difference in agonist concentration required to activate the nAChR (EC_{50} for ACh-induced receptor activation ~10-100 μM) and the affinity for [^{3}H]ACh measured in equilibrium binding assays (K_d ~ 10 nM) clearly reflects different receptor states (Raftery *et al.*, 1983). This presents a quantitative predicament on the role of high affinity binding sites measured under equilibrium conditions in ion channel activation. Most models assume that agonist occupancy of the two identified binding sites leads to both ion channel activation and desensitization.

However, an alternative model that was based originally on the sequence homology of the subunits proposed that the receptor carries additional low affinity sites whose occupancy may lead to channel activation. Experimental evidence for the existence of additional agonist binding sites on the *Torpedo* nAChR came from studying the

properties of agonist-induced fluorescent changes of receptors covalently labeled with an extrinsic fluorescent probe, 4-[[(iodoacetoxy)ethyl]methylamino]-7-nitro-2,1,3-benzoxaidazole (IANBD) (Dunn and Raftery, 1982a,b; Dunn *et al.*, 1983). As yet, the location of these putative low affinity site(s) that are distinct from the high affinity binding sites remains elusive. The presence of multiple ligand binding sites (Dunn and Raftery, 1993) raises the question of their role(s) in ion-channel activation and desensitization. The existence of homopentameric receptor complexes (e.g. AChBP, α7 neuronal acetylcholine receptor and 5-HT_3 receptor) and sequence homology among all LGIC subunits also raises the possibility of as many as five ligand binding sites occurring at each of the homologous subunit interfaces in the pentamer (see Fig. 2-2).

Residues from loop D on the non-α-subunits of the *Torpedo* nAChR i.e. the secondary component on γ- and δ-subunit were identified by photoaffinity labeling with [^{3}H]nicotine and [^{3}H]dTC as Trp55 and Trp57 respectively (Chiara and Cohen, 1997; Chiara *et al.*, 1998; Pederson and Cohen, 1990; Xie and Cohen, 2001). In contrast, residues from loop D of the α-subunits of the muscle nAChR have not been yet implicated in either ligand binding or channel activation. Loop D of the α-subunits nAChR from various species presents a unique amino acid motif, as they all have a conserved arginine (Arg55) at the equivalent position to γW55 and δW57. The presence of a charged residue in this position is unique to the peripheral nAChR α-subunits, since aromatic residues are highly conserved in all other subunits in the receptor family (see Fig. 2-1). In addition, loop D of the α-subunits is located at the other end of the α-subunit (so-called minus (-) interface, see Fig. 2-2). Based on the above considerations and sequence homology of subunits, the aim of this study was to investigate whether

amino acids in loop D, in particular αR55, have a role to play in modulating receptor properties. We have made multiple substitutions of this α-subunit residue and co-expressed each of these mutated subunits with wild type β, γ and δ subunits in *Xenopus* oocytes. The interactions of agonists and antagonists with these receptors were examined using both two-electrode voltage clamp techniques and radioligand binding assays. Using this approach, we show that this residue, Arg55 in a hitherto unexplored domain of the α-subunits plays a role in modulating agonist sensitivity. This raises the possibility that it forms a complementary component of ligand interaction at the α-subunits (see Fig. 2-12).

We further speculated that αArg55 may interact with other residue(s) from loops A-C of the neighboring γ-subunit (and possibly the β-subunit). A potential candidate was Glu93 from loop A of the γ-subunit (homologous to αTyr93), which is located at the opposing interface (Fig. 2-13). Molecular modeling based on the structure of the AChBP suggested that these two residues are in reasonably close proximity (see Fig. 2-14A). Furthermore, an arginine and glutamic acid is present at equivalent position (to α55 and γ93 respectively) in all species of muscle α- and γ-subunits nAChR respectively (see Fig. 2-14B). The opposite charges of these conserved residues (Arg55 and Glu93) suggested that their interaction (ion-pairing) might be important for receptor structure and/or channel function. To investigate this possibility, we mutated Glu93 of the γ-subunit to an arginine (γE93R) and show that this residue also significantly affects ACh sensitivity. We further investigated the possibility of a charge interaction between αArg55 and γGlu93, by studying the effect of double mutant (αR55F-γE93R) on

channel function. Our results demonstrate that interactions between amino acids of adjacent subunit (γ-α) may be important in channel function.

MATERIALS AND METHODS

Materials

ACh, carbamylcholine, α-BgTx and dTC were obtained from Sigma-RBA (Natick, MA). ^{125}I-α-BgTx (2000Ci/mmol) was obtained from Amersham Life Science (Arlington Heights, IL.). Restriction enzymes and cRNA transcript preparation materials were purchased from Invitrogen (Burlington, ON), Promega (Madison, WI) or from New England Biolabs (Pickering, ON). *Pfu* Turbo DNA polymerase for mutagenesis experiments was purchased from Stratagene (La Jolla, CA). All other chemicals were obtained from Sigma or other standard sources.

The α-, β- (in the SP64 plasmid) and δ-subunit (in the SP65 plasmid) cDNA clones of the *Torpedo* nAChR were generous gifts from Dr. Henry A. Lester (California Institute of Technology, CA). The γ-subunit cDNA (in the SP64-based plasmid, pMXT) was a gift from Dr. Jonathan B. Cohen (Harvard Medical School, Boston).

Site-directed Mutagenesis

The α-subunit mutants (R55F, R55W, R55K and R55E) were constructed using Stratagene's QuikChange site-directed mutagenesis protocol. Synthetic oligonucleotide mutagenic primers were typically 23-34 base pairs long (with 10-15 base pairs on either side of the mismatch region) and incorporated a silent mutation designed to allow for the screening of mutants by removing an endogenous *Bsu*361 restriction site in the α-subunit. A similar approach was undertaken to engineer the mutation of a loop A residue in the γ-subunit, Glu93 (γE93R). The following oligonucleotides (for the sense strand) were designed for mutagenesis:

αR55F, 5' GAAACAAATGTGTTTCTAAGGCAGTGG 3'

αR55W, 5' GTGGAAACAAATGTG**TGG**CTAAGGCAGCAATGG 3'

αR55K, 5' TGTGGAAACAAATGTG**AAG**CTAAGGCAGCAATGG 3'

αR55E, 5' GTGGAAACAAATGTG**GAG**CTAAGGCAGCAATGG 3'

αR55F-R57F, 5' TGTG**TTT**CTA**TTC**CAGCAATGGA 3'

γE93R, 5' GATGTTGTCCTT**CGG**AACAACAACGTTGAT 3'

The annealing temperature for the oligonucleotides in PCR was found to be optimal between 53 and 55°C. Restriction endonuclease digestion and DNA sequencing subsequently verified the presence of the mutation.

***In Vitro* Transcription**

The plasmid cDNAs were linearized by digestion with either *EcoR*I (for the α-subunit), *Fsp*I (for the wild-type β-subunit) or *Xba*I (for wild-type γ- and δ-subunit). *In vitro* cRNA transcription was performed using the methods described by Goldin and Sumikawa (1992). Briefly, the linearized cDNA (5μg) was incubated with 10 mM dithiothreitol, 0.5 mM NTP mix (Invitrogen), 60U of RNase inhibitor (RNaseOut, Promega), 0.5 mM of 7-methyldiguanoise triphosphate (RNA capping analogue, NEB) and 45U of SP6 RNA polymerase (Promega) in transcription buffer at 37 °C for 1 hour. An additional 45U of SP6 RNA polymerase was then added and the reaction was allowed to continue for an additional 1 hour. This was followed by addition of 5U of RNase-free DNase. The reaction mixture was then incubated at 37°C for 15 minutes. The RNA transcripts were extracted using 25:24:1 (v/v) phenol/chloroform/isoamyl alcohol, precipitated with 3M sodium acetate, and washed with 70% ethanol. Finally, the RNA pellets were resuspended in DEPC-treated water at a concentration of 1μg/μl.

Expression in *Xenopus* oocytes and Electrophysiology

Isolated, follicle-free oocytes were microinjected with 50 ng of total subunit cRNAs in a ratio of 2α:1β:1γ:1δ. Oocytes were maintained in ND96 buffer containing 96 mM NaCl, 2 mM KCl, 1.8 mM $CaCl_2$, 1 mM $MgCl_2$, 5 mM HEPES (pH7.6) and supplemented with 50 μg/ml gentamicin at 14 °C for at least 48 hours prior to recording. Currents elicited by bath application of ACh or carbamylcholine were measured using a GeneClamp500 amplifier (Axon Instruments, Foster City, CA) using standard two-electrode voltage clamp at a holding potential of –60mV. Electrodes were filled with 3M KCl and those with resistances of 0.5-3.0 MΩ were used. The recording chamber was perfused continuously by gravity (at a flow rate of ~ 5ml/min) with low calcium ND96 buffer containing 96 mM NaCl, 2 mM KCl, 0.1 mM $CaCl_2$, 1 mM $MgCl_2$, 5 mM HEPES supplemented with 1 μM atropine (pH7.6). Atropine was included in the perfusion buffer to block any endogenous muscarinic acetylcholine receptors present in the oocytes (Barnard *et al.*, 1982). Modified ND96 perfusion buffer with low Ca^{2+} was used to reduce receptor desensitization (Miledi, 1980). The responses of the receptors to agonists (in the absence or presence of antagonist) were measured by drug solution application via the perfusion system for 15-20 seconds with a 15-min wash out period between applications to ensure full recovery from desensitization. For measuring the apparent affinity (K_I) of the antagonist, dTC, oocytes were preincubated with various concentrations of dTC by perfusing the oocytes for 2-min with dTC in low Ca^{2+} ND96 before application of solution containing ACh (at concentration eliciting 50% of the maximum response, EC_{50}) and including the same concentration of dTC as used for preincubation.

Radioligand Binding of [^{125}I]α-BgTx to Intact Oocytes

Binding assays were performed on the same oocyte used in voltage clamp electrophysiology experiments. To measure the binding to nAChR expressed on the oocyte surface (fmol), oocytes were incubated with 5 nM [^{125}I]α-BgTx in a final volume of 100 µl of low Ca^{2+} ND96 buffer (containing 5 mg/ml bovine serum albumin) for 2 hours (Sullivan and Cohen, 2000; Tamamizu *et al.*, 2000). Excess unbound toxin was removed by washing the oocytes 3 times with 1ml of ice-cold low Ca^{2+} ND96 buffer. Non-specific binding was estimated by incubating uninjected oocytes with [^{125}I]α-BgTx. Non-specific binding determined in oocytes expressing wild type or mutant receptor in presence of excess cold ACh was comparable to that estimated using uninjected oocytes (data not shown). Bound [^{125}I]αBgTx was measured by γ-counting (Gamm8000, Beckman). Using these data, the maximum currents (I_{max}) measured for wild type and mutant receptors were normalized to the concentration of binding sites in terms of nA/fmol. For competition curves, oocytes were incubated for 40-min with various concentrations of ACh in a 96-well plate prior to the addition of 2.5 nM [^{125}I]α-BgTx. After 40-min, [^{125}I]α-BgTx binding was stopped by the addition of 1 µM unlabeled α-BgTx. In the absence of the competing ligand, ACh, [^{125}I]α-BgTx binding was ~ 30% of the available α-BgTx-binding sites (data not shown). Non-specific binding was determined in the presence of 100 mM ACh.

Data and Statistical Analysis

Competition and concentration-effect curves for both electrophysiological and radioligand binding experiments were analyzed by nonlinear regression techniques using

GraphPad Prism 3.0 software (GraphPad, San Diego, CA). Data from individual oocytes were normalized to the I_{max} value obtained for that oocyte.

For receptor activation, concentration-effect curves for agonist activation were analyzed using the following equation:

$$I = I_{max} * [L]^n / (EC_{50} + [L])^n$$

where I is the measured agonist-evoked current, [L] is the agonist concentration, EC_{50} is the agonist concentration that evokes half the maximal current (I_{max}) and n is the Hill coefficient. In each experiment, the current (I) is normalized to the I_{max} and the normalized data are presented as % response to plot concentration-effect curves.

The IC_{50} was determined from competition-inhibition curves by fitting to the following equation:

$$f = 100/[1+([X]/[IC_{50}])^n]$$

where f is the fractional (%) response remaining in the presence of inhibitor at concentration [X], IC_{50} is the inhibitor concentration that reduced the amplitude of ACh-evoked current by 50% and n is the Hill coefficient. ACh inhibition of initial rate of $[^{125}I]\alpha$-BgTx binding was also fit by the above equation.

The K_I (apparent) value was calculated using the Cheng-Prusoff equation (Cheng and Prusoff, 1973):

$$K_I = IC_{50}/[1 + [L]/(EC_{50})]$$

where [L] is the ACh concentration used in the experiment and EC_{50} is the ACh concentration that evokes half the maximal current.

Statistical analysis was performed using one-way analysis of variance (ANOVA) followed by Dunnett's post-test to determine the level of significance.

RESULTS

Functional Effects of αR55 Mutations on the Binding of Agonist and Antagonist–

Wild type or mutant receptors expressed in *Xenopus* oocytes were studied using two-electrode voltage clamp techniques. Figures 2-4 and 2-5 show the concentration-effect curves for ACh and carbamylcholine respectively. The wild-type nAChR receptor has an EC_{50} value for ACh-induced activation of ~ 24 μM with an estimated Hill coefficient of 1.6. The substitution of αArg55 with glutamic acid (αR55E) or lysine (αR55K) results in a subtle shift but statistically insignificant in the EC_{50} values for ACh activation to 29 and 47 μM, respectively without having a significant effect on the cooperativity of receptor activation (Hill slope >1.0). In contrast, the αR55F and αR55W mutations caused greater shifts in the EC_{50} for ACh activation to 112 μM and 151 μM respectively. In addition, the Hill coefficients for ACh induced activation for these latter mutant receptors were significantly reduced in comparison to the wild type nAChR (Table 2-1). Since the Hill coefficient is a function of both ligand binding and channel gating, a reduction of n_H is often difficult to interpret (Amin and Weiss, 1993). However, the reduced Hill coefficients for the αR55F and αR55W mutant receptors suggests that cooperative interactions amongst agonist binding sites are reduced by the mutations. The carbamylcholine (CCh) activation constants on the αR55F and αR55W mutant receptors also showed a similar rightward trend (~3-fold) albeit to a lesser extent as compared to ACh (Fig. 2-5, Table 2-1).

The effects of the partial agonist, phenyltrimethylammonium (PTMA, Fig. 2-3C) on activation of wild type and mutant receptors were also investigated. The wild type

nAChR was activated by PTMA with an EC_{50} of approximately 57 μM and a Hill coefficient of 2 (Fig. 2-6, Table 2-1). In contrast, PTMA failed to activate the αR55F and αR55W mutant receptors even at concentrations up to 10 mM. Instead, PTMA acted as a competitive antagonist at these mutant receptors (Fig. 2-7 A,B). Co-application of PTMA and ACh to the αR55F and αR55W receptors resulted in a PTMA–mediated concentration dependent inhibition of ACh-evoked currents with an IC_{50} value of 206 μM and 220 μM respectively. Furthermore, PTMA-induced channel activation (in wild type nAChR) and inhibition (in mutant receptors) occurs over a comparable concentration range (see Fig. 2-7A,B). The IC_{50} value of PTMA inhibition of ACh-evoked currents was not significantly different from the EC_{50} values for ACh-induced channel activation on the mutant receptors (Table 2-2).

Desensitization Properties of Wild Type and Mutant nAChR –

Desensitization of nAChRs was determined by analyzing the reduction in the amplitude of current evoked by ACh application responses in oocytes expressing wild type or the mutant receptor (Fig. 2-8). The half-life of desensitization was determined as described by Lee *et al.*, (1994) i.e. by measuring the time taken for the peak amplitude evoked by ACh to decline to half this value in the continuous presence of ACh. The desensitization rates of ACh-evoked current were concentration dependent. At high ACh concentrations (EC_{50} and EC_{100}), the desensitization half-life of the wild type and mutant receptors were similar (data not shown). However, at a concentration of ACh eliciting ~ 10% of the maximum current amplitude (EC_{10}), the average times taken for the current to decline to half of its peak amplitude for the αR55F and αR55W mutants ($t_{1/2}$ ~ 34 ± 10 s, n=3 and 37 ± 9 s, n=3 respectively) were approximately three-fold faster

than the time seen with wild-type nAChR ($t_{1/2}$ ~ 95 ± 5 s, n=5). The αR55K desensitization time-course did not differ significantly from that of the wild type nAChR.

Sensitivity of αR55 Mutant nAChR to Competitive Antagonist–

We also examined the ability of the competitive antagonist, dTC to inhibit ACh-evoked currents in wild type and mutant receptors (Fig. 2-10). For wild type nAChR, pre-perfusion with dTC produced a concentration dependent inhibition of ACh-evoked currents characterized by an apparent K_I of ~ 42 nM. dTC also inhibited ACh evoked currents in the receptors carrying the αR55K, αR55W and αR55F mutations with apparent K_I's of ~ 23 nM, 34 nM and 52 nM respectively (see Table 2-4). In these experiments, we observed that low concentrations of dTC (1-3 nM) potentiated ACh-evoked currents (by up to 25%) in the wild type and mutant receptors (see Fig. 2-10), although dTC alone did not elicit detectable whole cell currents. These findings are consistent with earlier reports, which have suggested that at low agonist concentrations, dTC acts as a weak agonist at the fetal nAChR (Steinbach and Chen, 1995). The simultaneous binding of one agonist molecule and one dTC molecule has been proposed to elicit channel opening. Our results indicate that the mutations have no effect on the ability of dTC to bind to the wild type or mutant receptors. Furthermore, dTC was able to abolish ACh-evoked currents completely at sub-micromolar concentrations.

Expression Levels and Maximum Amplitude of Wild-Type and Mutant nAChR–

Fig. 2-9 shows the density of binding sites on the wild type and mutant receptors as determined by [^{125}I]α-BgTx binding and compared to the maximum current, evoked by saturating concentrations of ACh in functional studies. Injection of 50 ng of wild type

subunit cRNAs resulted in a robust expression level of [^{125}I]α-BgTx binding sites (approximately 3.1 fmol/oocyte). All of the αR55 mutations were well-tolerated and showed high receptor expression when co-expressed with wild type β-, γ- and δ-subunits. The values of maximum ACh-evoked current normalized to the number of [^{125}I]α-BgTx binding sites for each mutant receptor are summarized in Table 2-3. The peak currents seen for the αR55F and αR55W mutants were considerably lower (~ 3- and 5-fold reduction respectively) than the wild type receptors, even though their expression levels were comparable to wild type. These results demonstrate that the αR55F and αR55W mutants significantly alters the magnitude of activation of these receptors by ACh and that the decrease in observed conductance was not due to altered receptor expression.

Influence of αR55F and αR55W Mutant receptors on the Binding of Acetylcholine–

The binding properties of ACh were investigated in intact *Xenopus* oocytes expressing wild type and mutant nAChR. The affinity of the mutant receptors for ACh was characterized by its inhibition of initial rate of [^{125}I]α-BgTx binding to *Torpedo* nAChR expressed on the surface of oocytes (Fig. 2-11, Table 2-4). ACh inhibited the initial rate of [^{125}I]α-BgTx binding to the wild-type nAChR in a concentration-dependent manner with an IC_{50} of 544 nM (n_H ~ -0.8). The IC_{50} and n_H of the αR55F and αR55W mutants was determined to be 454 nM (n_H ~ -1.0) and 313 (n_H ~ -0.9) respectively, and did not differ from that of the WT nAChR. Despite the reduction in potency of ACh at the mutant receptors seen in the functional characterization studies

(Fig. 2-4), the equilibrium (high affinity) binding of ACh to these receptors appears to be unaltered.

Functional Effects of γE93R Mutation on the Sensitivity of Agonist and Antagonist–

Oocytes expressing the γE93R mutation showed a leftward shift in the concentration-effect curve for ACh-elicited currents (Fig. 2-15A). The EC_{50} value for ACh activation of the γE93R mutant receptor was reduced to 3 μM (Hill coefficient of 1.4) compared with an EC_{50} of 24 μM observed for the wild type nAChR, i.e. 8-fold increase in ACh sensitivity (see Table 2-5). In contrast, the apparent affinity of the competitive antagonist, dTC (determined by inhibition of ACh-evoked currents in oocytes), at the γE93R mutant receptor was unaltered as compared to the oocytes expressing wild type nAChR (K_I ~ 55 nM and 42 nM respectively, see Fig. 2-16).

In order to investigate whether the αR55F and γE93R mutations had an additive effect, we investigated the receptors carrying the double mutation, γE93R-αR55F. This double mutant receptor had an EC_{50} for channel activation by ACh of ~ 13 μM (Fig. 2-15B), which is similar to that of the wild type nAChR. Furthermore, the Hill coefficient for ACh induced activation on this double mutant (n_H ~ 1.3) was comparable to that observed on wild type receptors (n_H ~ 1.6), which was in contrast to the significant reduction observed in the αR55F single mutant (n_H ~ 0.8, see Table 2-5).

DISCUSSION

It is widely accepted that the nAChR carries two high affinity binding sites located at the interfaces between α-γ and α-δ subunits (Corringer, 2000). The aim of the present study was to investigate the possibility that additional agonist binding sites may be present at subunit interfaces that are distinct from these high affinity binding interfaces. We investigated the role of Arg55 in loop D in receptor function. This residue lies in a putative binding domain that is present at the minus (-) side of the α-subunit (see Fig. 2-2, 2-12). Our findings suggest that αArg55 plays a modest but significant role in modulating ACh-mediated channel activation.

Amino acid sequence alignments of loop D reveals a lack of conservation of Arg55 of the nAChR α-subunit in comparison with the aromatic residues occurring in homologous positions of other subunits of the LGIC family e.g. γTrp55 and δTrp57 (in the complementary domain of *Torpedo* nAChR ligand binding site), the α1Phe64, β2Tyr62 and γ2Phe57 of the $GABA_A$ receptor, Trp89 of the $5HT_{3A}$ receptor and Trp54 of the α7 neuronal nicotinic receptor (see Fig. 2-1). Previously, it was shown that the EC_{50} for GABA activation of the $GABA_A$ receptor is altered significantly by the α1Phe64 mutation (F64L) (Sigel *et al.*, 1992). Mutations of γ2Phe77 of the $GABA_A$ receptor significantly altered ligand affinity at the benzodiazepine site and it was suggested that this residue may be part of the benzodiazepine-binding domain (Buhr *et al.*, 1997). The homologue to αR55 in the $5HT_{3A}$ receptor, Trp89 has been demonstrated to contribute to both dTC and granisetron binding (Yan *et al.*, 1999). Similarly, Trp54 in the neuronal nicotinic α7 receptor has been shown to contribute to

the binding of agonists (Corringer *et al.*, 1995). The nAChR γW55 was shown to modulate the apparent affinity of dTC and ACh (O'Leary *et al.*, 1994; Xie and Cohen, 2001). Single-channel kinetic analysis suggested that the loop D residue, δW57 of nAChR effects channel gating without altering the agonist binding (Akk, 2002). These studies demonstrate that residues lying in the homologous position to αR55 from subunits across the LGIC family play a role in modulating agonist/antagonist sensitivity.

The α-subunit-specific conserved arginine residue, R55, is not essential for subunit assembly or subunit-subunit interaction as our results demonstrate that mutations at this position did not have a detrimental effect on the expression of functional receptors. The conservative substitution, αR55K displayed a small but insignificant ~ 2-fold rightward shift in the concentration-dependent activation elicited by ACh. Surprisingly, the charge reversal mutation, αR55E displayed almost no difference in its ACh sensitivity from the wild type nAChR. However, it has been suggested that the positive charge surrounding the quaternary ammonium ion of agonists such as ACh is diffused and not localized (Dougherty and Stauffer, 1990). Hence, there exists the possibility that the charge on ACh interacts with more than one residue in the receptor's binding site. The amino acid sequence of the α-subunit revealed the presence of an additional Arg residue (Arg57) downstream to αArg55 (see Fig. 2-1). The residue at homologous position to αR57 in the 5-HT_{3A} receptors, (Trp91) was shown to be important for the binding of the agonist, serotonin (Yan *et al.*, 1999). In addition, the homologue of αR57 in the α7 neuronal nicotinic receptors, (Gln56) has been demonstrated to contribute to the binding of both ACh and nicotine (Corringer *et al.*, 1995). With this in mind, we also introduced a mutation of αArg57 (αR57F, data not shown). Our results on the αR57F-αR55F double

mutation revealed a reduction in receptor expression to levels that were barely above background. The very small ACh-evoked currents in functional studies precluded its further characterization. These preliminary results suggest that αR57 is important for either receptor assembly or expression.

The αR55F and αR55W mutations resulted in a modest but significant decrease in the sensitivity to ACh (by ~ 5- and 6-fold respectively). In contrast, a single charge reversal in the α1 subunit (D57K) (preceding loop D) of the $GABA_A$ receptor produced a <2-fold reduction in GABA sensitivity on its own (Kash *et al.*, 2003). However, when combined with an additional mutation in the extracellular linker domain between transmembrane 2-3 (K279D), it was shown to modulate gating. The larger rightward shift in ACh EC_{50} for receptor activation observed with the Trp and Phe substitution of the Arg55 residue could also be a consequence of the bulkiness of these aromatic residues causing greater stearic hindrance in agonist binding or the conformational transition of the agonist-receptor complex.

The partial agonist, PTMA failed to activate the αR55F and αR55W mutant receptors. However, PTMA is a poor agonist on the wild type nAChR (Fig. 2-6A) and its lack of functional response in the mutant receptors could be a consequence of a conductance that was reduced to undetectable levels or a greatly reduced sensitivity of the receptor towards the agonist. The lack of any response to PTMA on the mutant receptors was exploited to investigate whether this was a consequence of a change in binding or conductance. PTMA acted as an antagonist at the αR55F and αR55W mutant receptors over the same concentration range for that it acted as an agonist on the wild type nAChR (Fig. 2-7A,B, Table 2-2) indicative of unaltered affinity of PTMA on

the mutant receptors. Thus the major effect of mutation was a change in efficacy for PTMA. A similar strategy was employed by O'Leary and White (1992) to investigate the reduced efficacy of αY190F and αY198F mutants for ACh to suggest that these mutants alter channel activation at a stage later to agonist binding. However, it should be noted that the difference between a partial agonist and an antagonist is a fine one and it is very difficult to discriminate between a binding and a gating effect.

A reduction in the maximum ACh-evoked peak conductances observed in the αR55F and αR55W mutants could have been due to either a change in receptor function or to a relative decrease in receptor number compared to wild type nAChR. ACh-evoked maximum currents normalized to oocyte expression levels (nA/fmol) displayed a reduction in the αR55F and αR55W mutant receptors in comparison with wild type nAChR.

There is some evidence in the literature that this region may form a binding site. A synthetic peptide equivalent to α55-74 of *Torpedo* nAChR was shown to be able to bind α-BgTx. The αR55G substitution in the synthetic peptide inhibited the α-toxin binding (Wahlsten *et al.*, 1993). These results should be interpreted with caution since a synthetic peptide does not have the same tertiary or quaternary arrangement as seen in the native receptor and hence cannot be directly compared to our studies of recombinant intact receptors. Our results are, however, consistent with previous reports that mutations in the α7 neuronal nicotinic receptor of the Trp54 residue (homologous position to αR55) resulted in a reduction of ACh potency but did not disrupt α-BgTx binding (Corringer *et al.*, 1995). These results suggest that αR55 (or its homologue in α7 neuronal receptors) modulates to some extent ACh sensitivity but is not involved in

binding of the snake toxin, α-BgTx. We also observed a significant reduction in the Hill slope of the activation curves in the mutant receptors. The Hill slope can be reduced if the receptor loses the ability to undergo a conformational change upon agonist binding or if the cooperativity of agonist binding between the two non-equivalent binding sites is lost (Colquhoun, 1998). As noted in Results, the interpretation of Hill slope data is problematic.

Although the αR55F and αR55W mutations resulted in a significant decrease in ACh EC_{50} for channel activation, the apparent affinity of the competitive antagonist, dTC seen in functional studies on these mutants was unaltered as compared to wild-type receptors. By classical definition, a competitive antagonist binds to some or all the agonist binding sites, and therefore a change in the apparent affinity of the antagonist might be a consequence of an alteration at the agonist binding site. Based on the fact that antagonist does not induce a conformational change in the receptor, it would be tempting to speculate that the selective reduction in sensitivity of agonists observed on these mutant receptors is a likely consequence of reduction in the coupling between agonist binding and receptor activation (channel opening). A caveat must be placed on drawing conclusions from mutagenesis experiments since the mutations created may have either affected agonist binding, or the coupling of agonist binding to channel gating. Moreover, it is possible that the αR55 residue may not be "directly" involved in the binding of agonist/antagonist and the mutation may be allosterically coupled to the agonist binding site resulting in the altered activation and maximum conductance properties. Furthermore, the EC_{50} is a macroscopic constant that is a combination of agonist association and dissociation, ion-channel gating and closing and it is difficult to

interpret the contributing aspect of altered activation constant. Moreover, ligand binding and channel gating are not independent processes (Colquhoun, 1998).

Our analysis of equilibrium binding of ACh (measured by inhibiting rate of initial [^{125}I]α-BgTx binding) to the αR55 mutant receptors establishes that the equilibrium ACh affinity is the same as observed for wild type nAChR. This experiment, performed under equilibrium conditions, is likely to reflect the high affinity desensitized state of the receptor and therefore suggests that αR55 does not contribute to high affinity ACh binding. These results suggest that the reduction in ACh potency in mutants observed in functional studies is not a consequence of alteration of the high affinity ACh binding sites.

The relationship between the high affinity binding sites and low affinity channel activation is unclear. The unequivocal demonstration that more than the two "classical" high affinity binding sites exist at the *Torpedo* nAChR was that saturation of the high affinity sites with carbamylcholine did not diminish the ion flux response to subsequent challenge with activating concentrations of this ligand (Dunn and Raftery, 2000). This provided further evidence that the high affinity sites are not involved directly in the low affinity channel activation process nor can they directly cause desensitization. Recently, β2Tyr62 was identified as a determinant for high affinity binding to the $GABA_A$ receptor (Newell *et al.*, 2000). Further characterization of the role of this residue suggested that these receptors lacking high affinity sites were functional and underwent desensitization upon challenge with agonist, but were unable to maintain the desensitized state in spite the continued presence of agonist (steady state of desensitization). This study suggested that the occupancy of the high affinity sites does

not induce desensitization but stabilizes the desensitized state once the receptor has entered this stage (Newell and Dunn, 2002). We were unable to study the effects of concentration dependence of agonist-induced desensitization under steady state conditions in the *Torpedo* nAChR as these receptors desensitized rapidly and were very slow to recover precluding further characterization (unpublished observation). Instead, we studied desensitization by looking at its time-course (as described in Materials and Methods). This rather qualitative approach suggested that the desensitization process was concentration dependent and the wild type nAChR desensitizes more slowly than the αR55 mutants (αR55F and αR55W) at low agonist concentrations. These results suggest that the αR55 modulates both channel activation and desensitization processes. However, because of the limitation of this approach, we cannot speculate on the mechanism behind the altered desensitization time-course.

In summary, we have for the first time, identified a residue, Arg55 in loop D of the extracellular ligand binding domain of α-subunit that modulates ACh sensitivity and that is distinct from the classical high affinity binding sites (see Fig. 2-12). Our data complement earlier work to suggest that in addition to loop D from the non-α-subunits of nAChR, the contribution of this domain of the α-subunits to channel function cannot be excluded. For the α1β2γ2 type of $GABA_A$ receptor, it has been suggested that the high affinity agonist site may be located at the α-β subunit interface while the putative low affinity site is located at the β-α interface (Newell *et al.*, 2000). By analogy to the $GABA_A$ receptor, in nAChR the high affinity binding sites are suggested to be at the α-γ and α-δ interface while the putative low affinity site(s) may perhaps be located at the opposite β-α and γ-α subunit interface. The positively charged Arg55 of the α-subunit

could reduce agonist affinity through repulsion of the charge on the quaternary ammonium group of the agonist resulting in this site being of relatively lower affinity for ACh. It is possible that the high-affinity binding sites may be allosterically coupled to the residues from loop D of the α-subunit, which may form an important link between ligand binding and ion channel gating. Our findings suggest that αR55 from loop D of the *Torpedo* nAChR directly or indirectly modulates agonist sensitivity and might contribute to one of the additional ligand interacting interface(s), possibly a complementary component on the α-subunit that is distinct from the high affinity binding pocket.

Based on the high homology between the subunits' primary sequences, intuitively, it was suggested that additional ligand-binding sites might be present on each subunit (reviewed by Conti-Tronconi and Raftery, 1982). Similarly, structural models of the adult human nAChR based on AChBP have hypothesized putative interactions at additional subunit interfaces e.g. a salt bridge between εE93 (loop A residue) and αR55 present at the non-ligand binding ε-α interface (Sine, 2002; Sine *et al.*, 2002). Our results on γGlu93 mutation (γE93R) clearly demonstrate that the mutation results in a "gain of function" receptor leading to a more potent effect of ACh in activating the receptor. In contrast, mutation of the equivalent residue in loop A of the α-subunit, the Y93 (αY93F), resulted in an approximate 20-fold reduction in ACh-sensitivity for channel activation (Aylwin and White, 1994). Furthermore, our findings on the double mutant, αR55F-γE93R demonstrate that the ACh EC_{50} value for channel activation is comparable with that of the wild type receptors. These findings demonstrate a counter-balancing role of αArg55 and γGlu93 in modulating agonist sensitivity suggesting their

role in stabilizing receptor function, a finding consistent with the conserved nature of these residues from different species (see Fig. 2-14 B). These ion-pairing interactions at subunit interfaces may play an important role in inter-subunits interaction during the conformational twisting of subunits promoted by channel activation process.

In conclusion, our findings demonstrate a role for αR55 from loop D and γGlu93 from loop A of the *Torpedo* nAChR in modulating the sensitivity of the agonist, ACh but not that of the competitive antagonist, dTC. Furthermore, the proximity of these oppositely charged residues (see Fig. 2-14 A) suggests that the γ-α subunit interface through an ion-pairing interaction may contribute to one of the additional ligand interacting interface(s), with the complementary component on the α-subunit and principal component being contributed by γ-subunit. Alternatively, interaction at the γ-α subunit interface in modulating agonist sensitivity may be indirect, promoted by the twisting of the subunits induced upon low affinity channel activation resulting in association or disruption of this putative salt-bridge. The findings reported here clearly suggest that the role of other subunits and interfaces in modulating channel function cannot be excluded and warrants a detailed look at putative interactions beyond the classical high affinity binding sites.

Figure 2-1

Amino Acid Sequence Alignment of Residues from Loop D of members of the LGIC family and AChBP. Sequences of α1, γ and δ subunits from *Torpedo californica* (T. Ca) nAChR, human (H) α1 subunit of nAChR, rat subunit α1 and β2 of the $GABA_A$ receptor, α1 subunit of the rat glycine receptor, rat $5\text{-}HT_{3A}$ subunit and AChBP were aligned using CLUSTAL W software. Numbering shown is for the *Torpedo* nAChR α1 subunit. The positively charged Arg residue (in bold under the asterisk) at position 55 in the muscle α1 subunit is conserved in several species of nAChR α1 subunit. αArg55 is located at a homologous position to conserved aromatic amino acid residues (in the open rectangular box) from different members of the LGIC superfamily that have been identified by labeling or mutagenesis studies (see text for details).

		48	49	50	51	52	53	54	55	56	57	58	59	60	61	62
									★							
T.Ca_nAChR	α1	Q	I	V	E	T	N	V	**R**	L	R	Q	Q	W	I	D
H_nAChR	α1	Q	I	V	T	T	N	V	**R**	L	K	Q	Q	W	V	D
T.Ca_nAChR	γ	E	A	L	T	T	N	V	W	I	E	I	Q	W	N	D
T.Ca_nAChR	δ	E	T	L	T	S	N	V	W	M	D	H	A	W	Y	D
Rat_GABA$_A$	α1	M	E	Y	T	I	D	V	F	F	R	Q	S	W	K	D
Rat_GABA$_A$	β2	M	D	Y	T	L	T	M	Y	F	Q	Q	A	W	R	D
Rat_Glycine	α1	M	D	Y	R	V	N	I	F	L	R	Q	Q	W	N	D
Rat_5HT3	A	Q	V	L	T	T	Y	I	W	Y	R	Q	F	W	T	D
AChBP		N	E	V	D	V	V	F	W	Q	Q	T	T	W	S	D

Figure 2-2

A schematic representation of the subunit arrangement of the *Torpedo* nAChR showing the loop model of high affinity ligand binding domains. In addition, loop D (in red) of α-subunit is shown at its minus interface (AChBP nomenclature), which might contribute to putative low affinity additional binding site(s). Loop D of the α-subunit has not been implicated to date in ligand binding or modulating agonist/antagonist sensitivity. αArg55 is located in loop D.

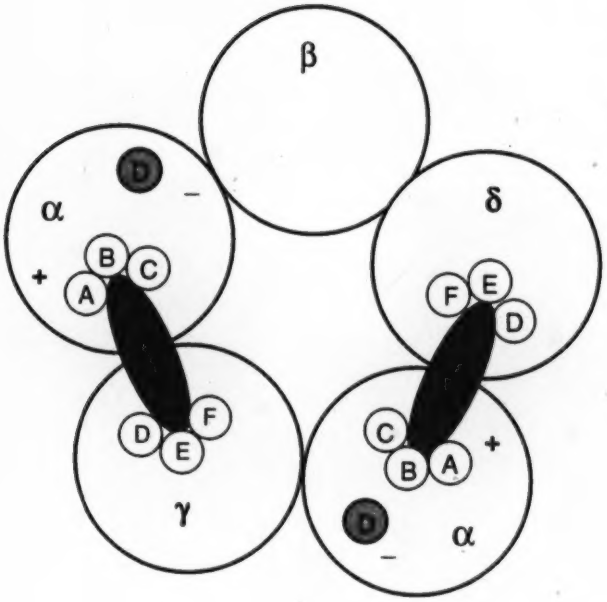
β
α
D
−
+
B
C
A
δ
F
E
D
D
F
E
γ
C
B
A
+
D
−
α

Figure 2-3

Chemical structures of the agonists (A) acetylcholine, (B) carbamylcholine and (C) phenyltrimethylammonium (PTMA), and the competitive antagonist, (D) *d*-tubocurarine (dTC).

A)

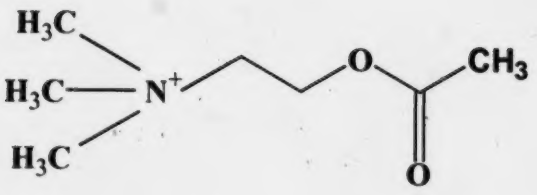
H3C
H3C
N+
H3C
O
CH3
O

B)

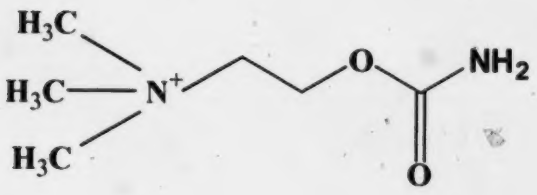
H3C
H3C
N+
H3C
O
NH2
O

C)

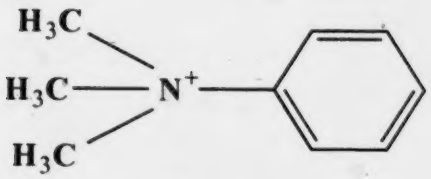
H3C
H3C
N+
H3C

D)

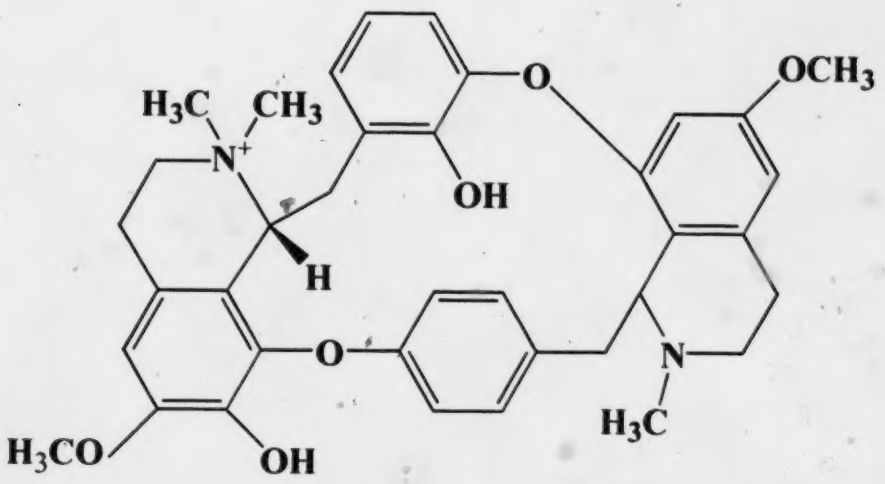
H3C
CH3
N+
H
O
OH
OCH3
O
N
H3C
H3CO
OH

Figure 2-4

ACh activation of wild type and mutant receptors. Concentration-effect curves obtained from oocytes expressing wild type (■), αR55E (□), αR55K (△), αR55W (◇) and αR55F (○) nAChR. Data are normalized to I_{max} for each individual point. The data represent the mean ± SEM from at least 3 oocytes. The shift in EC_{50} value for the αR55F and αR55W mutant receptor is approximately 5 and 6-fold respectively. Data for wild type and all mutants are summarized in Table 2-1.

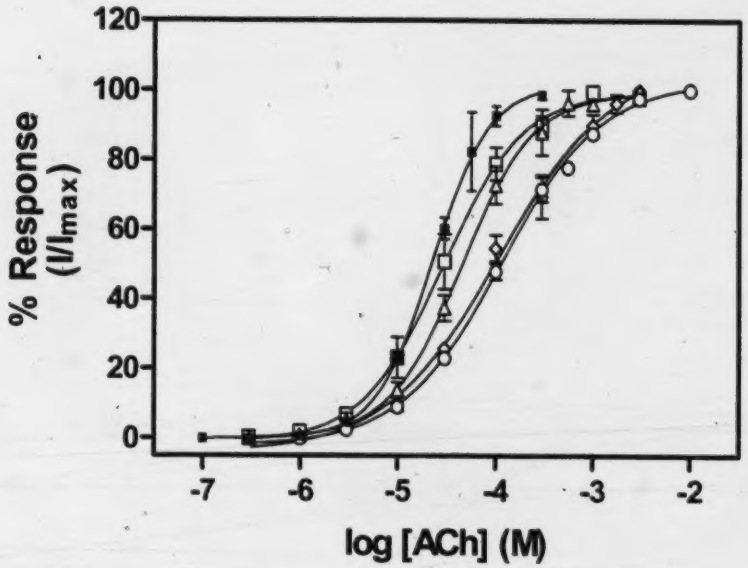
120
100
80
60
40
20
0
% Response
(I/Imax)
-7
-6
-5
-4
-3
-2
log [ACh] (M)

Figure 2-5

Carbamylcholine (CCh) activation of wild-type and mutant receptors. Concentration-effect curves obtained from oocytes expressing wild type (■), αR55E (□), αR55K (△), αR55W (◇) and αR55F (○) nAChR. Data are normalized to I_{max} for each individual point. The data represent the mean ± SEM from at least 3 oocytes. The shift in EC_{50} value for the αR55F and αR55W containing mutant receptor is approximately 3-fold. Data for wild type and all mutants are summarized in Table 2-1.

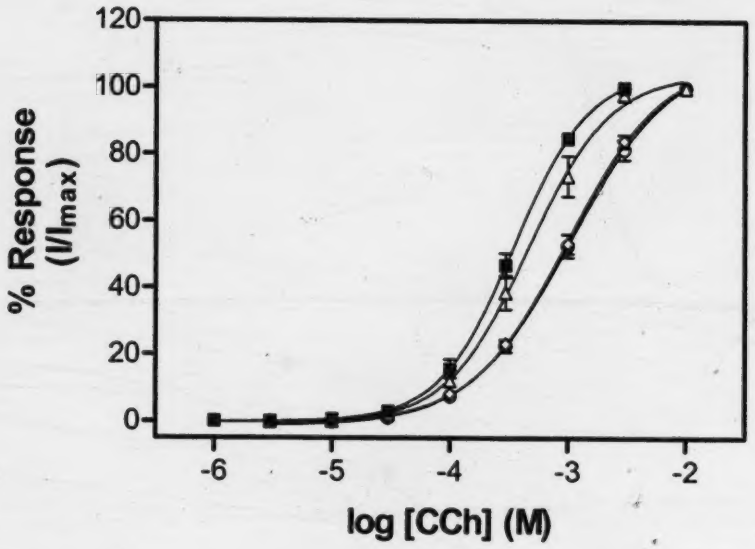
120
100
80
60
40
20
0
% Response
(I/Imax)
-6
-5
-4
-3
-2
log [CCh] (M)

Figure 2-6

Functional properties of the partial agonist, phenyltrimethylammonium (PTMA). (A) Concentration-effect curves for PTMA (□) and ACh (■) on oocytes expressing wild type nAChR. Data are normalized to I_{max} for each individual point. The data represent the mean ± SEM from at least 3 oocytes. PTMA failed to evoke any response in the αR55F and αR55W containing mutant receptor at concentrations up to 10 mM. Data are summarized in Table 2-1. (B) Maximal responses, I_{max}, for ACh and PTMA on the same oocyte expressing wild type receptors was determined using concentrations established from concentration-effect curves (Fig. 2-5). Percentage I_{max} observed with PTMA was 1.5 ± 0. 13 SEM compared to ACh.

A)

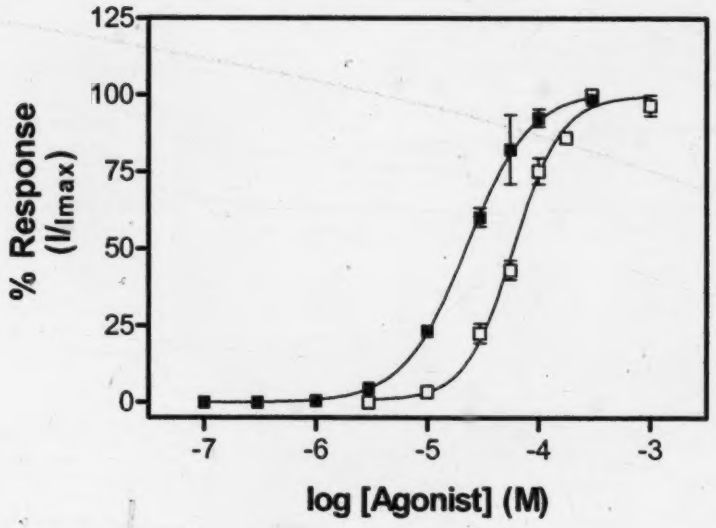
125
100
75
50
25
0
% Response
(I/Imax)
-7
-6
-5
-4
-3
log [Agonist] (M)

B)

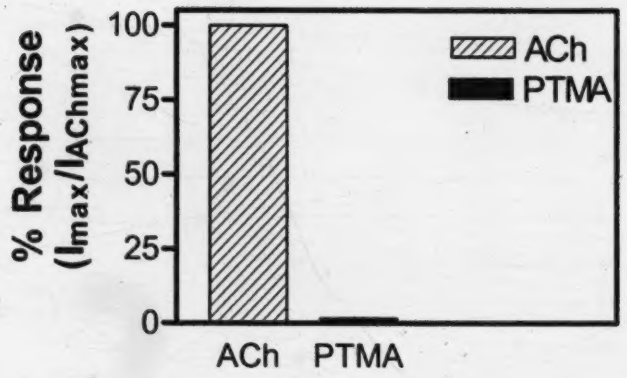
100
75
50
25
0
% Response
(Imax/IAChmax)
ACh
PTMA
ACh
PTMA

Figure 2-7

Phenyltrimethylammonium (PTMA) activation of wild type and inhibition of mutant receptors. (A) Concentration effect curves for PTMA (activation) on WT (■) and inhibition (PTMA + ACh co-application, □) on αR55F mutant receptors. (B) Concentration effect curves for PTMA (activation) on WT (■) and inhibition (PTMA + ACh co-application, □) on αR55W mutant receptors. Data are normalized to I_{max} for each individual point. The data represent the mean ± SEM from at least 3 oocytes except for the αR55W mutant (n=1). PTMA failed to evoke any response in the oocytes expressing αR55F or αR55W mutant receptors at concentrations up to 10mM but it now acted as a competitive antagonist on these mutant receptors. Data are summarized in Table 2-2. PTMA inhibition of the mutant nAChR occurs over a similar concentration range as activation of the wild type nAChR

A)

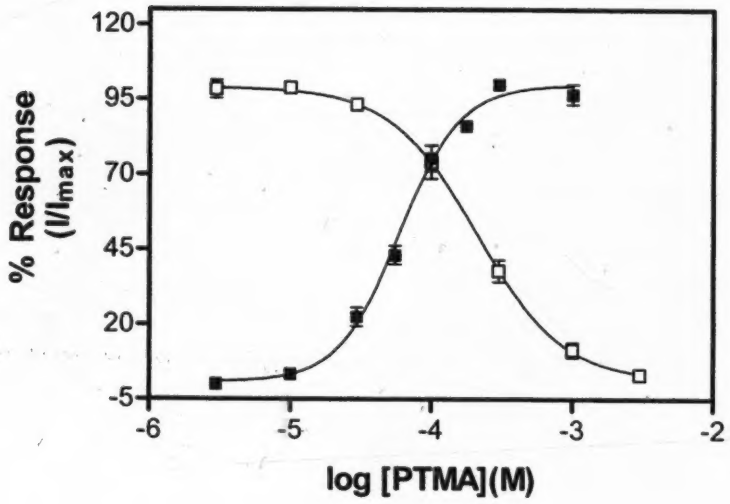
120
95
70
45
20
-5
% Response
(I/I$_{max}$)
-6
-5
-4
-3
-2
log [PTMA](M)

B)

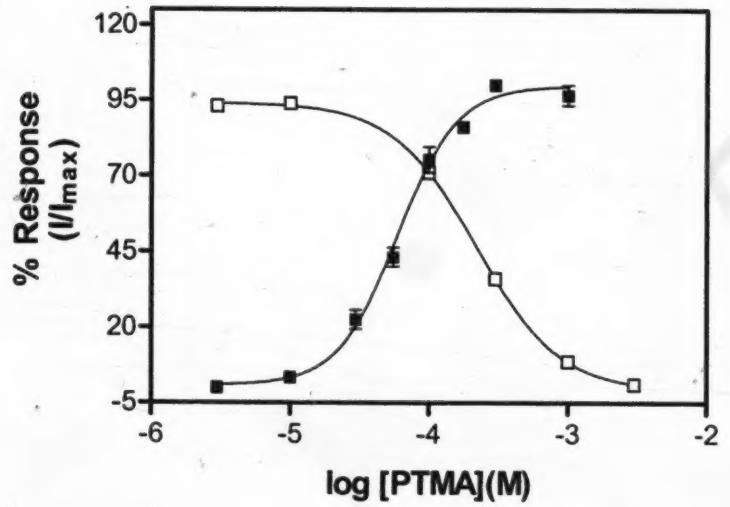
120
95
70
45
20
-5
% Response
(I/I$_{max}$)
-6
-5
-4
-3
-2
log [PTMA](M)

Figure 2-8

Representative traces of current evoked by EC_{10} concentrations of ACh in *Xenopus* oocytes expressing A) wild type, B) αR55F and C) αR55W mutant receptors. The average time taken for ACh-evoked peak current to decrease to half of its amplitude in the continuous presence of agonist is taken as a measure of the time course of desensitization. Arrowheads represents wash out of agonist application with agonist free buffer. Data represent mean ± SEM of three to five determinations using separate oocytes. The average desensitization time course for the αR55F and αR55W mutants was 34 ± 10s and 37 ± 9s respectively, which was about 3-fold faster than in oocytes expressing wild-type nAChR (95 ± 5s) (see the timescale of the trace). EC_{10} concentrations of ACh used were 5.3 μM, 10.6 μM and 8.2 μM for wild type, αR55F and αR55W nAChR respectively.

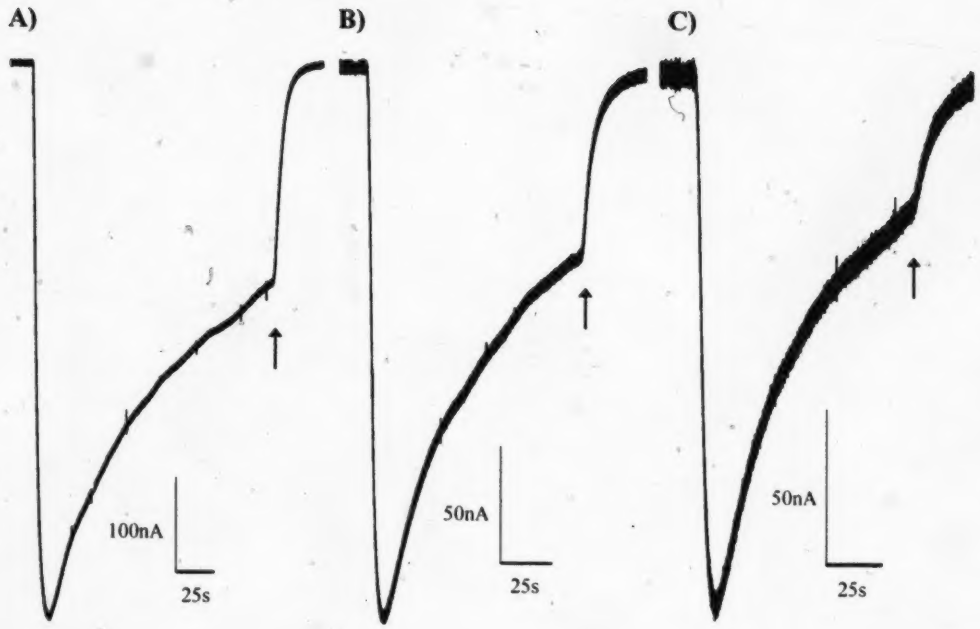
A)
B)
C)
100nA
25s
50nA
25s
50nA
25s

Figure 2-9

Surface nAChR expression in *Xenopus* oocytes labeling as determined by [^{125}I]α-BgTx binding. Maximum ACh-evoked currents (I_{max}) were determined using concentrations determined from concentration-effect curves (as shown in Fig. 2-4) using two-electrode voltage clamp techniques. Surface receptor levels were determined in the same oocyte by measuring [^{125}I]α-BgTx binding as described under "Materials and Methods." The data represent mean ± SEM of 3-11 determinations from individual oocytes and are presented in Table 2-3.

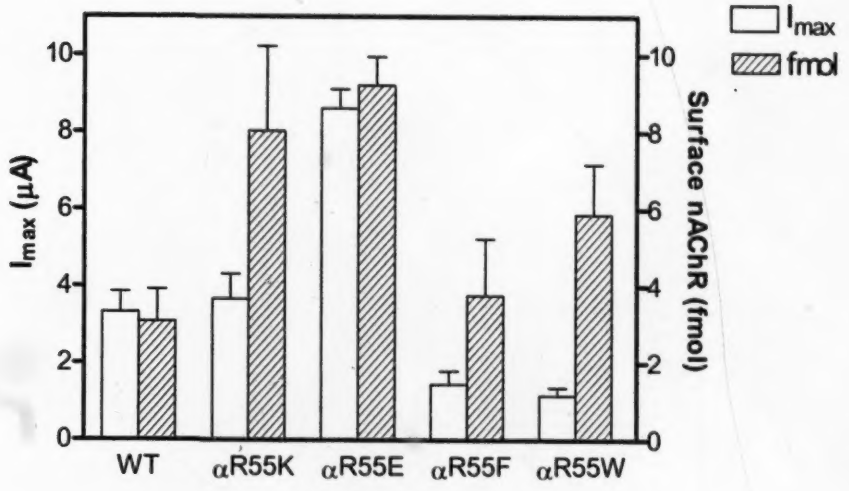
I_{max}
fmol
I_{max} (μA)
Surface nAChR (fmol)
0
2
4
6
8
10
WT
αR55K
αR55E
αR55F
αR55W

Figure 2-10

Concentration dependent inhibition of ACh-evoked currents by dTC in oocytes expressing the wild type (■), αR55K (△), αR55W (◇) and αR55F (○) mutant receptors. The ACh concentrations used in the experiments corresponded to their EC_{50} determined for each receptor. The protocol is described in the "Materials and Methods" section. Each curve was generated from at least three oocytes. The apparent K_I of dTC on oocytes expressing the αR55K, αR55F and αR55W mutant receptors is not significantly different from the wild type nAChR. Data for wild type and mutant receptors are summarized in Table 2-4.

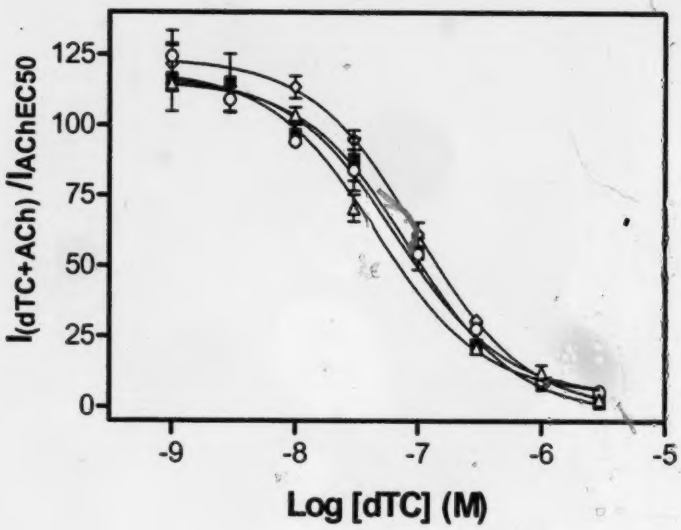
I(dTC+ACh) /IAChEC50
125
100
75
50
25
0
-9
-8
-7
-6
-5
Log [dTC] (M)

Figure 2-11

ACh binding to *Torpedo* nAChR expressed on surface of *Xenopus* oocytes. Binding studies were done on intact oocytes as described in "Materials and Methods". ACh inhibited the initial rate of [^{125}I]α-BgTx binding in a concentration dependent manner in WT (■), αR55F (O) and αR55W (□) receptors. The data represent the mean ± SEM of two-three determinations performed in duplicate and are summarized in Table 2-4.

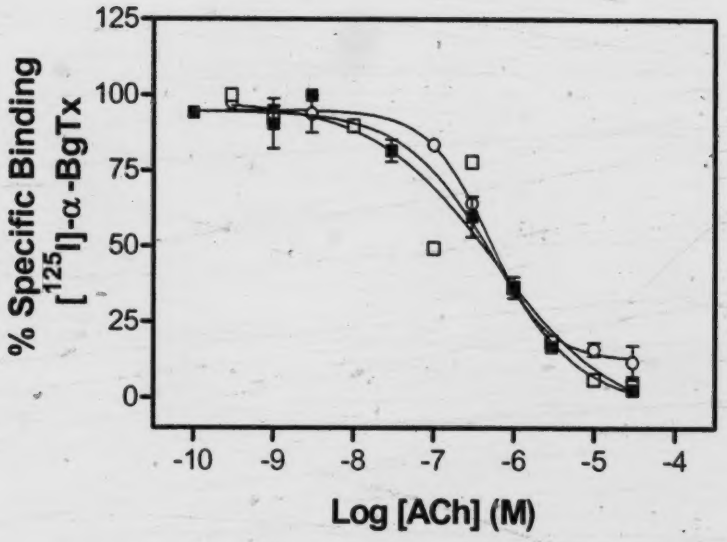
% Specific Binding
[125I]-α-BgTx
125
100
75
50
25
0
-10
-9
-8
-7
-6
-5
-4
Log [ACh] (M)

Figure 2-12

Location of Arg55 (in red) from loop D of the α-subunit (in yellow) based on the crystal structure of the AChBP. Loop D residue, αR55 lies on the β2 strand (see Fig.1-6B) and is located at the (-)-face of the α-subunit at the opposite side of the subunit, at some distance from the classical high affinity binding. Also shown are some of the residues (in black) from the primary component of the α-subunit located at the subunit-subunit interface implicated in forming the high affinity binding pocket. The illustration is a ribbon representation of two adjacent subunit perpendicular to the axes of symmetry created using WebLab ViewerLite software (Molecular Stimulations Inc).

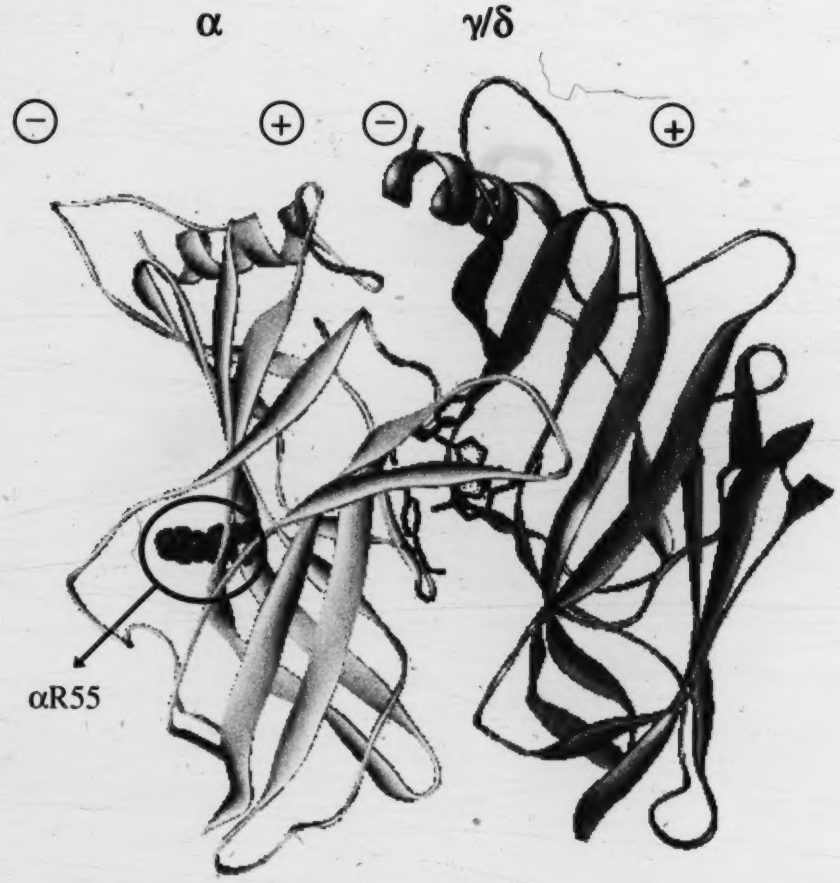
α
γ/δ
αR55

Figure 2-13

Illustration of the subunit arrangement perpendicular to the axis of symmetry based on the crystal structure of AChBP. (A) Ribbon representation of the two alpha subunits (in yellow) with a gamma subunit (line ribbon illustration in blue) located in between, in an α-γ-α manner. (B) Location of Glu93 (in green) from loop A of the γ-subunit (in blue) relative to Arg55 (in red) from loop D of the α-subunit (in yellow). Glu93 in the γ-subunit is homologous to αY93 from loop A. γE93 and αR55 lie at the γ-α subunit-subunit interface. The illustration is a ribbon representation created using WebLab ViewerLite software (Molecular Stimulations Inc).

A)

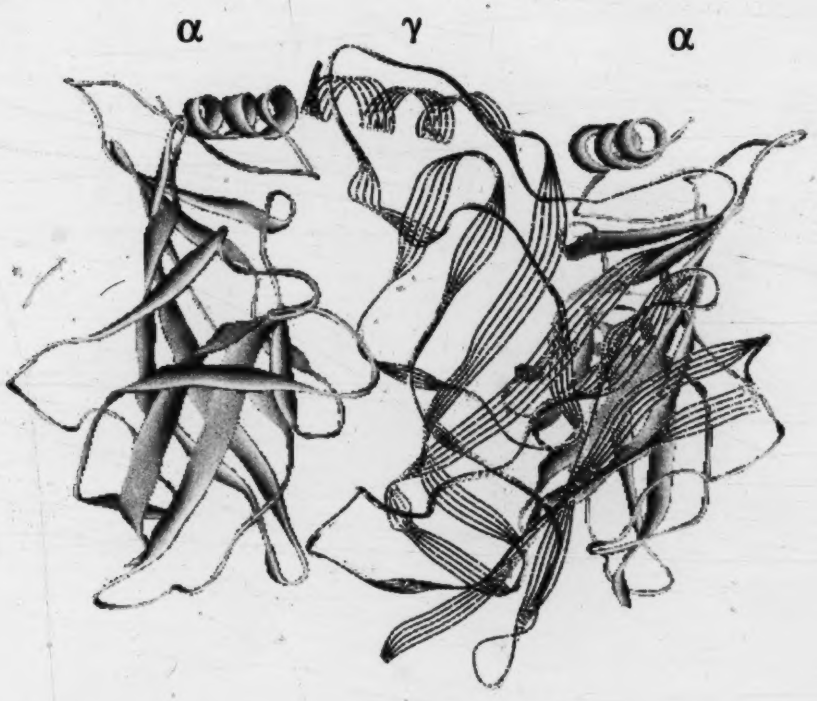

B)

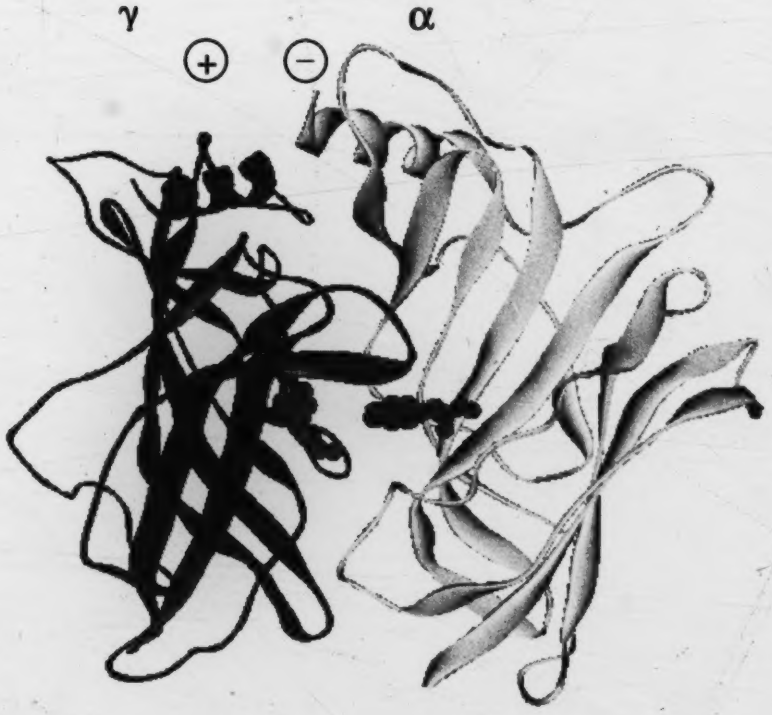

Figure 2-14

(A) Distance between γGlu93 and αArg55 located at the γ-α subunit interface is approximately 6Å. These two residues are located close enough to form a putative ion-pairing interaction (Sine, 2002). (B). Sequence alignment of residues from loop A and loop D of the γ- and α-subunit respectively from various species. Glu93 and Arg55 are conserved across different species (in bold present in open rectangular box) suggesting a potential role in receptor function. Numbering shown is for the *Torpedo* nAChR. Also depicted are residues at equivalent position to γGlu93 in loop A: Tyr93 (in the circle) from the α-subunit of *Torpedo* nAChR that has been implicated in forming the ACh binding site (Galzi *et al.*, 1990) and His101 (in open square) from the rat $GABA_A$ receptor α1 subunit that modulates benzodiazepine sensitivity (Dunn *et al.*, 1999).

A)

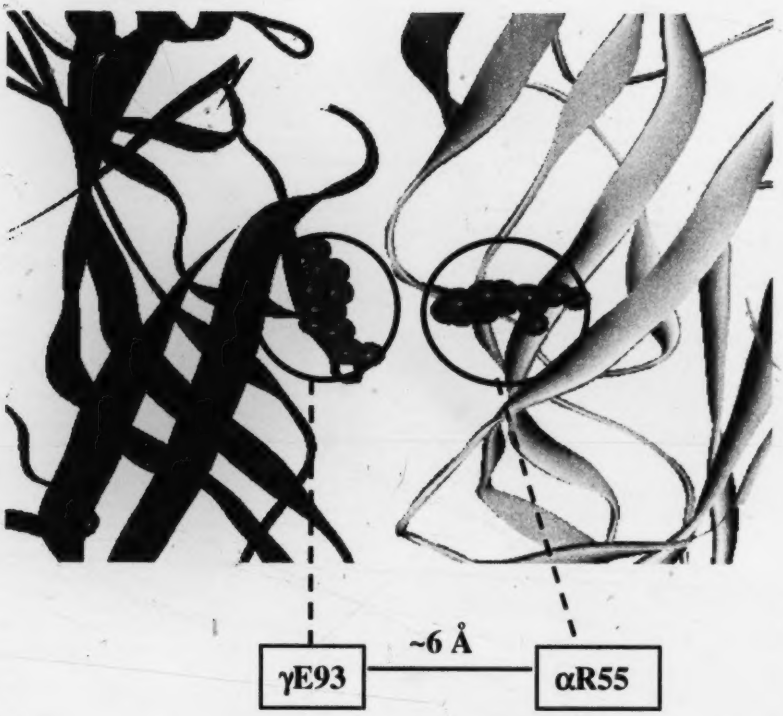

B)

Loop A	89	90	91	92	93	94	95	96	97
*Torpedo*_γ	D	V	V	L	**E**	N	N	V	D
Human_ε	E	I	V	L	**E**	N	N	I	D
Mouse_ε	E	I	V	L	**E**	N	N	I	D
*Torpedo*_α	D	L	V	L	Y	N	N	A	D
Rat_GABA$_A$ α1	D	T	F	F	H	N	G	K	K

Loop D	51	52	53	54	55	56	57	58	59
*Torpedo*_α	E	T	N	V	**R**	L	R	Q	Q
Human_α1	T	T	N	V	**R**	L	K	Q	Q
Rat_α1	T	T	N	V	**R**	L	K	Q	Q

Figure 2-15

ACh activation of γE93 mutant receptors. (A) Concentration-effect curves obtained from oocytes expressing wild type (■), γE93R (□) and αR55F (○) nAChR. The γE93R mutant results in a leftward shift of the ACh activation curve and its EC_{50} value is approximately 8-fold lower as compared with the wild type nAChR. In contrast, the αR55F results in a rightward shift of the ACh activation curve. (B) Concentration-effect curve for wild type (■) and the double mutant, γE93R-αR55F (◆). The EC_{50} for ACh channel activation on γE93R-αR55F nAChR is quite similar to the wild type nAChR. Data are normalized to I_{max} for each individual point. The data represent the mean ± SEM from at least 3 oocytes. The shift in EC_{50} value for the αR55F mutant receptor is approximately 5-fold towards higher concentration of ACh. Data for wild type and all mutants are summarized in Table 2-5.

A)

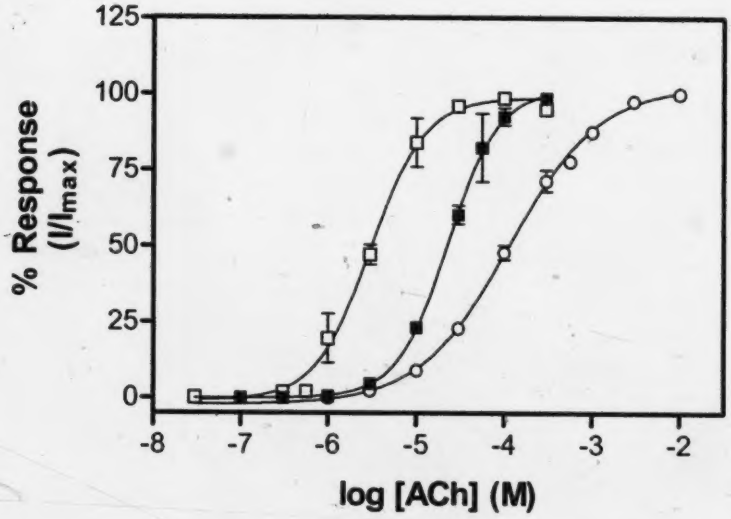
125
100
75
50
25
0
% Response
(I/Imax)
-8
-7
-6
-5
-4
-3
-2
log [ACh] (M)

B)

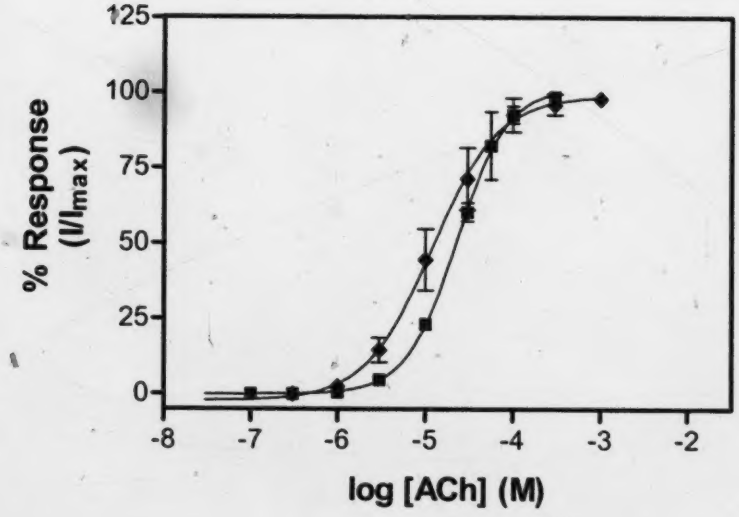
125
100
75
50
25
0
% Response
(I/Imax)
-8
-7
-6
-5
-4
-3
-2
log [ACh] (M)

Figure 2-16

Concentration dependent inhibition of ACh evoked currents by dTC in oocytes expressing the wild type (■) and γE93R (□) mutant receptors. The ACh concentration used in the experiments corresponded to their EC_{50} concentrations determined for each receptor. The protocol is described in the "Materials and Methods" section. Each curve was generated from at least three oocytes. The apparent K_I of dTC on oocytes expressing the γE93R receptors (55 nM) is not significantly different from the wild type nAChR (42 nM).

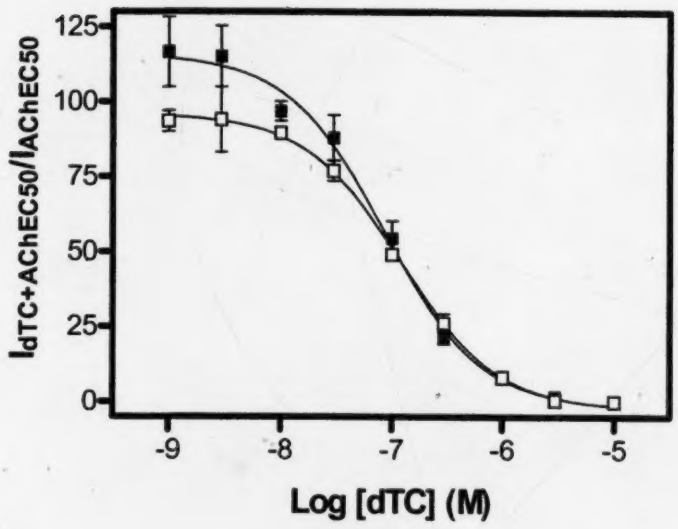
125
100
75
50
25
0
-9
-8
-7
-6
-5
IdTC+AChEC50/IAChEC50
Log [dTC] (M)

TABLE 2-1

Concentration-effect data for ACh, carbamylcholine and PTMA activation of wild type and mutant receptors expressed in Xenopus *oocytes.*

	Log EC_{50} ± SEM (M)	EC_{50} (μM)	n_H ± SEM	EC_{50}Mutant/ EC_{50}WT
ACh				
WT	-4.614 ± 0.04 (9)	24.3	1.6 ± 0.1	1
αR55E	-4.543 ± 0.12 (3)	28.6	1.2 ± 0.1	1.2
αR55K	-4.326 ± 0.08 (3)	47.2	1.2 ± 0.1	1.9
αR55F	-3.952 ± 0.06 (4)**	112	0.8 ± 0.02**	4.6
αR55W	-3.822 ± 0.18 (4)**	151	0.8 ± 0.1**	6.2
CCh				
WT	-3.434 ± 0.02 (3)	368	1.3 ± 0.2	1
αR55E	NT	NT	NT	
αR55K	-3.330 ± 0.07 (3)	468	1.3 ± 0.03	1.3
αR55F	-2.946 ± 0.08 (4)**	1130	1.05 ± 0.1	3.1
αR55W	-2.993 ± 0.05 (3)**	1020	1.1 ± 0.1	2.8
PTMA				
WT	-4.244 ± 0.06 (3)	57.0	2.1 ± 0.2	
αR55F	NR (Antagonist)	NR	NR	
αR55W	NR (Antagonist)	NR	NR	

Data represent the mean ± SEM. Values for log EC_{50} and Hill coefficient (n_H) were determined from concentration-effect curves (Fig. 2-4, 2-5, 2-6) using GraphPad Prism software. Log EC_{50} and Hill coefficient value from individual curves was averaged to generate final mean estimates. The value in parentheses is the number of oocytes used for each receptor type. NT- not tested because αR55E mutant was found to be similar to WT receptors to its response to ACh. NR- no response was observed with up to 10 mM concentration of PTMA on the αR55F and αR55W mutant receptors.

Statistical analysis performed by comparing the log EC_{50} and n_H of the mutant receptors to the wild-type nAChR using one-way analysis of variance (ANOVA) followed by Dunnett's post-test to determine the level of significance. **$p<0.001$.

TABLE 2-2

Concentration-effect data for PTMA inhibition (IC_{50}) of ACh-evoked currents and EC_{50} for ACh-induced channel activation in mutant receptors expressed in Xenopus *oocytes.*

Receptor	PTMA		ACh[$]	PTMA/ACh
	Log IC_{50} ± SEM (M)	IC_{50} (μM)	EC_{50} (μM)	IC_{50}/EC_{50}
WT	-4.244 ± 0.06 (3)[#]	57.0[#]	24.3 (9)	2.3
αR55F	-3.685 ± 0.04 (3)	206	112 (4)	1.8
αR55W	-3.658 (1)	220	151 (4)	1.5

PTMA did not activate oocytes expressing the αR55F and αR55W mutant receptors. However, PTMA still retained the ability to bind to these mutant receptors as is demonstrated by its ability to act as a competitive antagonist. Furthermore, the IC_{50} values for PTMA inhibition of ACh-evoked current on the mutant receptor is quite similar to the ACh EC_{50} for channel activation on these receptors.

EC_{50} for PTMA induced channel activation
$ From Table 2-1.

TABLE 2-3

Surface expression and normalized ACh-evoked maximum currents in wild type and mutant receptors expressed in Xenopus *oocytes.*

	Surface Binding (fmol/oocyte ± SEM)	**I_{max} (nA ± SEM)**	**Normalized Peak Current (nA/fmol)**	**% Peak Current (Mutant I_{max}/ WT I_{max})**
WT	3.1 ± 0.8 (11)	3316 ± 537	1081	100
αR55E	9.2 ± 0.7 (3)	8680 ± 501	934.4	86.4
αR55K	8.0 ± 1.5 (5)	3652 ± 654	455.1	42.1
αR55F	3.8 ± 0.7 (6)	1445 ± 340	384.6	35.6
αR55W	5.9 ± 1.3 (7)	1154 ± 210	197.0	18.2

All oocytes were injected with 50ng of total cRNA encoding wild type or mutant subunit nAChR. The value in parentheses is the number of oocytes used for each receptor type.

Table 2-4

Data generated from dTC and ACh competition inhibition curves in functional and radioligand binding studies respectively.

Receptor Type	dTC[a]			ACh[b]	
	Log IC_{50} ± SEM (M)	IC_{50} (nM)	App K_I (nM)	Log IC_{50} ± SEM (M)	IC_{50} (nM)
WT	-7.071 ± 0.11	85.0	41.5	-6.264 ± 0.14	544
αR55K	-7.342 ± 0.07	45.5	23.3	nd	
αR55E	nd	nd		nd	
αR55F	-7.159 ± 0.10	69.3	34.3	-6.343 ± 0.06	454
αR55W	-7.007 ± 0.07	98.4	51.5	-6.504 ± 0.20	313

Log IC_{50} values were determined from inhibition curves (Fig. 2-10, 2-11) using GraphPad Prism software. The log IC_{50} value from individual curves was averaged to generate final mean estimates. nd- not determined.

[a] Inhibition of ACh-evoked currents by dTC in functional studies. Apparent K_I was determined by using the Cheng-Prusoff equation as described in the "Materials and Methods" section. The experiment was repeated in 3-4 oocytes for each receptor type. No significant differences were observed between the wild type and mutant receptors.

[b] The IC_{50} from equilibrium binding of ACh was determined from inhibition of the initial rate of [^{125}I]α-BgTx binding. The data represent the mean ± SEM of two-three determinations performed in duplicates. No significant differences were found between the log IC_{50} values.

TABLE 2-5

Concentration-effect data for ACh activation of γE93 mutant receptors expressed in Xenopus *oocytes.*

Receptor	Log EC_{50} ± SEM (M)	EC_{50} (μM)	n_H ± SEM	EC_{50}Mutant/ EC_{50}WT
γE93R	-5.518 ± 0.1 (4)**,$	3.03	1.4 ± 0.02	0.12
γE93R-αR55F	-4.890 ± 0.2 (4)$	12.9	1.3 ± 0.1	0.53
αR55F	-3.952 ± 0.06 (4)**	112	0.8 ± 0.02	4.6
WT	-4.614 ± 0.04 (9)	24.3	1.6 ± 0.1	1

Data represent the mean ± SEM. Values for log EC_{50} and Hill coefficient (n_H) were determined from concentration-effect curves (Fig. 2-4, 2-14 and 2-15) using GraphPad Prism software. Log EC_{50} and Hill coefficient values from individual curves were averaged to generate final mean estimates. The value in parentheses is the number of oocytes used for each receptor type.

The log EC_{50} of the mutant receptors is compared with that of the wild-type nAChR using one-way analysis of variance (ANOVA) followed by Dunnett's post-test to determine the level of significance. **$p<0.001$, $^{\$}p<0.001$ (comparison between γE93R and αR55F mutant receptors).

BIBLIOGRAPHY

AKK, G. (2002). Contributions of the non-α subunit residues (loop D) to agonist binding and channel gating in the muscle nicotinic acetylcholine receptor. *J. Physiol.*, **544.3,** 695-705.

AMIN, J. AND WEISS, D.S. (1993). $GABA_A$ receptor needs two homologous domains of the beta-subunit for activation by GABA but not by pentobarbital. *Nature*, **366,** 510-511.

AYLWIN, M.L. AND WHITE, M.M. (1994). Ligand-receptor interactions in the nicotinic acetylcholine receptor probed using multiple substitutions at conserved tyrosines on the α subunit. *FEBS Lett.*, **349,** 99-103.

ARIAS, H.R. (2000). Localization of agonist and competitive antagonist binding sites on nicotinic acetylcholine receptor. *Neurochem. Int.*, **36,** 595-645.

BARNARD, E. A., MILEDI, R. AND SUMIKAWA, K. (1982). Translational of exogenous messenger RNA coding for nicotinic acetylcholine receptors produces functional receptors in *Xenopus* oocytes. *Proc. R. Soc. Lond . B.*, **215**, 241-246.

BERTRAND, D. AND CHANGEUX, J.-P. (1995). Nicotinic receptor: an allosteric protein specialized for intracellular communication. *Sem. Neurosci.*, **7,** 75-90.

BLOUNT, P. AND MERLIE, J.P. (1989). Molecular basis of the two nonequivalent ligand binding sites of the muscle nicotinic acetylcholine receptor. *Neuron*, **3**, 349-357.

BREJC, K., DIJK, W.J.V., KLAASSEN, R.V., SCHUURMANS, M., OOST, J.V.D., SMIT, A.B. AND SIXMA, T.K. (2001). Crystal structure of an ACh-binding protein reveals the ligand-binding domain of nicotinic receptors. *Nature*, **411**, 269-276.

BUHR, A., BAUR, R. AND SIGEL, E. (1997). Subtle changes in residue 77 of the gamma subunit of alpha1beta2gamma2 GABAA receptors drastically alter the affinity for ligands of the benzodiazepine binding site. *J Biol. Chem.*, **272,** 11799-804.

CHENG, Y. AND PRUSOFF, W.H. (1973). Relationship between the inhibition constant (K1) and the concentration of inhibitor which causes 50 per cent inhibition (I50) of an enzymatic reaction. *Biochem. Pharmacol.*, **22**, 3099-3108.

CHIARA, D.C. AND COHEN, J.B. (1997). Identification of amino acids contributing to high and low affinity d-tubocurarine sites in the *Torpedo* nicotinic acetylcholine receptor. *J. Biol. Chem.*, **272,** 32940-32950.

CHIARA, D.C., MIDDLETON, R.E. AND COHEN, J.B. (1998). Identification of tryptophan 55 as the primary site of [3H]nicotine photoincorporation in the gamma-subunit of the *Torpedo* nicotinic acetylcholine receptor. *FEBS Lett.*, **423**, 223-226.

COLQUHOUN, D. (1998). Binding, gating, affinity and efficacy: the interpretation of structure-activity relationships for agonists and of the effects of mutating receptors. *Br. J. Pharmacol.*, **125**, 924-947.

CONTI-TRONCONI, B.M. AND RAFTERY, M.A. (1982). The nicotinic cholinergic receptor: Correlation of molecular structure with functional properties. *Ann. Rev. Biochem.*, **51**, 491-530.

CORRINGER, P.J., GALZI, J.L., EISELE, J.L., BERTRAND, S., CHANGEUX, J.-P. AND BERTRAND, D. (1995). Identification of a new component of the agonist binding site of the nicotinic alpha 7 homooligomeric receptor. *J. Biol. Chem.*, **270**, 11749-11752.

CORRINGER, P.J., LE-NOVÈRE, N. AND CHANGEUX, J.-P. (2000). Nicotinic receptors at the amino acid level. *Ann. Rev. Pharmacol. Toxicol.*, **40**, 431-458.

DOUGHERTY, D.A. AND STAUFFER, D.A. (1990). Acetylcholine binding by a synthetic receptor: Implications for biological recognition. *Science*, **250**, 1558-1560.

DUNN, S.M.J. (1993). Structure and function of the nicotinic acetylcholine receptor. *Adv. Struc. Biol.*, **2**, 225-244.

DUNN, S.M.J., BLANCHARD, S.G. AND RAFTERY, M.A. (1980). Kinetics of carbamylcholine binding to membrane-bound acetylcholine receptor monitored by fluorescence changes of a covalently bound probe. *Biochem.*, **22**, 5645-5652.

DUNN, S.M.J. AND RAFTERY, M.A. (1982a). Activation and desensitization of *Torpedo californica* acetylcholine receptor: Evidence for separate binding sites. *Proc. Nat. Acad. Sci. USA.*, **79**, 6757-6761.

DUNN, S.M.J. AND RAFTERY, M.A. (1982b). Multiple binding sites for agonists on *Torpedo californica* acetylcholine receptor. *Biochem.*, **21**, 6264-6272.

DUNN, S.M.J., CONTI-TRONCONI, B.M. AND RAFTERY, M.A. (1983). Separate sites of low and high affinity for agonists on *Torpedo californica* acetylcholine receptor. *Biochem.*, **22**, 2512-2518.

DUNN, S.M.J. AND RAFTERY, M.A. (1993). Cholinergic binding sites on the pentameric acetylcholine receptor of *Torpedo californica*. *Biochem.*, **32**, 8608-8615.

DUNN, S.M.J., DAVIES, M., MUNTONI, A.L. AND LAMBERT, J.L. (1999). Mutagenesis of the rat α1 subunit of the γ-aminobutyric acid$_A$ receptor reveals the importance of residue 101 in determining the allosteric effects of benzodiazepine site ligands. *Mol. Pharmacol.*, **56**, 768-774.

DUNN, S.M.J. AND RAFTERY, M.A. (2000). Roles of agonist-binding sites in nicotinic acetylcholine receptor function. *Biochem. Biophys. Res. Commun.*, **279**, 358-362.

GOLDIN, A.L. AND SUMIKAWA, K. (1992). Preparation of RNA for injection into *Xenopus* oocytes. *Methods Enzmol.*, **207**, 279-297.

GRUTTER, T. AND CHANGEUX, J.-P. (2001). Nicotinic receptors in wonderland. *Trends Biochem. Sci.*, **26,** 459-463.

KARLIN, A. (2002). Emerging structure of the nicotinic acetylcholine receptors. *Nature Neurosci.*, **3,** 102-114.

KARLIN, A. AND AKABAS, M.H. (1995). Toward a structural basis for the function of nicotinic acetylcholine receptors and their cousins. *Neuron,* **15**, 1231-1244.

KASH, T.L., JENKINS, A., KELLY, J.C., TRUDELL, J.R. AND HARRISON, N.L. (2003). Coupling of agonist binding to channel gating in the GABA(A) receptor. *Nature,* **421,** 272-275.

LEE, Y.H., LI, L., LASALDE, J., ROJAS, L., MCNAMEE, M. AND ORTIZ-MIRANDA, S.I. (1994). Mutations in the M4 domain of *Torpedo californica* acetylcholine receptor dramatically alter ion channel function. *Biophy. J.*, **66**, 646-653.

MILEDI, R. (1980). Intracellular calcium and the desensitization of acetylcholine receptors. *Proc. R. Soc. Lond. B.*, **209**, 447-452.

MIYAZAWA, A., FUJIYOSHI, F. AND UNWIN, N. (2003). Structure and gating mechanism of the acetylcholine receptor pore. *Nature*, **423**, 949-955.

NEWELL, J.G., DAVIES, M., BATESON, A.N. AND DUNN, S.M.J. (2000). Tyrosine 62 of the γ-aminobutyric acid type A receptor β2 subunit is an important determinant of high affinity agonist binding. *J. Biol. Chem.*, **275,** 14198-14204.

NEWELL, J.G. AND DUNN, S.M.J. (2002). Functional consequences of the loss of high affinity agonist binding to the γ-aminobutyric acid type A receptor. Implications for receptor desensitization. *J. Biol. Chem.*, **277,** 21423-21430.

O'LEARY, M.E., FILATOV, G.N. AND WHITE, M.M. (1994). Characterization of *d*-tubocurarine binding site of *Torpedo* acetylcholine receptor. *Am. J. Physiol.*, **266,** C648-C653.

PEDERSON, S.E. AND COHEN, J.B. (1990). *d*-Tubocurarine binding sites are located at α-γ and α-δ subunit interfaces of the nicotinic acetylcholine receptor. *Proc. Nat. Acad. Sci., USA.*, **87**, 2785-2789.

RAFTERY, M.A., HUNKAPILLER, M.W., STRADER, C.D. AND HOOD, L.E. (1980). Acetylcholine receptor: Complex of homologous subunits. *Science,* **208,** 1454-1456.

RAFTERY, M.A., DUNN, S.M.J., CONTI-TRONCONI, B.M., MIDDLEMAS, D.S. AND CRAWFIRD, R.D. (1983). The nicotinic acetylcholine receptor: subunit structure, functional binding sites, and ion transport properties. *Cold Spring Harb. Symp. Quant. Biol.*, **48**, 21-33.

SIGEL, E., BAUR, R., KELLENBERGER, S. AND MALHERBE, P. (1992). Point mutations affecting antagonist affinity and agonist dependent gating of the $GABA_A$ receptor channels. *EMBO J.*, **11,** 2017-2023.

SINE, S.M. (2002). The nicotinic receptor ligand binding domain. *J. Neurobiol.*, **53**, 431-446.

SINE, S.M., WANG, H.L. AND BREN, N. (2002). Lysine scanning mutagenesis delineates structural model of the nicotinic receptor ligand binding domain. *J. Biol. Chem.*, **277,** 29210-29223.

STEINBACH, J.H. AND CHEN, Q. (1995). Antagonist and partial agonist actions of d-tubocurarine at mammalian muscle acetylcholine receptors. *J. Neurosci.*, **15,** 230-240.

SULLIVAN, D.A. AND COHEN, J.B. (2000). Mapping the agonist binding site of the nicotinic acetylcholine receptor. Orientation requirements for activation by covalent agonist. *J. Biol. Chem.*, **275,** 12651-12660.

TAMAMIZU, S., GUZMÀN, G.R., SANTIAGO, J., ROJAS, L.V., MCNAMEE, M.G. AND LASALDE-DOMINICCI, J.A. (2000). Functional effects of periodic tryptophan substitutions in the α M4 transmembrane domain of the *Torpedo californica* nicotinic acetylcholine receptor. *Biochem.*, **39**, 4666-4673.

WAHLSTEN, J.L., LINDSTROM, J.M. AND CONTI-TRONCONI, B.M. (1993). Amino acid residues within the sequence region α55-74 of *Torpedo* nicotinic acetylcholine receptor interacting with antibodies to the main immunogenic region and with snake α-neurotoxins. *J. Rec. Res.*, **13**, 989-1008.

UNWIN, N. (1995). Acetylcholine receptor channel imaged in the open state. *Nature*, **373,** 37-43.

XIE, Y. AND COHEN, J.B. (2001). Contributions of *Torpedo* nicotinic acetylcholine receptor γTrp-55 and δTrp-57 to agonist and competitive antagonist function. *J. Biol. Chem.*, **276,** 2417-2426.

YAN, D., SCHULTE, M.K., BLOOM, K.E. AND WHITE, M.M. (1999). Structural features of the ligand-binding domain of the serotonin 5HT3 receptor. *J. Biol. Chem.*, **274,** 5537-5541.

CHAPTER 3[2]

Contribution of Tryptophan-86 in the Alpha Subunit of the *Torpedo* Nicotinic Acetylcholine Receptor to Channel Activation by the Bisquaternary Ligand Suberyldicholine

[2] *A version of this chapter is in preparation for submission.* Kapur, A., Davies, M., Dryden, W.F. and Dunn, S.M.J. (2004). Ankur Kapur carried out all experimental work.

INTRODUCTION

The nicotinic acetylcholine receptor (nAChR) is a ligand-gated ion channel protein that mediates the fast excitatory effects of the endogenous neurotransmitter, acetylcholine (reviewed by Conti-Tronconi and Raftery, 1982). The *Torpedo* nAChR is homologous with the muscle-type nicotinic receptor. It is a pentameric transmembrane protein complex composed of four homologous subunits that exist in a stoichiometry of $(\alpha 1)_2\beta 1\gamma\delta$ arranged pseudosymmetrically around a central cation-selective ion-channel (Raftery *et al.*, 1980; Dunn, 1993). Biochemical and mutational studies have revealed that high affinity ACh binding sites are formed at the α-γ and α-δ subunit-subunit interfaces (reviewed by Corringer *et al.*, 2000; Arias, 2000; Karlin, 2002). Evidence from these studies led to the suggestion of a "multiple loop model" for the ligand binding sites in which a group of aromatic and hydrophobic amino acid from non-contiguous extracellular regions of the protein (designated as loops A-C) of the α-subunits together with residues from the adjacent γ- and δ-subunits (loops D-F) form the high affinity binding sites.

It has been demonstrated that, at least for some competitive antagonists, these high affinity binding sites are non-equivalent being formed by the association of the α-γ and the α-δ subunits (Blount and Merlie, 1989; Pederson and Cohen, 1990). Three distinct regions of the α-subunit implicated in the formation of the principal component of the binding site include: Tyr93 (loop A), Trp149 (loop B) and Tyr190, Cys192, Cys193 and Tyr198 (loop C) (Kao *et al.*, 1984; Dennis *et al.*, 1988; Galzi *et al.*, 1990; Middleton and Cohen, 1991). Recently, the crystal structure of a soluble homopentameric acetylcholine-binding protein (AChBP), secreted by the snail, *Lymnaea stagnalis* glial

cell was reported (Brejc *et al.*, 2001). This protein is a truncated homologue of the nAChR (homologous to the extracellular amino terminal domains but lacking the membrane spanning domains) and its structure has supported earlier findings from biochemical and mutational studies that the ligand binding sites occur in discrete 'Loops' lying at subunit interfaces (Brejc *et al.*, 2001). While this crystal structure is a model of the LGIC receptor family, it cannot shed light on the processes initiated by the agonist binding to the receptor and the subsequent gating of the ion channel. Nevertheless, AChBP provides us with a valuable template to model binding sites on the *Torpedo* nAChR and other members of the Cys-loop LGIC superfamily.

Suberyldicholine is a potent agonist (more potent than ACh and CCh) of the nAChR (Dreyer *et al.*, 1978; Dionne *et al.*, 1978). The bisquaternary nature and long chain length of suberyldicholine (see Fig. 3-2) suggests that it simultaneously associates with two distinct binding sites and this may explain its high potency (Dunn and Raftery, 1997a,b). To investigate further the interaction of suberyldicholine with the *Torpedo* nAChR, Dunn and Raftery (1997a,b) studied the kinetics of association and dissociation of acetylcholine and suberyldicholine. Results from these studies suggested that although both these agonists had comparable affinity in equilibrium binding studies, they displayed significantly different kinetics of binding to the high affinity sites. Upon saturation of the high affinity sites with [^{3}H]ACh under equilibrium conditions, subsequent addition of higher (micromolar) concentrations of unlabeled ACh resulted in an acceleration of [^{3}H]ACh rate of dissociation as compared to dissociation caused by dilution of the receptor-agonist complex. In contrast, the dissociation kinetics of bound [^{3}H]suberyldicholine was relatively immune to displacement by addition of micromolar

concentrations of unlabeled agonists. These findings led to the suggestion that each of the high affinity site in *Torpedo* nAChR is made up of two "subsites" and suberyldicholine, by virtue of its bisquaternary character, is able to bridge the two subsites while ACh is unable to do so. Thus the high affinity sites are predicted to be allosterically coupled to sites of 'intermediate affinity' and these form the two subsites within each high affinity site.

Photoaffinity labeling studies on nAChR from *Torpedo* membranes with the competitive antagonist, *p*-[^{3}H] dimethylaminobenzene diazonium fluoroborate (DDF) led to the identification of αTry93 (in loop A) as a critical cholinergic ligand binding residue (Galzi *et al.*, 1990). In the same study, an additional residue, αTrp86 was inconclusively identified as a result of low amount of photolabel incorporation. Based on the crystal structure of AChBP (Brejc *et al.*, 2001, see Fig. 3-3), it appears that Trp82 (homologous to *Torpedo* αTrp86) lies approximately 15Å away from the putative binding site. This residue may not, therefore, be located within the well characterized high affinity ACh binding domain. Sequence alignments of loop A residues from different members of the ligand-gated ion-channel (LGIC) superfamily show that this residue (Trp86) is highly conserved at the homologous position in various subunits (see Fig. 3-1), suggesting that it may have an important role in receptor structure and/or function.

The quaternary ammonium group of ACh, which is suggested to interact primarily through a cation-π interaction with electron rich aromatic residues in the extracellular binding site of the receptor (Dougherty and Stauffer, 1990), is located within 6.4Å of the carbonyl carbon (Sullivan and Cohen, 2000). Suberyldicholine, a bisquaternary ligand

has two quaternary ammonium groups (see Fig. 3-2) separated by an interonium distance of ~ 18Å. The structure of AChBP suggests that the αTrp86 residue may lie 15-18Å from αTyr93 identified as a residue participating in the binding site (see Fig. 3-4 A,B). We, therefore, speculate that αTrp86 may contribute to the 'secondary' binding subsite(s) for suberyldicholine.

In this study, we have constructed mutations of the conserved Trp residue at position 86 of the α-subunit and co-expressed this mutant subunit with recombinant wild-type β, γ and δ subunits in *Xenopus laevis* oocytes. The changes in receptor function in response to the application of the agonists, ACh and suberyldicholine were studied using two-electrode voltage clamp techniques in wild-type and mutant receptors. Our results show that the mutation αW86F has a significant effect on suberyldicholine-mediated channel activation and desensitization properties. In contrast, ACh potency at this mutant was not different from the wild type nAChR. We conclude that αW86 contributes a secondary suberyldicholine-binding site that is important for mediating both channel activation and desensitization.

Materials and Methods

Materials

ACh, suberyldicholine, α-BgTx and dTC were obtained from Sigma-RBA (Natick, MA). ^{125}I-α-BgTx (2000Ci/mmol) was obtained from Amersham Life Science (Arlington Heights, IL.). Restriction enzymes and cRNA transcript preparation materials were purchased from Invitrogen (Burlington, ON), Promega (Madison, WI) or from New England Biolabs (Pickering, ON). *Pfu* Turbo DNA polymerase for mutagenesis experiments was purchased from Stratagene (La Jolla, CA). All other chemicals were obtained from Sigma or other standard sources.

The α-, β- (in the SP64 plasmid) and δ-subunit (in the SP65 plasmid) cDNA clones of the *Torpedo* nAChR were generous gifts from Dr. Henry A. Lester (California Institute of Technology, CA). The γ-subunit cDNA (in the SP64-based plasmid, pMXT) was a gift from Dr. Jonathan B. Cohen (Harvard Medical School, Boston).

Site-directed Mutagenesis

The α-subunit mutants (W86A and W86F) were constructed using Stratagene's QuikChange site-directed mutagenesis protocol. Synthetic oligonucleotide mutagenic primers were typically 27-35 base pairs long (with 12-16 base pairs on either side of the mismatch region). The following oligonucleotides (for the sense strand) were designed for mutagenesis:

αW86A, 5' CCTTCTGATGATGTT**GCG**CTGCCAGATTTAGTT 3'

αW86F, 5' GCCTTCTGATGATGTT**TTC**CTGCCAGATTTAGTTC 3'

A similar approach was undertaken to engineer mutation of conserved proline residues from the α-subunit that were in the vicinity of αW86.

αP21A, 5' AAGGTGATTCGT**GCA**GTGGAGCATCAC 3'

αP88A, 5' GATGTTTGGCTG**GCA**GATTTAGTTCTG 3'

α W86F-P88A, 5' GATGATGTT**TTC**CTG**GCA**GATTTAGTT 3'

The annealing temperature for the oligonucleotides in the PCR was found to be optimal between 54 and 55°C. Restriction endonuclease digestion and DNA sequencing subsequently verified the presence of the mutation.

***In Vitro* Transcription**

The plasmid cDNAs were linearized by digestion with *EcoR*I (for the α-subunit), *Fsp*I (for the wild-type β-subunit) or *Xba*I (for wild-type γ- and δ-subunit). *In vitro* cRNA transcription was performed using the method described by Goldin and Sumikawa (1992). Briefly, the linearized cDNA (5 μg) was incubated with 10 mM dithiothreitol, 0.5 mM NTP mix (Invitrogen), 60U of RNase inhibitor (RNaseOut, Promega), 0.5 mM of 7-methyldiguanoise triphosphate (RNA capping analogue, NEB) and 45U of SP6 RNA polymerase (Promega) in transcription buffer at 37 °C for 1 hour. An additional 45U of SP6 RNA polymerase was then added and the reaction was allowed to continue for an additional 1 hour. This was followed by addition of 5U of RNase-free DNase. The reaction mixture was then incubated at 37°C for 15 minutes. The RNA transcripts were extracted using 25:24:1 (v/v) phenol/chloroform/isoamyl alcohol, precipitated with 3M sodium acetate, and washed with 70% ethanol. Finally, the RNA pellets were resuspended in DEPC-treated water at a concentration of 1μg/μl.

Expression in *Xenopus* oocytes and Electrophysiology

Isolated, follicle-free oocytes were microinjected with 50 ng of total subunit cRNAs in a ratio of 2α:1β:1γ:1δ. Oocytes were maintained in ND96 buffer containing 96 mM

NaCl, 2 mM KCl, 1.8 mM $CaCl_2$, 1 mM $MgCl_2$, 5 mM HEPES (pH7.6) and supplemented with 50 μg/ml gentamicin at 14 °C for at least 48 hours prior to recording. Currents elicited by bath application of ACh or suberyldicholine were measured using a GeneClamp500 amplifier (Axon Instruments, Foster City, CA) using standard two-electrode voltage clamp at a holding potential of -60mV. Electrodes were filled with 3M KCl and those with resistances of 0.5-3.0MΩ were used. The recording chamber was perfused continuously by gravity (at a flow rate of ~ 5ml/min) with low calcium ND96 buffer containing 96 mM NaCl, 2 mM KCl, 0.1 mM $CaCl_2$, 1 mM $MgCl_2$, 5 mM HEPES supplemented with 1 μM atropine (pH7.6). Atropine was included in the perfusion buffer to block any endogenous muscarinic acetylcholine receptors present in the oocytes (Barnard *et al.*, 1982). Modified ND96 perfusion buffer with low Ca^{2+} was used to reduce receptor desensitization (Miledi, 1980). The sensitivity of receptors to agonists (in the absence or presence of antagonist) was measured by drug solution application via the perfusion system for 15-20 seconds (or 2-min suberyldicholine application on mutant receptors) with a 15-min wash out period between applications to ensure full recovery from desensitization. For measuring apparent affinity of antagonist, oocytes were preincubated with various concentrations of dTC by perfusing the oocytes for 2-min with dTC in low Ca^{2+} ND96 before application of solution containing the agonist (at a concentration eliciting 50% of the maximum response, EC_{50} unless otherwise indicated) and including the same concentration of dTC as used for preincubation.

Radioligand Binding of [^{125}I]α-BgTx to Intact Oocytes

Binding to nAChR expressed on the oocyte surface (fmol) was determined on the same oocyte as used in functional assays. Briefly, the maximum current (I_{max}) evoked in the voltage clamped oocyte was measured, followed by an adequate wash-out with buffer. The same oocyte was then incubated with 5 nM [^{125}I]α-BgTx in a final volume of 100 µl of low Ca^{2+} ND96 buffer (containing 5 mg/ml bovine serum albumin) for 2 hours in a 96-well plate (Sullivan and Cohen, 2000; Tamamizu *et al.*, 2000). Excess unbound toxin was removed by washing the oocytes 3 times with 1ml of ice-cold low Ca^{2+} ND96 buffer. Non-specific binding was determined by incubating uninjected oocytes with [^{125}I]α-BgTx. Bound [^{125}I]αBgTx was measured by γ-counting (Gamm8000, Beckman). Using these data, I_{max} was normalized to ACh in wild-type and mutant receptors to the concentration of binding sites in terms of nA/fmol.

Data and Statistical Analysis

Competition and concentration-effect curves for both electrophysiological and radioligand binding experiments were analyzed by nonlinear regression techniques using GraphPad Prism 3.0 software (GraphPad, San Diego, CA). Data from individual oocytes were normalized to the I_{max} value obtained for that oocyte.

For receptor activation, concentration-effect curves for agonist activation were analyzed using the following equation:

$$I = I_{max} * [L]^n / (EC_{50} + [L])^n$$

where I is the measured agonist-evoked current, [L] is the agonist concentration, EC_{50} is the agonist concentration that evokes half the maximal current (I_{max}) and n is the Hill

coefficient. In each experiment, the current (I) is normalized to the I_{max} and the normalized data are presented as % response to plot concentration-effect curves.

The IC_{50} was determined from competition-inhibition curves by fitting to the following equation:

$$f = 100/[1+([X]/[IC_{50}])^n]$$

where f is the fractional response (%) remaining in the presence of inhibitor at concentration [X], IC_{50} is the inhibitor concentration that reduced the amplitude of agonist-evoked current by 50% and n is the Hill coefficient. SubDc inhibition of initial rate of [^{125}I]α-BgTx binding was also fit by the above equation.

The apparent K_I value were calculated using the Cheng-Prusoff equation (Cheng and Prusoff, 1973):

$$K_I = IC_{50}/[1 + [L]/(EC_{50})]$$

where [L] is the ACh concentration used in the experiment and EC_{50} is the ACh concentration that evokes half the maximal current. Data is reported as mean ± SEM. Statistical analysis was performed using one-way analysis of variance (ANOVA) followed by Dunnett's post-test to determine the level of significance.

RESULTS

Functional Effect of αW86 and αW86A Mutants on the Binding of Agonist and Antagonist–

Wild type or αW86F and αW86A mutant receptors expressed in *Xenopus* oocytes were studied using two-electrode voltage clamp techniques. Fig. 3-5 summarizes the activation characteristics of ACh and suberyldicholine-induced currents on the wild type and αW86F mutant receptors. For the wild-type nAChR, exposure to ACh or suberyldicholine resulted in a concentration-dependent increase in evoked currents characterized by EC_{50} values of ~ 24 μM (n_H of 1.6) and ~ 3 μM (n_H of 1.4) respectively (Table 3-1).

The αW86A mutation abolished any detectable currents for ACh, even at concentrations as high as 10 mM. In contrast, the αW86F mutant receptors were functional and the mutation resulted in a small but insignificant (~ 2-fold) shift in the EC_{50} for ACh-evoked channel activation (~ 53 μM). However, the αW86F caused a dramatic and very significant (~ 500-fold) shift in suberyldicholine sensitivity towards higher concentration (EC_{50} ~ 1.7 mM). In addition, the Hill coefficients for both ACh- and suberyldicholine-induced activation for this mutant receptor was significantly reduced (to 0.9 and 0.7 respectively) as compared with the wild type nAChR (1.6) (Table 3-1). The currents evoked by agonist acting on the αW86F mutant were small compared to wild type, possibly as a consequence of reduced expression levels in the mutant (see Fig. 3-9).

Both ACh and suberyldicholine evoked currents desensitized in the wild type nAChR. In the mutant, although the ACh-elicited current desensitized,

suberyldicholine-evoked currents failed to desensitize after reaching its peak amplitude (Fig. 3-6). Furthermore, the suberyldicholine-concentration dependent activation process in the mutant was significantly slower and required ~ 2-min exposure to agonist solution to reach peak current as compared to a 15-20s exposure in the wild type.

Altered Sensitivity of αW86F nAChR to Competitive Antagonist–

We further examined the ability of the competitive antagonist, dTC to inhibit ACh and suberyldicholine-evoked currents in wild type and mutant receptors (Fig. 3-8 A, B). For wild-type nAChR, pre-perfusion with dTC produced a concentration-dependent inhibition of suberyldicholine-evoked currents characterized by an apparent K_I of ~ 58 nM. In contrast, dTC did not inhibit suberyldicholine-evoked responses in the αW86F mutant receptors. dTC did, however, completely inhibit ACh-elicited currents in both wild type and αW86F nAChR with an apparent K_I value of ~ 42 nM and ~ 5 nM respectively (see Fig. 3-8 A, Table 3-2). These results indicate that the substitution of αTrp86 by Phe (αW86F) resulted in a specific loss of the mutant receptor's sensitivity to dTC to inhibit suberyldicholine-mediated conductance changes.

Expression Levels and Maximum Currents of Wild-Type and Mutant nAChR–

Fig. 3-9 shows a comparison of the density of binding sites on the surface of oocytes expressing the wild type and mutant receptor (as determined by [^{125}I]α-BgTx binding) and the maximum current evoked by saturating concentrations of ACh. Injection of 50 ng of wild type subunit cRNAs resulted in a robust expression level of 2.9 fmol/oocyte of [^{125}I]α-BgTx binding sites. However, the αW86F mutation when co-expressed with the wild type β-, γ- and δ- subunit resulted in a significant reduction (approximately 10-fold reduction) in the number of [^{125}I]α-BgTx binding sites. In addition, the maximum

current observed for the αW86F mutant were much lower than those observed in wild type nAChR. The αW86F mutant receptors were functional albeit the receptor expression levels were significantly reduced. In contrast, the αW86A mutant abolished all [^{125}I]α-BgTx binding explaining the loss of function seen in electrophysiology experiments. Table 3-3 shows a comparison of the ACh and suberyldicholine maximum currents normalized to the [^{125}I]α-BgTx binding sites (nA/fmol).

Other Mutant nAChR Engineered

The difficulty faced in investigating the αW86F mutant was the small current size evoked by agonist application as a consequence of its reduced expression level. We probed the simultaneous influence of neighboring conserved residues on the αW86F mutant nAChR. Deane and Lummis (2001) have suggested that highly conserved proline residues in the 5-HT$_{3A}$ receptors have a role in maintaining the overall structure of the receptor. These prolines present a unique amino acid motif in terms of having an adjacent aromatic (e.g. Trp) or bend-forming amino acid suggesting that all these residues have a structural role (also see Discussion). Mapping the residue distance based on the crystal structure of AChBP revealed that αP21 and αP88 in the *Torpedo* nAChR were within 5Å from the αW86 residue (Fig. 3-7). We probed the effect of αP88A, double mutant αW86F-P88A, αW86F-P21A and triple mutant αW86F-P21A-P88A on receptor function and expression (data not shown). Our preliminarily findings revealed that all the proline mutants were functional although with reduced current and [^{125}I]α-BgTx binding much like that observed for the αW86F mutant receptor. Furthermore, substituting the proline residues (to alanine) did not enhance receptor expression or function of the αW86 mutant nAChR and hence were not further characterized.

DISCUSSION

An understanding of the role of different molecular domains involved in receptor activation and inactivation processes is critical for defining structure-function relationships of the nAChR. Cholinergic agonists recognize electron rich residues in the binding site of the receptor primarily through cation-π interactions (Dougherty and Stauffer, 1990). The bisquaternary agonist, suberyldicholine was found to be approximately 8-fold more potent than the classical agonist ACh as measured by the EC_{50} for receptor activation of the wild type nAChR expressed in *Xenopus* oocytes (see Table 3-1). However, in terms of current amplitudes, high concentrations of suberyldicholine evoked only about 50 % of the maximum current of ACh i.e. it acted as a partial agonist (data not shown). Similar results have been reported from earlier work on the frog neuromuscular junction (Dreyer *et al.*, 1978; Dionne *et al.*, 1978). Suberyldicholine by virtue of its two quaternary ammonium functional groups has been suggested to cross-link "subsites" within the binding site (Dunn and Raftery, 1997a,b) and this may explain its higher potency. The aim of the present study was to investigate the location of the putative secondary site that interacts with the second quaternary ammonium group of suberyldicholine. To do so, we used the crystal structure of AChBP as a template to model the binding site. Trp86 from loop A of the α-subunit emerged as an attractive choice since this residue lies distal to the binding site, but close enough for suberyldicholine to interact there simultaneously with the high affinity binding site. Furthermore, this residue was also identified by earlier photolabeling studies (see Introduction).

Previously, a mutagenesis approach in which unnatural amino acids were incorporated into the receptor, ruled out αTrp86 as a contributing residue for a strong cation-π interaction with ACh (Zhong *et al.*, 1998). Using various Trp86 analogues with electron withdrawing groups attached, the authors demonstrated that the EC_{50} values for ACh-induced receptor activation were <2-fold different from the wild type nAChR. Our results on the ACh activation properties of the αW86F mutant receptors are consistent with these findings and suggest that αW86 may not be important for modulating ACh sensitivity.

The most important finding of our results is the drastic reduction in the sensitivity of suberyldicholine-evoked currents (~500-fold) mediated by the αW86F mutant receptors as compared to the subtle reduction of ACh sensitivity (~2-fold). Another important observation was that the suberyldicholine-evoked currents in αW86F nAChR failed to desensitize even at saturating concentrations. This suggests that αW86 plays a crucial role in modulating both suberyldicholine-induced activation and desensitization. This was in contrast to ACh-evoked currents in the αW86F mutant that still underwent desensitization. Based on the current data, it is difficult to predict the reason for these significantly different desensitization properties of the two agonists. However, the possibility that suberyldicholine is no longer acting through the primary high affinity site(s) cannot be discounted.

We also observed a significant reduction in Hill coefficient of the activation curves in the mutant receptor suggesting a loss of cooperativity of either binding or the evoked response. Since binding and gating are not independent processes it is difficult to differentiate the two (Colquhoun, 1998; Amin and Weiss, 1993). Another interesting

observation was the total loss of sensitivity of dTC to inhibit suberyldicholine-evoked currents at the αW86F mutant. In contrast, ACh evoked currents were inhibited by dTC in the mutant receptor. This behavior of suberyldicholine in addition to its altered activation and desensitization properties as compared to ACh on the mutant, suggests that it is no longer associating with the same components of the binding sites as ACh and possibly not binding at the ACh-binding sites e.g. αTyr93.

To characterize further whether suberyldicholine is now binding to a distinct site in the mutant receptor, equilibrium binding of suberyldicholine to *Torpedo* nAChR expressed on the surface of intact oocytes was measured by its ability to inhibit toxin binding ($[^{125}I]$α-BgTx binding) was performed. Suberyldicholine inhibited the initial rate of $[^{125}I]$α-BgTx binding to the wild-type nAChR in a concentration-dependent manner with an IC_{50} of ~ 66 nM (n_H = -0.4) (Fig. 3-10). However, due to low receptor expression in oocytes expressing the αW86F mutant receptors, we were unable to determine the IC_{50} of suberyldicholine on the αW86F mutant and hence cannot comment whether the high affinity suberyldicholine-binding in the mutant receptors is altered in comparison with the wild type nAChR.

The presence of a conserved Trp residue at the homologous position to 86 in the α1-subunit (from loop A) through out the LGIC superfamily suggests that it may have a crucial structural role (see Fig. 3-1). We found that the αW86F mutant receptors were functional although the density of receptors was significantly reduced as compared to the wild type. Furthermore, the lack of receptor expression of the αW86A mutant suggests that the presence of an aromatic residue at αTrp86 may be important for receptor assembly or surface expression. Mutational studies on the homologous Trp121 residue

(W121S/Y) in the homopentameric $5HT_{3A}$ receptors revealed a complete loss of both binding and function suggesting that the residue has a critical role in receptor expression (Spier and Lummis, 2000). Similarly, in the $GABA_A$ receptor, mutations of the Trp residue in the α1 subunit (homologous to W86) resulted in an inability of the subunits to form pentamers (Srinivasan *et al.*, 1999). In contrast, for the W86F mutant nAChR, the normalized peak current (nA/fmol) was not significantly different from that of the wild type nAChR. Our results demonstrate that the αW86F mutant receptors were functional and showed some surface nAChR expression.

Lummis and colleagues (Deane and Lummis, 2001) investigated the role of the highly conserved proline residues in the $5HT_{3A}$ receptors. The authors demonstrated that Pro56 and Pro123 (homologous to αPro21 and αPro88 in *Torpedo* nAChR) were crucial for receptor expression. Furthermore, it was suggested that certain proline residues require the presence of adjacent "favourable" residues such as Trp, Tyr, Phe, Pro and Gly. Amino acid sequence alignments revealed that residues homologous to αPro21 and αPro88 are highly conserved throughout the LGIC receptor family (see Fig. 3-7C). Furthermore, these prolines were in the vicinity of αTrp86 (see Fig. 3-7A,B). We reasoned that the low receptor expression observed with the αW86F might be a further consequence of the removal of one of the "favorable" residues adjacent to the conserved prolines. To try to improve the expression of the αW86F mutant receptor, we generated a series of mutations such as αP88A, double mutant αW86F-P88A, αW86F-P21A and triple mutant αW86F-P21A-P88A. Our preliminary findings showed that all the proline mutants responded to agonist challenge, albeit with much smaller currents as compared to the wild type nAChR. These findings suggest that the αP88 and αP21 may be more

important in proper receptor expression rather than modulating agonist mediated channel activation in concert with αTrp86.

Previous studies in nAChR from *Torpedo* membranes have suggested the existence of additional suberyldicholine binding sites. Binding of suberyldicholine to *Torpedo* nAChR covalently labeled with the fluorescent probe, IANBD (4-[[(iodoacetoxy)ethyl]methylamino]-7-nitro-2,1,3-benzoxaidazole) had revealed the presence of two binding sites with dissociation constants of ~ 2 μM (correlating closely with the EC_{50} for suberyldicholine induced channel activation) and lower affinity of ~ 2 mM (Dunn and Raftery, 1993). These affinities were significantly lower than the K_d estimates seen in direct equilibrium binding studies using [^{3}H]suberyldicholine (~ 16 nM) (Dunn and Raftery, 1997a). Quench-flow experiments in *Torpedo* membranes vesicles have also revealed that suberyldicholine at high concentrations (>50 μM) inhibits ion flux in a concentration dependent fashion without affecting the rate of receptor inactivation, suggesting a "regulatory binding site" mediated inhibition (Pasquale *et al.*, 1983). Suberyldicholine was demonstrated to bind to the putative regulatory site with a dissociation constant of 500 μM. Furthermore, this regulatory mechanism was not observed with acetylcholine. Similarly, suberyldicholine mediated self-inhibition of $^{86}Rb^+$ efflux from *Torpedo* membrane vesicles has been reported with a K_d of 3 mM though a putative low affinity inhibitory site(s) (Forman *et al.*, 1987). These findings clearly suggested the presence of specific low affinity site(s) on the receptor for suberyldicholine. Our present findings can be considered in the context of these earlier findings to suggest that αW86 may constitute the putative regulatory (additional) site and possibly represent the lower affinity binding site of the two high

affinity subsite model proposed that is responsible for modulating the sensitivity of suberyldicholine and not that of ACh.

Although for classical agonists such as ACh and CCh, it has been demonstrated that the high affinity binding sites in *Torpedo* nAChR are not directly involved in receptor activation and the occupancy of these sites does not *per se* desensitize the receptor; suggesting that there might be additional low affinity binding domains that modulate receptor activation (Dunn and Raftery, 2000). Our current findings demonstrate that for the bisquaternary agonist, suberyldicholine, the putative lower affinity site, contributed by αTrp86, is important for its channel activation and desensitization properties.

In summary, data from this present study demonstrate that Trp86 of the α-subunits is important for modulating the effects of suberyldicholine. We suggest that this residue in the *Torpedo* nAChR constitutes a secondary binding site for the bisquaternary ligand, suberyldicholine and is important for modulating both channel activation and desensitization induced by this ligand. Previous work in our laboratory using bisquaternary ligands of varying chain lengths had suggested that compounds with an interonium distance of >14Å (such as adipyldicholine, pimelyldicholine) may be long enough to bridge binding sites (Dunn and Raftery, 1997b). These preliminary studies were undertaken to characterize the properties of a series of bisfunctional ligands and to give an indication to the approximate distances between distinct binding sites. In light of the findings reported here, it is predicted that similarly, other bisquaternary ligands (e.g. glutaryldicholine, azelyldicholine) possibly interact with residue(s) in the vicinity of the high affinity binding sites i.e. αTrp86. Further characterization of bisfunctional compounds of different chain lengths on αTrp86 mutant receptors may help to study the

cut-off chain length that is adequate to cross-link residues in the extracellular ligand binding domain. Studies that probe the structural basis for ligand-selectivity will help widen not only the knowledge of the receptor structure but also help in designing better therapeutic agents. Mutagenesis experiments must be interpreted with prudence, as these mutants may alter the overall tertiary and quaternary arrangement of the receptors. However until we have a crystal structure of the nAChR, combining the receptor's structural information with functional experiments will aid in identification of residues involved in agonist-mediated receptor activation and provide mechanistic insights in ligand binding and ion-channel gating mechanisms.

Figure 3-1

Amino acid sequence alignment of residues from loop A of members of the LGIC family and AChBP. Sequences of α1, β1, γ and δ subunits from *Torpedo californica* (T. Ca) nAChR, rat subunit α1, β2 and γ2 of the $GABA_A$ receptor, rat $5\text{-}HT_{3A}$ subunit and AChBP were aligned using CLUSTAL W software. Numbering shown is for the *Torpedo* nAChR α1 subunit. The Trp residues (in the open rectangular box) are conserved throughout the different members of the LGIC superfamily. The αTrp86 residue of nAChR has been implicated in the photoaffinity labeling of DDF (Galzi *et al.*, 1990) and is homologous to Trp82 (in AChBP).

		80	81	82	83	84	85	86	87	88	89	90	91	92	93
T.Ca_nAChR	α1	L	P	S	D	D	V	W	L	P	D	L	V	L	Y
T.Ca_nAChR	β1	I	P	S	S	D	V	W	Q	P	D	I	V	L	M
T.Ca_nAChR	γ	I	P	S	E	L	L	W	L	P	D	V	V	L	E
T.Ca_nAChR	δ	L	P	P	E	L	V	W	I	P	D	I	V	L	Q
Rat_$GABA_A$	α1	L	M	A	S	K	I	W	T	P	D	T	F	F	H
Rat_$GABA_A$	β2	R	V	A	D	Q	L	W	V	P	D	T	Y	F	L
Rat_ $GABA_A$	γ2	N	M	V	G	K	I	W	I	P	D	T	F	F	R
Rat_5HT3	A	I	P	T	D	S	I	W	V	P	D	I	L	I	N
AChBP		V	P	I	S	S	L	W	V	P	D	L	A	A	Y

Figure 3-2

Chemical structures of the agonists (A) acetylcholine and (B) suberyldicholine.

A)

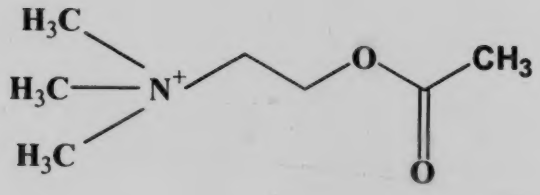

B)

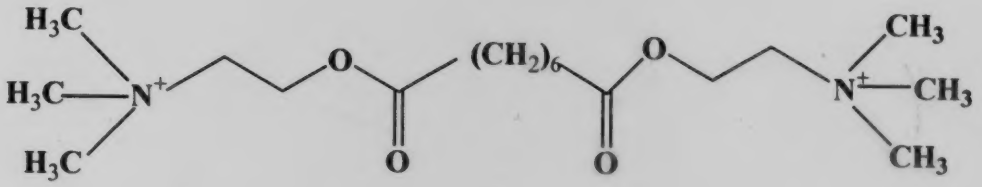

Figure 3-3

The location of αTrp86 from loop A of *Torpedo* nAChR (photolabeled by [^{3}H]DDF, Galzi *et al.*, 1990) based on the crystal structure of AChBP. The illustration is a ribbon representation of α-subunit (yellow) and the neighboring γ- or δ-subunit (blue), perpendicular to the axis of symmetry created using WebLab ViewerLite software (Molecular Simulations Inc). αW86 (in blue) in *Torpedo* nAChR is homologous to W82 in AChBP. αW86 is located distal to the aromatic binding pocket represented here by αY93 (red), αW149 (green) and αY198 (black) and has been predicted not to participate directly in agonist binding (Brejc *et al.*, 2001).

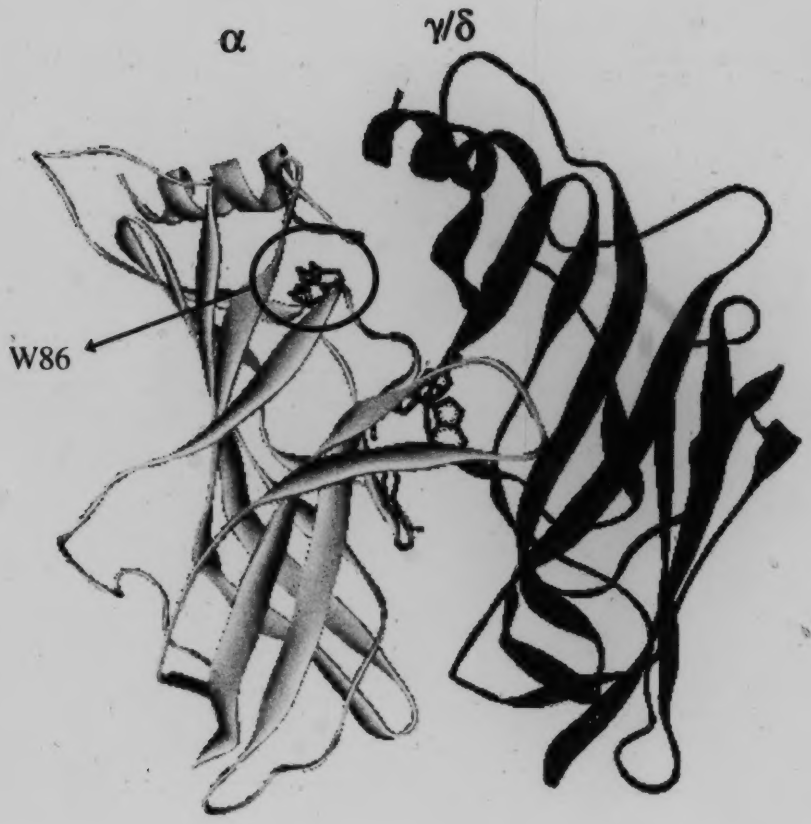
α
γ/δ
W86

Figure 3-4

(A) Zoomed in illustration of Figure 3-3 depicting partial structure of the α-subunit (in yellow) and αW86 (in blue), αY93 (red), αW149 (green) and αY198 (black) residues. (B) Approximate distance between αW86 and the high ACh binding pocket (represented here by αY93) is ~ 15.5Å.

A)

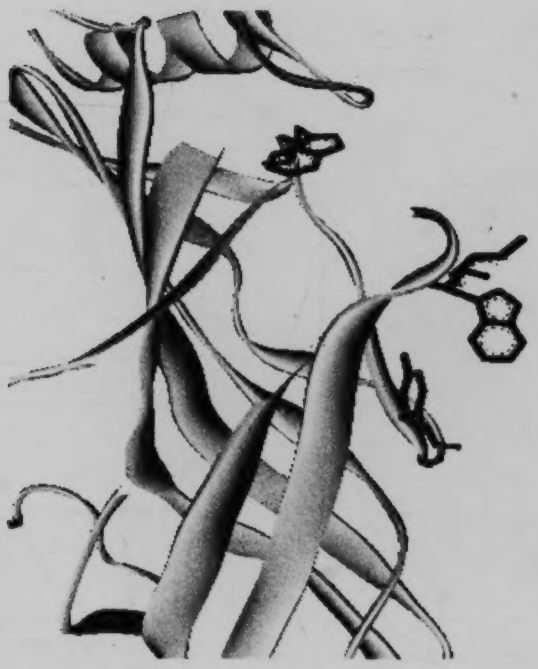

B)

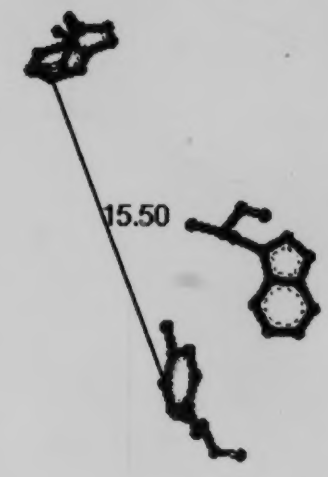

Figure 3-5

Concentration-effect curves for ACh and suberyldicholine (SubDc) in *Xenopus* oocytes expressing wild-type (WT) and αW86F mutant nAChR. (A) ACh activation of WT (■) and αW86F (□) respectively, and (B) SubDc on WT (●) and αW86F (○) respectively. Data normalized to I_{max} for each individual point. The data represents mean ± SEM from at least 3 oocytes. The increase in EC_{50} value for channel activation on the mutant receptor by ACh is subtle (~2-fold) as compared to the ~500-fold shift observed for suberyldicholine. Data for wild type and all mutants are summarized in Table 3-1.

A)

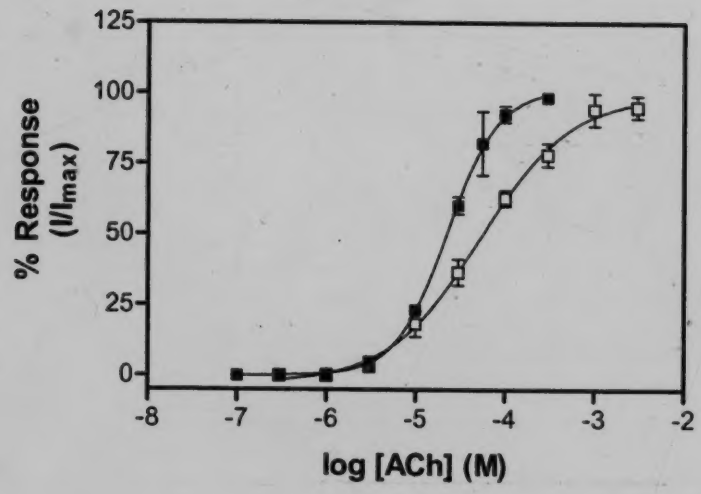
% Response
(I/Imax)
125
100
75
50
25
0
-8
-7
-6
-5
-4
-3
-2
log [ACh] (M)

B)

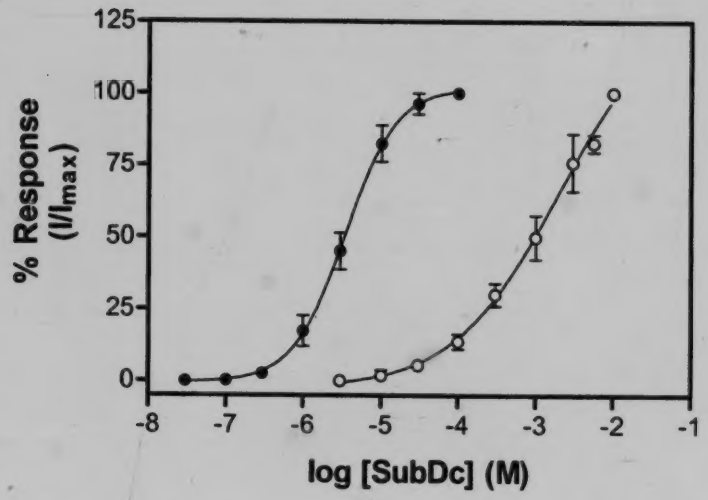
% Response
(I/Imax)
125
100
75
50
25
0
-8
-7
-6
-5
-4
-3
-2
-1
log [SubDc] (M)

Figure 3-6

Representative current traces showing ACh and suberyldicholine (SubDc) activation of *Xenopus* oocytes expressing wild-type (WT) and αW86F mutant nAChR. (A) ACh I_{max} on WT, (B) SubDc I_{max} on WT, (C) ACh I_{max} on αW86F and (D) SubDc I_{max} on αW86F nAChR. I_{max}-evoking concentrations used were from the concentration-effect curves (see Fig. 3-5 A, B). The bar above the current trace represents agonist application.

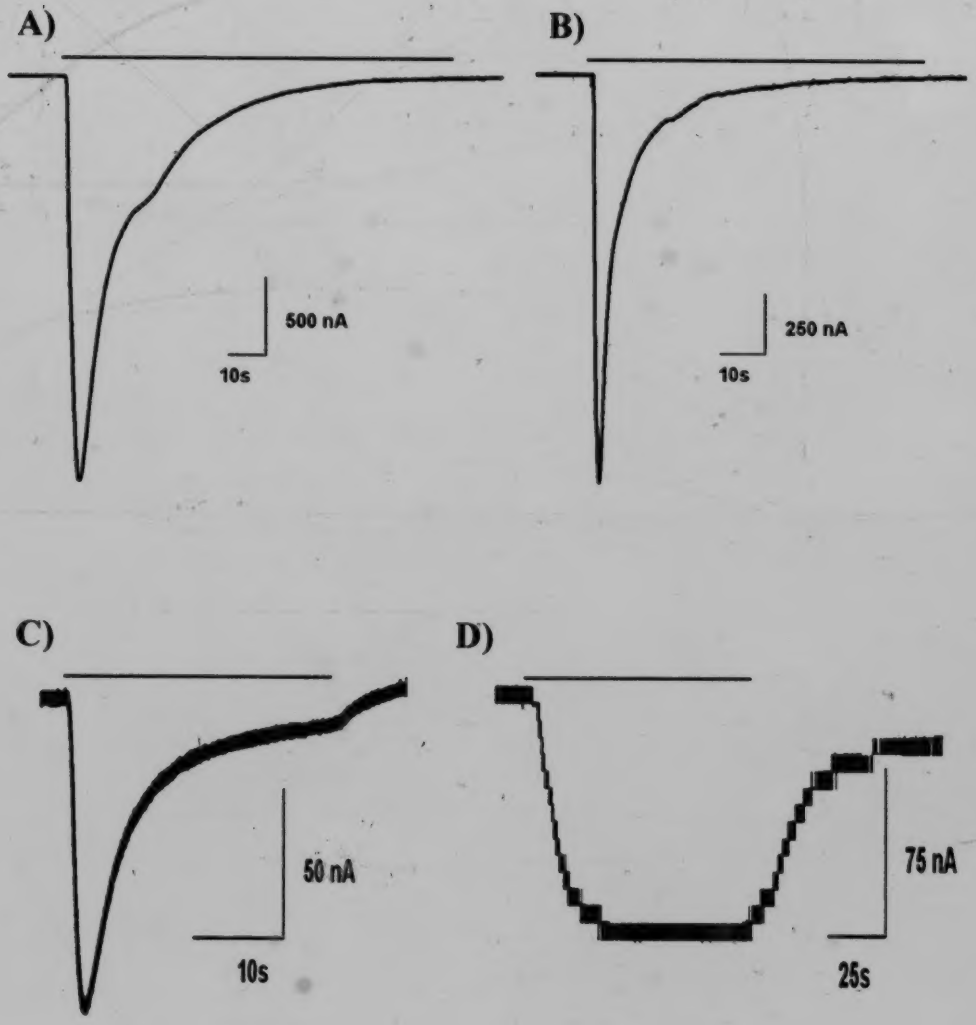
A)
500 nA
10s
B)
250 nA
10s
C)
50 nA
10s
D)
75 nA
25s

Figure 3-7.

Location of conserved proline residues in the vicinity of αTrp86. (A) The illustration is a line ribbon representation of α-subunit (green) depicting αPro21 (blue), αPro88 (black) and αTrp86 (red). (B) αP21 and αP88 are both located within 5Å of αW86. Homologous residues in AChBP are P20 and P84. (C) Amino acid sequence alignment depicting conserved proline residues (in rectangular box) throughout the LGIC family. Numbering shown is for the *Torpedo* nAChR α1 subunit. Homologous residues in the $5HT_3$ receptors, P56 and P123 have been suggested to be crucial for receptor assembly (Deane and Lummis, 2001).

A)

B)

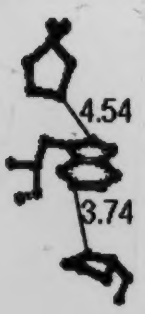

C)

		21	22	23	86	87	88	89
T.Ca_nAChR	α1	P	V	E	W	L	P	D
T.Ca_nAChR	γ	P	A	K	W	L	P	D
T.Ca_nAChR	δ	P	V	K	W	I	P	D
Rat_GABA$_A$	α1	P	G	L	W	T	P	D
Rat_ GABA$_A$	β2	P	D	F	W	V	P	D
Rat_5HT3	A	P	V	R	W	V	P	D
AChBP		P	T	Q	W	V	P	D

Figure 3-8

Concentration dependent inhibition of agonist-evoked currents by dTC in oocytes expressing the wild type and αW86F mutant receptors. (A) affect of dTC on ACh-evoked current in WT (■) and αW86F (□), and (B) affect of dTC on SubDc-evoked current on WT (●) and αW86F (○) respectively. ACh and suberyldicholine concentration used in the experiment corresponded to EC_{50} determined at each receptor except for EC_{90} ACh concentration used in αW86F since evoked-currents were quite small in these mutant receptors. Each curve was generated from at least three independent oocytes. The apparent K_I is obtained from IC_{50} values using Cheng-Prusoff equation. The protocol is described in the "Material and Methods" section.

A)

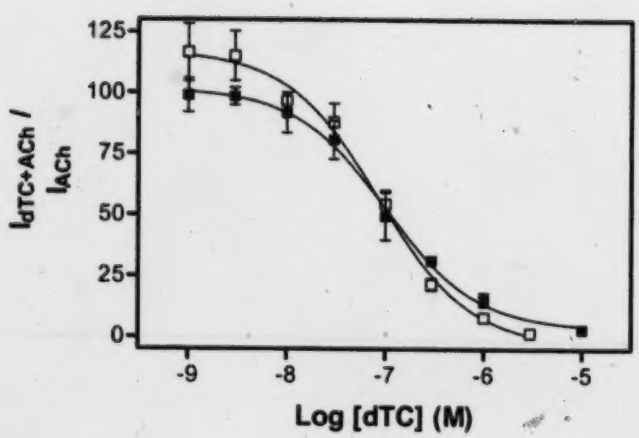
125
100
75
50
25
0
-9
-8
-7
-6
-5
Log [dTC] (M)
I dTC+ACh / I ACh

B)

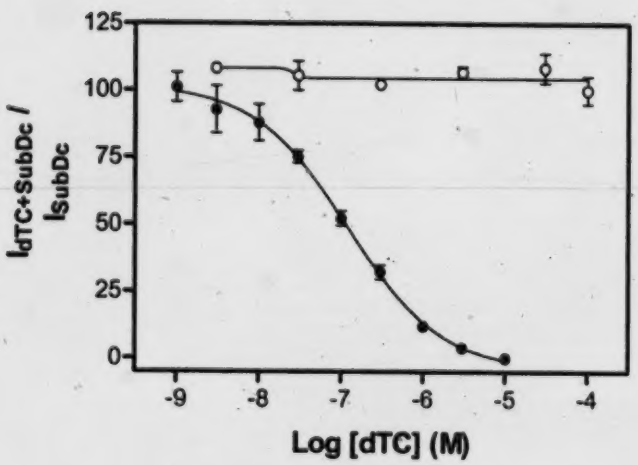
125
100
75
50
25
0
-9
-8
-7
-6
-5
-4
Log [dTC] (M)
I dTC+SubDc / I SubDc

Figure 3-9

Surface nAChR expressed in *Xenopus* oocytes labeled with [^{125}I]α-BgTx. Maximum ACh-evoked currents (I_{max}) were determined using concentrations determined from concentration-effect curves (as shown in Fig. 3-5) using two-electrode voltage clamp technique. Surface receptor levels were determined in the same oocyte by measuring the [^{125}I]α-BgTx binding as described in "Materials and Methods". Data represents mean ± SEM of 3-14 determinations from individual oocytes and are presented in Table 3-3.

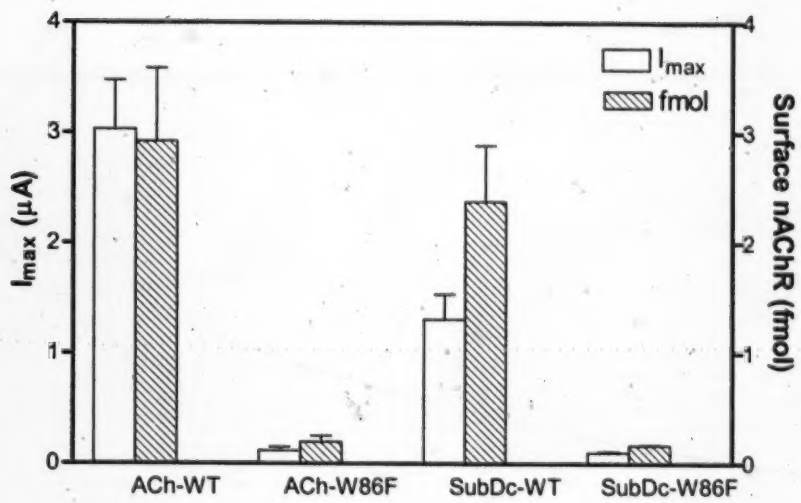
I_{max}
fmol
I_{max} (μA)
Surface nAChR (fmol)
0
1
2
3
4
ACh-WT
ACh-W86F
SubDc-WT
SubDc-W86F

Figure 3-10

Suberyldicholine binding to *Torpedo* nAChR expressed on surface of *Xenopus* oocytes. Binding studies were done on intact oocytes as described in "Materials and Methods". in Chapter 2. SubDc inhibited the initial rate of [^{125}I]α-BgTx binding in a concentration dependent manner in WT (■) with an IC_{50} of ~ 66 nM. Low receptor expression in oocytes expressing the αW86F mutant nAChR precluded its characterization. The data represent the mean ± SEM of two determinations performed in duplicate.

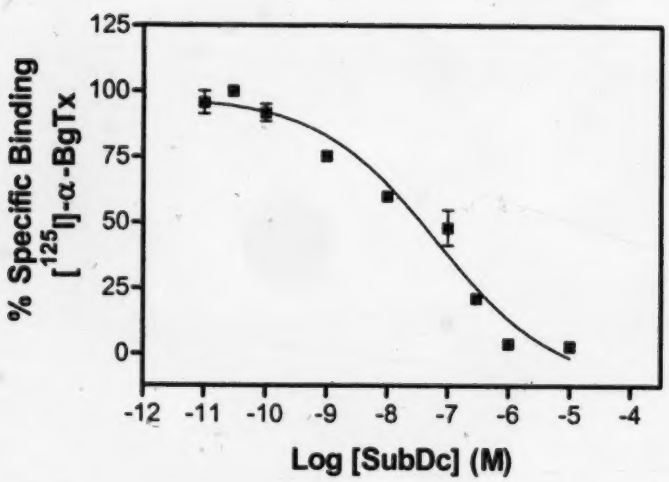
% Specific Binding
[125I]-α-BgTx
125
100
75
50
25
0
-12
-11
-10
-9
-8
-7
-6
-5
-4
Log [SubDc] (M)

TABLE 3-1

Concentration-effect data for ACh and suberyldicholine activation of the wild type and mutant receptors expressed in Xenopus *oocytes*

	Log EC_{50} ± SEM (M)	EC_{50} (μM)	n_H ± SEM	EC_{50}Mut/ EC_{50}WT
ACh				
WT	-4.614 ± 0.04 (9)	24.3	1.6 ± 0.1	1
αW86A	NR	NR		-
αW86F	-4.28 ± 0.08 (4)	52.5	0.9 ± 0.1**	2.2
Suberyldicholine				
WT	-5.471 ± 0.08 (3)	3.38	1.4 ± 0.04	1
αW86A	ND	ND		-
αW86F	-2.774 ± 0.16 (5)**	1680	0.7 ± 0.04**	500

Data represent the mean ± SEM. Values for log EC_{50} and Hill coefficient (n_H) were determined from concentration-effect curves using GraphPad Prism software. The log EC_{50} and Hill coefficient values from individual oocytes were averaged to generate final mean estimates. The value in parenthesis is the number of oocytes used for each receptor type. NR – no response with up to 10 mM ACh. ND - not determined. Statistical analysis performed by comparing the log EC_{50} and n_H of the mutant receptors to the wild-type nAChR using one-way ANOVA followed by Dunnett's post test. **$p<0.001$

TABLE 3-2

Apparent K_I values for dTC inhibition of ACh and suberyldicholine evoked currents in wild type and mutant receptors expressed in Xenopus *oocytes*

	Log IC_{50} ± SEM (M)	Log IC_{50} (nM)	App K_I (nM)
ACh			
WT	-7.071 ± 0.11 (4)	85	41.5
αW86F	-7.055 ± 0.23 (3)	88	4.5
Suberyldicholine			
WT	-6.925 ± 0.05 (3)	120	58.3
αW86F	No Inhibition		

TABLE 3-3

Surface expression and normalized maximum current seem in wild type and mutant receptors expressed in Xenopus *oocytes*

	Surface Binding (fmol/oocyte ± SEM)	I_{max} (nA ± SEM)	Normalized Peak Current (nA/fmol)	% Peak Current (MutI_{max}/WT I_{max})
ACh				
WT	2.9 ± 0.7 (14)	3030 ± 440	1045	100
αW86A	NB	NR		
αW86F	0.2 ± 0.05 (7)	117 ± 32	585.0	56
Suberyldicholine				
WT	2.4 ± 0.5 (3)	1310 ± 230	545.8	100
αW86A	ND	ND		
αW86F	0.17 ± 0.01 (3)	100 ± 20	588.2	107

All oocytes were injected with 50ng of cRNA. The value in parentheses is the number of oocytes used for each receptor type. NB- no binding of [^{125}I]α-BgTx was observed. NR- no response observed in functional studies with up to 10 mM ACh. ND- not determined.

BIBLIOGRAPHY

AMIN, J. AND WEISS, D.S. (1993). $GABA_A$ receptor needs two homologous domains of the beta-subunit for activation by GABA but not by pentobarbital. *Nature*, **366**, 510-511.

ARIAS, H.R. (2000). Localization of agonist and competitive antagonist binding sites on nicotinic acetylcholine receptor. *Neurochem. Int.*, **36**, 595-645.

BARNARD, E. A., MILEDI, R. AND SUMIKAWA, K. (1982). Translational of exogenous messenger RNA coding for nicotinic acetylcholine receptors produces functional receptors in *Xenopus* oocytes. *Proc. R. Soc. Lond . B.*, **215**, 241-246.

BLOUNT, P. AND MERLIE, J.P. (1989). Molecular basis of the two nonequivalent ligand binding sites of the muscle nicotinic acetylcholine receptor. *Neuron*, **3**, 349-357.

BREJC, K., DIJK, W.J.V., KLAASSEN, R.V,, SCHUURMANS, M., OOST, J.V.D., SMIT, A.B. AND SIXMA, T.K. (2001). Crystal structure of an ACh-binding protein reveals the ligand-binding domain of nicotinic receptors. *Nature*, **411**, 269-276.

CHENG, Y. AND PRUSOFF, W.H. (1973). Relationship between the inhibition constant (K1) and the concentration of inhibitor which causes 50 per cent inhibition (I50) of an enzymatic reaction. *Biochem. Pharmacol.*, **22**, 3099-3108.

COLQUHOUN, D. (1998). Binding, gating, affinity and efficacy: the interpretation of structure-activity relationships for agonists and of the effects of mutating receptors. *Br. J. Pharmacol.*, **125**, 924-947.

CONTI-TRONCONI, B.M. AND RAFTERY, M.A. (1982). The nicotinic cholinergic receptor: Correlation of molecular structure with functional properties. *Ann. Rev. Biochem.*, **51**, 491-530.

CORRINGER, P.J., LE-NOVÈRE, N. AND CHANGEUX, J.-P. (2000). Nicotinic receptors at the amino acid level. *Ann. Rev. Pharmacol. Toxicol.*, **40**, 431-458.

DEANE, C.M. AND LUMMIS, S.C. (2001). The role and predicted propensity of conserved proline residues in the 5-HT3 receptor. *J. Biol. Chem.*, **276**, 37962-37966.

DENNIS, M., GIRAUDAT, J., KOTZYBA-HIBERT, F., GOELDNER, M., HIRTH, C., CHANG, J.Y., LAZURE, C., CHRETIEN, M. AND CHANGEUX, J.-P. (1988). Amino acids of the *Torpedo marmorata* acetylcholine receptor alpha subunit labeled by a photoaffinity ligand for the acetylcholine binding site. *Biochem.*, **27**, 2346-2357.

DIONNE, V.E., STEINBACH, J.H. AND STEVENS, C.F. (1978). An analysis of the dose-response relationship at voltage-clamped frog neuromuscular junctions. *J. Physiol.*, **281**, 421-444.

DOUGHERTY, D.A. AND STAUFFER, D.A. (1990). Acetylcholine binding by a synthetic receptor: Implications for biological recognition. *Science*, **250**, 1558-1560.

DREYER, F., PEPER, K. AND STERZ, R. (1978). Determination of dose-response curves by quantitative ionophoresis at the frog neuromuscular junction. *J. Physiol.*, **281**, 395-419.

DUNN, S.M.J. (1993). Structure and function of the nicotinic acetylcholine receptor. *Adv. Struc. Biol.*, **2**, 225-244.

DUNN, S.M.J. AND RAFTERY, M.A. (1993). Cholinergic binding sites on the pentameric acetylcholine receptor of *Torpedo californica*. *Biochem.*, **32**, 8608-8615.

DUNN, S.M.J. AND RAFTERY, M.A. (1997a). Agonist binding to the *Torpedo* acetylcholine receptor. 1. Complexities revealed by dissociation kinetics. *Biochem.*, **36**, 3846-3853.

DUNN, S.M.J. AND RAFTERY, M.A. (1997b). Agonist binding to the *Torpedo* acetylcholine receptor. 2. Complexities revealed by association kinetics. *Biochem.*, **36**, 3854-3863.

DUNN, S.M.J. AND RAFTERY, M.A. (2000). Roles of agonist-binding sites in nicotinic acetylcholine receptor function. *Biochem. Biophys. Res. Commun.*, **279**, 358-362.

FORMAN, S.A., FIRESTONE, L.L. AND MILLER, K.W. (1987). Is agonist self-inhibition at the nicotinic acetylcholine receptor a nonspecific action? *Biochem.*, **26**, 2807-2814.

GALZI, J.-L., REVAH, F., BLACK, D., GOELDNER, M., HIRTH, C. AND CHANGEUX, J.-P. (1990). Identification of a novel amino acid alpha-tyrosine 93 within the cholinergic ligands-binding sites of the acetylcholine receptor by photoaffinity labeling. Additional evidence for a three-loop model of the cholinergic ligands-binding sites. *J. Biol. Chem.*, **265**, 10430-10437.

GOLDIN, A.L. AND SUMIKAWA, K. (1992). Preparation of RNA for injection into *Xenopus* oocytes. *Methods Enzmol.*, **207**, 279-297.

GRUTTER, T. AND CHANGEUX, J.-P. (2001). Nicotinic receptors in wonderland. *Trends Biochem. Sci.*, **26**, 459-463.

KAO, P.N., DWORK, A.J., KALDANY, R.R., SILVER, M.L., WIDEMAN, J., STEIN, S. AND KARLIN, A. (1984) Identification of the alpha subunit half-cysteine specifically labeled by an affinity reagent for the acetylcholine receptor binding site. *J. Biol. Chem.*, **259**, 11662-11665.

KARLIN, A. (2002). Emerging structure of the nicotinic acetylcholine receptors. *Nature Neurosci.*, **3**, 102-114.

MIDDLETON, R.E. AND COHEN, J.B. (1991). Mapping of the acetylcholine binding site of the nicotinic acetylcholine receptor: [3H]nicotine as an agonist photoaffinity label. *Biochem.*, **30,** 6987-6997.

MILEDI, R. (1980). Intracellular calcium and the desensitization of acetylcholine receptors. *Proc. R. Soc. Lond. B.*, **209**, 447-452.

PASQUALE, E.B., TAKEYASU, K., UDGAONKAR, J.B., CASH, D.J., SEVERSKI, M.C. AND HESS, G.P. (1983). Acetylcholine receptor: evidence for a regulatory binding site in investigations of suberyldicholine-induced transmembrane ion flux in Electrophorus electricus membrane vesicles. *Biochem.*, **22**, 5967-5973.

PEDERSON, S.E. AND COHEN, J.B. (1990). *d*-Tubocurarine binding sites are located at α-γ and α-δ subunit interfaces of the nicotinic acetylcholine receptor. *Proc. Nat. Acad. Sci., USA.*, **87**, 2785-2789.

RAFTERY, M.A., HUNKAPILLER, M.W., STRADER, C.D. AND HOOD, L.E. (1980). Acetylcholine receptor: Complex of homologous subunits. *Science,* **208,** 1454-1456.

RAFTERY, M.A., DUNN, S.M.J., CONTI-TRONCONI, B.M., MIDDLEMAS, D.S. AND CRAWFIRD, R.D. (1983). The nicotinic acetylcholine receptor: subunit structure, functional binding sites, and ion transport properties. *Cold Spring Harb. Symp. Quant. Biol.*, **48**, 21-33.

SPIER, A.D. AND LUMMIS, S.C. (2000). The role of tryptophan residues in the 5-Hydroxytryptamine(3) receptor ligand binding domain. *J. Biol. Chem.*, **275**, 5620-55625.

SRINIVASAN, S., NICHOLS, C.J., LAWLESS, G.M., OLSEN, R.W., TOBIN, A.J. (1999). Two invariant tryptophans on the alpha1 subunit define domains necessary for GABA(A) receptor assembly. *J. Biol. Chem.*, **274**, 26633-26638.

SULLIVAN, D.A. AND COHEN, J.B. (2000). Mapping the agonist binding site of the nicotinic acetylcholine receptor. Orientation requirements for activation by covalent agonist. *J. Biol. Chem.*, **275,** 12651-12660.

TAMAMIZU, S., GUZMAN, G.R., SANTIAGO, J., ROJAS, L.V., MCNAMEE, M.G. AND LASALDE-DOMINICCI, J.A. (2000). Functional effects of periodic tryptophan substitutions in the α M4 transmembrane domain of the *Torpedo californica* nicotinic acetylcholine receptor. *Biochem.*, **39**, 4666-4673.

ZHONG, W., GALLIVAN, J.P., ZHANG, Y., LI, L., LESTER, H.A. AND DOUGHERTY, D.A. (1998). From *ab initio* quantum mechanics to molecular neurobiology: a cation-pi binding site in the nicotinic receptor. *Proc. Natl. Acad. Sci. USA*, **95,** 12088-12093.

CHAPTER 4

General Discussion and Conclusions

GENERAL DISCUSSION

The present day knowledge of the nicotinic acetylcholine receptor as a complex allosteric protein has been achieved by many years of technological and conceptual advances. The information accumulated over the years is extensive and it is not possible here to discuss many of the important contributions. However, some examples that are listed below are an attempt to place previous work in the context of our current understanding of the receptor. The early era (1950's to early 70s) used classical pharmacology/physiology approaches to study the nAChRs at the frog neuromuscular junction. Later, in conjunction with voltage clamp techniques, these studies helped to elucidate some aspects of neurotransmitter binding and the consequent depolarization of the receptor (Katz and Thesleff, 1957; Dreyer and Peper, 1975; Dreyer *et al.*, 1978; Dionne *et al.*, 1978). The mid 1970's to late 80's witnessed the extensive use of biochemical techniques to determine the structural components of the nAChR. Although the subunit composition was controversial for many years, the N-terminal sequencing of the *Torpedo* nAChR subunits and the subsequent cloning of all receptor subunits (Raftery *et al.*, 1980; Noda *et al.*, 1982; 1983; Ballivet *et al.*, 1982) provided a new understanding of nAChR structure. During the same time period the development of patch-clamp techniques by Sakmann and colleagues (Neher and Sakmann, 1976; Saxmann *et al.*, 1980) provided researchers with a powerful tool to study receptor activation properties at the single channel level.

The 1980s through 1990s marked a new era in our ability to identify key structural elements of the receptor and how these were involved in receptor function. This was possible largely due to extensive biochemical characterization of nAChR, abundantly

available from *Torpedo* electric organ. Further characterization of the receptor has been facilitated by the availability of cloned nAChR subunits together with the advent of molecular biology techniques (e.g. site-directed mutagenesis) and the establishment of heterologous expression system (e.g. *Xenopus* oocytes).

The first documented use of *Xenopus* oocytes as an expression system dates back to 1971 when Gurdon and colleagues (Gurdon *et al.*, 1971) demonstrated its ability to synthesize the globin protein from foreign mRNA. The large size of the *Xenopus* oocyte (~1.2mm) makes it amenable to electrophysiogical analysis of recombinant receptors and more recently for radioligand assays. Many different ion channels and receptors have since been successfully expressed in *Xenopus* oocytes, including the nAChR as the first of the LGIC family (Sumikawa *et al.*, 1981). This landmark paper demonstrated that microinjection of heterologous nAChR mRNA (extracted from the electric organ of *Torpedo*) into oocytes led to expression of α-BgTx binding nAChRs in the oocyte membrane. Soon after, the same group demonstrated that only the extracellular application of ACh could activate these expressed receptors, suggesting that they were efficiently assembled in the membrane (Barnard *et al.*, 1982). Shortly thereafter, subunit cloning and the expression of the recombinant wild type and mutant nAChRs helped to identify regions of the protein that are important for conferring functional properties (Mishina *et al.*, 1985). Oocytes have become a model for studying exogenously expressed ion channels that have no natural role in the development and function of the oocyte. The high translational capacity, ability to express receptors from their encoding cRNAs or cDNAs and the relative scarcity of endogenous ion channels in the oocyte membrane make it a versatile tool for the study a range of heterologously

expressed ion channel and receptor proteins (reviewed by Colman, 1984; Dascal, 1987; Quick and Lester, 1994; Theodoulou and Miller, 1995).

Like any heterologous expression system, the *Xenopus* oocyte has its share of limitations. Oocytes exhibit seasonal variations that affect the levels of protein expression. Furthermore, there can be significant variation in receptor proteins levels seen within and across different batches of oocytes. We attempted to address this issue in individual oocytes by correcting the peak ACh evoked current to the receptor expression level (as determined by toxin binding) (nA/fmol) to give us a more reliable estimate of peak conductances (see Chapter 2). However, there is no assurance that all receptors detected by binding represent functional receptors. Another area of concern is the presence of endogenous muscarinic acetylcholine receptors in the oocyte membrane (Kusano *et al.*, 1982; Barnard *et al.*, 1982). Such receptors can interfere with the analysis and interpretation of small currents from exogenous ion channels. To overcome this, for electrophysiological recordings on the *Torpedo* nAChR expressed in oocytes, we added 1μM atropine to block any muscarinic AChRs present.

Since *Xenopus* oocytes must be individually injected, they are not readily suited for radioligand binding studies, as hundreds of oocytes would have to be injected to harvest sufficient amounts of membrane-bound receptor. In the studies described in this thesis, the inability of recombinant nAChR to be adequately expressed in a suitable mammalian cell line (see Introduction) made *Xenopus* oocytes a favored choice for expression studies. In addition, *Torpedo* nAChR express and function well at 16-22°C (Eertmoed *et al.*, 1998), a temperature range that is ideal for use of oocytes.

Most of the current knowledge on functional correlation with the structure of the nAChR has been generated by the use of mutant receptors. Site-directed mutagenesis experiments are routinely used to probe the role of specific residues of the receptor involved in channel function. Amino acids identified through biochemical means were the initial targets in mutagenesis studies and these complementary approaches have proven to be a powerful approach in characterizing the contribution of individual amino acids to ligand recognition. However, not all residues are susceptible to photoaffinity labeling and hence there may be additional regions in the receptor that also interact with the ligand. In addition, findings from mutational studies should be interpreted with caution as there exists a possibility of the mutant receptor producing global structural changes rather than just a localized change in the primary sequence of the region of interest and consequently the observed alterations in function could be wrongly attributed to a specific region. Perhaps, the biggest limitation of mutagenesis experiments is that it is difficult to determine whether the alteration in ligand sensitivity is directly attributable to the mutated residue to or is an allosteric, indirect influence of the that residue. Furthermore, it is difficult to predict whether the mutated region has altered the affinity of the ligand to bind or effected a step subsequent to binding i.e. channel gating. Since, binding and gating are inter-dependent processes, they are difficult to separate experimentally (Colquhoun, 1998).

Although the use of two-electrode voltage clamp techniques to measure whole cell currents precludes making detailed kinetic interpretations and cannot replace the rigorous analysis possible with single channel recordings, it is a good starting point to

investigate ligand concentration dependent activation of receptor that can lead to further detailed characterization.

A related approach that has been used by a number of researchers is the substituted cysteine accessibility method (SCAM) and this can provide information about binding site residue(s) that makes contact with the ligand (reviewed by Karlin and Akabas, 1995; Karlin, 2002). This approach could help in providing additional information on residues investigated in this thesis i.e. whether residues from loop D (i.e. Arg55) and loop A (i.e. Trp86) of the α-subunit are involved directly in associating with ligands. However, SCAM studies are not exempt from the limitations of mutagenesis studies. A similar approach that was recently employed to predict secondary structural feature in the ε-subunit is lysine scanning mutagenesis (Sine *et al.*, 2002). Such techniques in conjunction with homology modeling based on the atomic structure of AChBP can shed light on the orientation of residues towards either the hydrophobic core or the hydrophilic surface.

The use of unnatural amino acid substitution of aromatic residues has been employed as an extension of site-directed mutagenesis studies to predict residues that associate with agonists (reviewed by Beene *et al.*, 2003). The attachment of a tethered agonist to the unnatural amino acid has been exploited to map residues that can directly associate with ligands. In one such elegant study, the replacement of αTrp149 by a tyrosine derivative with a tethered quaternary ammonium groups ($Tyr\text{-}O\text{-}(CH_2)_3\text{-}N(CH_3)_3^+$) resulted in a constitutively active receptor (Zhong *et al.*, 1998). The use of such innovative approaches can further help in mapping ligand-binding residues.

A major challenge in interpretation of mutational studies involving the α-subunits of *Torpedo* nAChR is the non-equivalence of the two 'classical' binding sites as a consequence of the different subunits adjacent to the α-subunits. These two binding sites have different affinities for some ligands (see Introduction). Hence, it cannot be definitely stated which interface is responsible for the altered sensitivity of the mutant receptor. The use of concatenated subunits (C-terminal of one subunit covalently linked to the N-terminal of the preceding subunit) permits the targeted introduction of a mutation in one specific subunit and can help in probing the influence of a positional mutation (reviewed by Minier and Sigel, 2004). This approach could help in further characterizing mutations at the γ-α subunit interface (and possibly β-α interface) of the *Torpedo* nAChR (see Chapter 2).

A major advance in the understanding of structure-function relationships of the nAChR has been the elucidation of the crystal structure of the AChBP (Brejc *et al.*, 2001). The AChBP structure has reinforced long-held predictions about the extracellular domain of nAChR (see Introduction). The AChBP structure now provides us with a template for comparative modeling of subunits of the LGIC family (Le Novère *et al.*, 2002; Sine, 2002; Sine *et al.*, 2002; Ernst *et al.*, 2003). A recent study using computational docking of agonists to a three-dimensional model of nAChR (based on AChBP structure) has predicted structural requirements for an agonist-bound state (Le Novère *et al.*, 2002). These studies have suggested that the agonist-binding pocket has a high degree of conservation and all the residues identified earlier by labeling and mutagenesis studies are localized to a cavity of 10-12Å in diameter. However, it should be noted that although the crystal structure of AChBP was characterized in the absence

of a ligand, a HEPES molecule (present in the crystallization buffer) was bound in the binding site. Since HEPES contains a positively charged quaternary ammonium group and thus may place the crystallized protein in an agonist bound state, it is not clear as to which conformation of the nAChR it might correspond. There have, however, been some suggestions that the AChBP structure corresponds to the desensitized conformation of nAChR (Grutter and Changeux, 2001). Since the nAChR must undergo conformational transitions upon agonist binding with a changing affinity for ligands, it is unclear whether the same residues that stabilize the desensitized high affinity state are also involved in the early stages of ligand recognition. Hence all predictions based on comparative modeling with AChBP should be interpreted with caution.

Exploitation of the AChBP structure has provided us with a starting point to make predictions of structure-function correlations of the LGIC family. One method as described earlier includes computational docking of ligands to the modeled 3-dimensional binding site. This, in combination with *in silico* mutagenesis, can help to identify residues that can potentially be involved ligand recognition. This would be a starting point for experimental mutagenesis and functional characterization of the mutant receptors. In this regard, advances in higher-throughput electrophysiology can be a very useful. For example, the Roboocyte system (Schnizler *et al.*, 2003) permits the automation of both cRNA injection and two-electrode voltage clamp recordings from multiple oocytes in standard 96-well plates.

The elucidation of structure of the extracellular binding region in both the closed (desensitized) and open (active) is going to be the focus of intense research in the near

future and this would help in solving the many unresolved mysteries of receptor transitions associated with synaptic transmission.

CONCLUSIONS AND FUTURE DIRECTIONS

My findings on the role of the Arg residue at position 55 from loop D of the α-subunit (Chapter 2) in channel function demonstrate that mutations of this residue (αR55F and αR55W) result in modest but significant rightward shifts (~5-6-fold) in the concentration-effect curves of ACh-induced channel activation and also cause a reduction in the maximum agonist-induced currents of these mutant receptors. Furthermore, the partial agonist, PTMA acted as an antagonist on these mutant receptors. Although, it would be tempting to speculate that αArg55 is important for modulating agonist sensitivity, based on the current data, it is not possible to determine whether the results are due to a specific change in ligand recognition or are a secondary consequence of global alterations in the structure of the receptor. However, the unaltered apparent affinity of the competitive antagonist, dTC on the mutants suggests that the effects of these mutations are ligand-specific and not due to a non-specific alteration in global structure of the receptor. The affinity of ACh at these mutant receptors (as determined by inhibition of initial rate of toxin binding) was not different from the wild-type nAChR. These results suggest that αArg55 does not alter high affinity ACh-binding, consistent with the notion that this residue is not part of the 'classical' high affinity binding site.

The main objective of the study (Chapter 2) was to identify putative low-affinity sites that are predicted to be important for channel activation (see Introduction). The

primary rationale for choosing the Arg residue at position 55 (from loop D) of the α-subunit was that it is positively charged unlike the conserved aromatic residues that are present at the homologous position in all other subunits of the LGIC family. Intuitively, it might be predicted that the positive charge of αArg55 could reduce agonist affinity through repulsion of the charge on the quaternary ammonium group of the ligand. This would result in this site being of relatively lower affinity for ACh. However, the lack of any significant effect of the charge reversal mutation at this residue (αR55E) ruled out the contribution of a direct charge interaction between the agonist molecule and this residue. However, there still exists the possibility that an aromatic or negatively charged residue(s) from the adjacent subunit (i.e. γ- or β-subunit) provides an anionic environment for ACh interaction. In studying this possibility, homology modeling (based on AChBP) showed that the γ-subunit residue, Glu 93 (from loop A; homologous to αTyr93) is in reasonable proximity close to αArg55. Mutation of γGlu93 (γE93R) resulted in an increase in ACh potency (~8-fold reduction in EC_{50} for channel activation). In contrast, the double mutation (γE93R-αR55F) restored ACh potency to wild-type levels, suggesting a counter-balancing influence in stabilizing the interaction with the agonist.

Channel activation has been suggested to involve rotational movements of the α-subunits towards the neighboring subunits (Miyazawa *et al.*, 2003). Additional interfaces (e.g. γ-α as investigated here) may therefore, play a crucial role in inter-subunit interactions during the channel activation process. Although we are limited in our ability to interpret the findings presented here, further studies are warranted using a series of substitutions at the γGlu93 to investigate whether this residue is crucial *per se*

or its charge has a role to play in modulating channel function. Future studies might also include investigating the contributions of residues from loops B and C of the γ-subunit as well as the residues in homologous positions of the β-subunit. Lysine scanning mutagenesis experiments of residues in the ε-subunit (homologue of γ-subunit) have suggested that W55 and E93 (at equivalent position to αR55 and γE93) are located on β-strands and project towards the protein surface hydrophilic environment rather than the hydrophobic core (Sine *et al.*, 2002). These results raise the possibility that these residues have the potential to associate with agonists approaching the receptor from the outside surface. In conclusion, our present findings show that residues at hitherto unexplored interfaces i.e. γ-α and/or β-α (see Fig. 1-2) modulate agonist activation. It remains to be established whether these interfaces are involved in forming distinct agonist binding sites.

Chapter 3 describes the identification of a binding site residue that is important for the action of the bisquaternary ligand, suberyldicholine. Bisquaternary ligands have been shown to have unusual binding interactions with the *Torpedo* nAChR (Dunn and Raftery, *et al.*, 1997a,b). Based on kinetic studies, it was suggested that suberyldicholine, by virtue of its two quaternary ammonium groups (approximately 16 Å apart) can cross-link separate binding sites. Molecular modeling based on the AChBP crystal structure, revealed the presence of αTrp86 located ~15Å from the high affinity ACh binding site e.g. αTyr93. Mutational analysis of αTrp86 (αW86F) demonstrated a selective increase in the EC_{50} for suberyldicholine-induced channel activation (~ 500-fold) while the EC_{50} of ACh was not significantly affected. This study clearly shows that αTrp86 plays a crucial role in receptor activation by suberyldicholine. Furthermore,

suberyldicholine-evoked currents in this mutant failed to desensitize and were insensitive to inhibition by dTC. These findings further confirm the prediction that αTrp86 is not located within a general binding pocket that accommodates both ACh and suberyldicholine. These results can be interpreted in context of earlier findings that each of the high affinity sites of nAChR is made up to two "subsites" and that αTrp86 contributes the second subsite for suberyldicholine.

Future characterization to map the distances between these putative subsites has been initiated by using a series of bisquaternary ligands with different interonium chain lengths (see Fig. 4-1A,B). Preliminary electrophysiological characterization of wild-type nAChR expressed in *Xenopus* oocytes has revealed significant effect of chain length on agonist potencies (see Fig. 4-2A,B). Compounds with longer chain length (methyl groups ≥ 4 with an interonium distance of ~ 15Å and above) are potent agonists on the wild type nAChR while shorter chain length ligands (e.g. succinylcholine) are significantly less potent and efficacious. The screening of these bisquaternary agonists on the αTrp86 mutant receptor (αW86F) could help to map binding sites distances and shed light on the structural determinants of the ligand potency.

A major problem encountered with the αW86F mutant receptors was the small size of currents observed in electrophysiological studies as a consequence of reduced receptor surface expression level. Screening of poor partial agonists such as succinylcholine (see Fig. 4-2B) may further exacerbate this problem. An alternative to the conventional mutagenesis undertaken here could be to employ the use of unnatural amino acid substitution (discussed earlier). In addition, low receptor expression levels of the mutant receptor in oocytes precluded its biochemical characterization. The use of

a suitable cell line (e.g. a fish cell line) may serve as an alternative heterologous expression system to permit radioligand binding experiments on these mutants.

Another approach that could be undertaken for further detailed characterization of the mutant receptors engineered is the analysis of single channel currents at a microscopic level using patch-clamp techniques. Oocytes can be used for patch-clamping (reviewed by Dascal, 1987; Quick and Lester 1994; Stühmer and Parekh, 1995) and more detailed kinetic characterization of mutant receptors would undoubtedly enhance the understanding of the processes involved in receptor activation and desensitization.

In conclusion, the data presented in this thesis show that elucidation of structural determinants for ligand binding to mutant nAChRs using a multidisciplinary approach will allow correlation with functional consequences and thereby enhance our understanding of the fundamental but poorly understood process of neurotransmission. The knowledge assimilated from the nAChR, the prototype of the LGIC family, can be extrapolated to other members of this family and this could have far reaching implications. The eventual determination of the crystal structure of the nAChR will be important to establish a clearer picture of the receptor and help to address various unanswered questions about receptor structure-function relationships.

Figure 4-1

Chemical structure of a generic bisquaternary agonist. (A) Depicted are the two quaternary ammonium groups separated by methyl group of various chain lengths, represented by "X". (B) Bisquaternary ligands represented by their methyl chain length and estimated interonium distance. Suberyldicholine and succinylcholine were purchased from Sigma chemical. All other compounds were a gift from Dr. William F. Dryden, Department of Pharmacology, University of Alberta, Edmonton.

A)

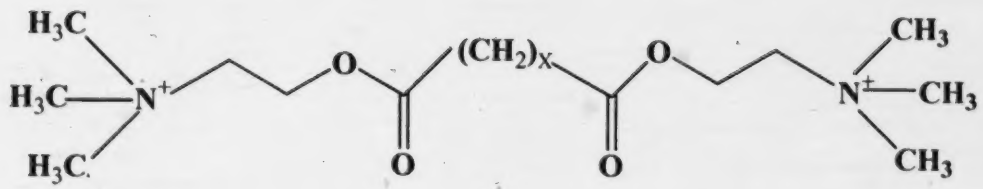

B)

Bisquaternary Ligand	X	~ Interonium Distance (Å)
Succinylcholine	2	13.2
Glutaryldicholine	3	14.5
Adipyldicholine	4	15.7
Suberyldicholine	6	18.0
Azelyldicholine	7	19.5

Figure 4-2

Activation of wild type nAChR by bisquaternary agonists. (A) Concentration-effect curves for bisquaternary agonists, azelyldicholine (■), suberyldicholine (□), adipyldicholine (✱), succinylcholine (●) and glutaryldicholine (◇) activation of *Xenopus* oocytes expressing wild-type nAChR. Data for each individual point are normalized to I_{max}. The data represent mean ± SEM from at least 2-3 oocytes. The potency order for channel activation by these compounds is: azelyldicholine > suberyldicholine > adipyldicholine > succinylcholine > glutaryldicholine. (B) Maximal responses (I_{max}) for the bisquaternary ligands compared to that of ACh. I_{max} for a particular bisquaternary agonist and ACh were determined on the same oocyte expressing wild type receptors using concentrations established from concentration-effect curves. The efficacy order of these agonists is: azelyldicholine (AzDc) > adipyldicholine (AdPc) > suberyldicholine (SubDc) > glutaryldicholine (Glu) > succinylcholine (Scc). Data for the agonists are summarized in Table 4-1.

A)

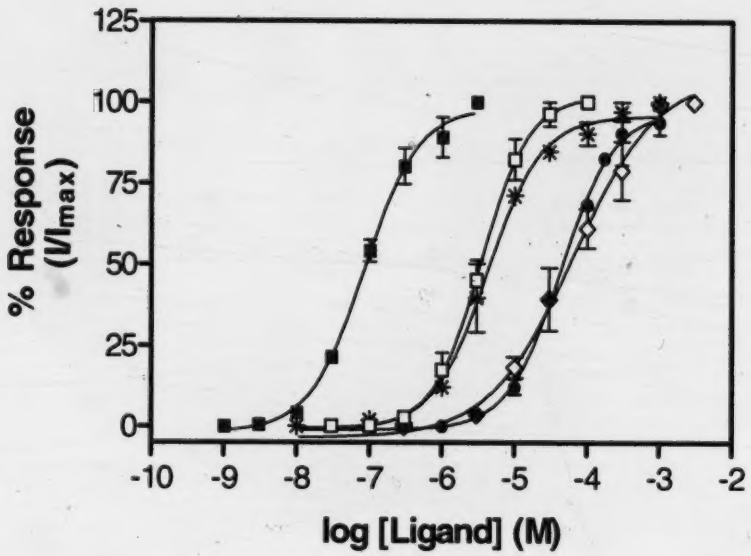
125
100
75
50
25
0
% Response
(I/Imax)
-10
-9
-8
-7
-6
-5
-4
-3
-2
log [Ligand] (M)

B)

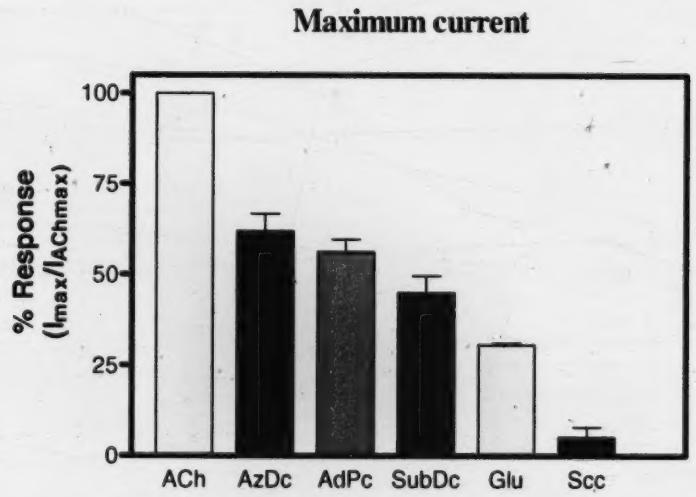
Maximum current
100
75
50
25
0
% Response
(Imax/IAChmax)
ACh
AzDc
AdPc
SubDc
Glu
Scc

TABLE 4-1

Concentration-effect data and maximum agonist-induced currents for bisquaternary ligand activation of Xenopus *oocytes expressing wild type nAChR.*

Ligand	Log EC_{50} ± SEM (M)	EC_{50} (μM)	n_H ± SEM	% Imax Bisquat./ ACh
Azelyldicholine	-7.074 ± 0.03 (2)	0.084	1.2 ± 0.13	62 ± 5 (2)
Suberyldicholine	-5.471 ± 0.08 (3)	3.4	1.4 ± 0.03	45 ± 5 (5)
Adipyldicholine	-5.378 ± 0.09 (2)	4.2	1.2 ± 0.04	56 ± 3 (2)
Glutaryldicholine	-4.180 ± 0.21 (2)	66	0.9 ± 0.04	30 ± 1 (2)
Succinylcholine	-4.393 ± 0.03 (3)	40	1.2 ± 0.1	5.2 ± 2.7 (2)

Data represent the mean ± SEM. Values for log EC_{50} and Hill coefficient (n_H) were determined from concentration-effect curves (Fig. 4-2) using GraphPad Prism software. Log EC_{50} and Hill coefficient values from individual oocytes were averaged to generate final mean estimates. The value in parentheses is the number of oocytes used for each drug.

BIBLIOGRAPHY

BALLIVET, M., PATRICK, J., LEE, J. AND HEINEMANN, S. (1982). Molecular cloning of cDNA coding for the γ subunit of *Torpedo* acetylcholine receptor. *Proc. Natl. Acad. Sci. USA*, **79,** 4466-4470.

BARNARD, E. A., MILEDI, R. AND SUMIKAWA, K. (1982). Translational of exogenous messenger RNA coding for nicotinic acetylcholine receptors produces functional receptors in *Xenopus* oocytes. *Proc. R. Soc. Lond . B.*, **215**, 241-246.

BEENE, D.L., DOUGHERTY, D.A. AND LESTER, H.A. (2003). Unnatural amino acid mutagenesis in mapping ion channel function. *Curr. Opin. Neurobiol.*, **13,** 264-270.

BREJC, K., DIJK, W.J.V., KLAASSEN, R.V., SCHUURMANS, M., OOST, J.V.D., SMIT, A.B. AND SIXMA, T.K. (2001). Crystal structure of an ACh-binding protein reveals the ligand-binding domain of nicotinic receptors. *Nature*, **411,** 269-276.

COLMAN, A. (1984). Translation of eukaryotic messenger RNA in *Xenopus* oocytes, in: *Transcription and Translation: a Practical Approach*, D. Rickwood and B. D. Hames, eds., Oxford University Press, Washington D.C., pp. 271-302.

COLQUHOUN, D. (1998). Binding, gating, affinity and efficacy: the interpretation of structure-activity relationships for agonists and of the effects of mutating receptors. *Br. J. Pharmacol.*, **125**, 924-947.

DASCAL, N. (1987). The use of *Xenopus* oocytes for the study of ion channels, *CRC Crit. Rev. Biochem.* **22**, 317-387.

DIONNE, V.E., STEINBACH, J.H. AND STEVENS, C.F. (1978). An analysis of the dose-response relationship at voltage-clamped frog neuromuscular junctions. *J. Physiol.*, **281**, 421-444.

DREYER, F. AND PEPER, K. (1975). Density and dose-response curve of acetylcholine receptors in frog neuromuscular junction. *Nature,* **253,** 641-643.

DREYER, F., PEPER, K. AND STERZ, R. (1978). Determination of dose-response curves by quantitative ionophoresis at the frog neuromuscular junction. *J. Physiol.,* **281,** 395-419.

DUNN, S.M.J. AND RAFTERY, M.A. (1997a). Agonist binding to the *Torpedo* acetylcholine receptor. 1. Complexities revealed by dissociation kinetics. *Biochem.,* **36,** 3846-3853.

DUNN, S.M.J. AND RAFTERY, M.A. (1997b). Agonist binding to the *Torpedo* acetylcholine receptor. 2. Complexities revealed by association kinetics. *Biochem.,* **36,** 3854-3863.

EERTMOED, A.L., VALLEJO, Y.F. AND GREEN, W.N. (1998). Transient expression of heteromeric ion channels. *Methods Enzymol.*, **293,** 564-585.

ERNST, E., BRAUCHART, D., BORESCH, S. AND SIEGHART, W. (2003). Comparative modeling of the $GABA_A$ receptors: Limits, insights, future developments. *Neurosci.,* **119,** 933-943.

GRUTTER, T. AND CHANGEUX, J.-P. (2001). Nicotinic receptors in wonderland. *Trends Biochem. Sci.*, **26,** 459-463.

GURDON, J. B., LANE, C. D., WOODLAND, H. R., AND MARBAIX, G. (1971). Use of frog eggs and oocytes for the study of messenger RNA and its translation in living cells. *Nature*, **233,** 177-182.

KARLIN, A. (2002). Emerging structure of the nicotinic acetylcholine receptors. *Nature Neurosci.*, **3,** 102-114.

KARLIN, A. AND AKABAS, M.H. (1995). Toward a structural basis for the function of nicotinic acetylcholine receptors and their cousins. *Neuron,* **15**, 1231-1244.

KATZ, B. AND THESLEFF, S. (1957). A study of the desensitization produced by acetylcholine at the motor end-plate. *J Physiol. (Lond.).*, **138**, 63-80.

KATZ, B. AND MILEDI, R. (1977). Transmitter leakage from motor nerve endings. *Proc. Royal Soc. Lond. - Series B: Biol. Sci.,* **196**, 59-72.

KUSANO, K., MILEDI, R. AND STINNAKRE, J. (1982). Cholinergic and catecholaminergic receptors in the *Xenopus* oocyte membrane, *J. Physiol.*, **328**, 143-170.

LE NOVÈRE, N., GRUTTER, T. AND CHANGEUX, J.-P. (2002). Models of the extracellular domains of the nicotinic receptors and of agonist- and Ca^{2+}-binding sites. *Proc. Natl. Acad. Sci. USA,* **99,** 3210-3215.

MINIER, F. AND SIGEL, E. (2004). Techniques: Use of concatenated subunits for the study of ligand-gated ion channels. *Trends Pharmacol. Sci.*, **25,** 499-503.

MISHINA, M., TOBIMATSU, T., IMOTO, K., TANAKA, K-I., FUJITA, Y., FUKUDA, K., KURASAKI, M., TAKAHASHI, H., MORIMOTO, Y., HIROSE, T., INAYAMA, S., TAKAHASHI, T., KUNO, M. AND NUMA. S. (1985). Location of functional regions of acetylcholine receptor α-subunit by site-directed mutagenesis. *Nature*, **313**, 364-369.

MIYAZAWA, A., FUJIYOSHI, F. AND UNWIN, N. (2003). Structure and gating mechanism of the acetylcholine receptor pore. *Nature*, **423**, 949-955.

NEHER, E. AND SAKMANN, B. (1976). Single-channel currents recorded from membrane of denervated frog muscle fibres. *Nature,* **260,** 799-802.

NODA, M., TAKAHASHI, H., TANABE, T., TOYOSATO, M., FURUTANI, Y., HIROSE, T., ASAI, M., INAYAMA, S., MIYATA, T. AND NUMA, S. (1982). Primary structure of α-subunit precursor of *Torpedo californica* acetylcholine receptor deduced from cDNA sequence. *Nature,* **299,** 793-797.

NODA, M., TAKAHASHI, H., TANABE, T., TOYOSATO, M., KILYOTANI, S., FURUTANI, Y., HIROSE, T., TAKASHIMA, H., INAYAMA, S., MIYATA, T. AND NUMA, S. (1983). Structural homology of *Torpedo californica* acetylcholine receptor subunits. *Nature,* **302,** 528-532.

QUICK, M. W. AND LESTER, H. A. (1994). Methods for expression of excitability proteins in *Xenopus* oocytes, in: *Methods in Neuroscience*, Academic Press, London, volume 19, pp. 261-279.

RAFTERY, M.A., HUNKAPILLER, M.W., STRADER, C.D. AND HOOD, L.E. (1980). Acetylcholine receptor: Complex of homologous subunits. *Science,* **208,** 1454-1456.

SAKMANN, B., PATLAK, J.B. AND NEHER, E. (1980). Single acetylcholine-activated channels show burst-kinetics in presence of desensitizing concentrations of agonist. *Nature,* **286,** 71-73.

SCHNIZLER, K., KUSTER M., METHFESSEL C. AND FEJTL, M. (2003). The roboocyte: automated cDNA/mRNA injection and subsequent TEVC recording on Xenopus oocytes in 96-well microtiter plates. *Rec. Chann.*, **9,** 41-48.

SINE, S.M. (2002). The nicotinic receptor ligand binding domain. *J. Neurobiol.*, **53,** 431-446.

SINE, S.M., WANG, H.L. AND BREN, N. (2002). Lysine scanning mutagenesis delineates structural model of the nicotinic receptor ligand binding domain. *J. Biol. Chem.*, **277**, 29210-29223.

STÜHMER, W. AND PAREKH, A. B. (1995). Electrophysiological recordings from *Xenopus* oocytes, in: *Single-Channel Recording, Second Edition*, B. Sakmann and E. Neher, eds., Plenum Press, New York, pp 341-356.

SUMIKAWA K., HOUGHTON, M., EMTAGE, J. S., RICHARDS, B. M., AND BARNARD, E. A. (1981). Active multi-subunit ACh receptor assembled by translation of heterologous mRNA in *Xenopus* oocytes. *Nature,* **292,** 862-864.

THEODOULOU, F. L. AND MILLER, A. J. (1995). *Xenopus* oocytes as a heterologous expression system. *Methods Mol. Biol.*, **49,** 317-340.

ZHONG, W., GALLIVAN, J.P., ZHANG, Y., LI, L., LESTER, H.A. AND DOUGHERTY, D.A. (1998). From *ab initio* quantum mechanics to molecular neurobiology: a cation-pi binding site in the nicotinic receptor. *Proc. Natl. Acad. Sci. USA,* **95,** 12088-12093.

APPENDIX

Sequence Alignment of *Torpedo* nAChR subunits with AChBP.

Shown is the Clustal W Multiple sequence alignment. Numbering on top and bottom is for that of *Torpedo* α1 and AChBP respectively. Asterisk denotes highly conserved residues. T. Ca- *Torpedo californica.*

																						21	
T.Ca_α1	E	H	E	T	R	L	V	A	N	L	L	E	N	-	-	Y	N	K	V	I	R	P	V
T.Ca_β	V	M	E	D	T	L	L	S	V	L	F	E	T	-	-	Y	N	P	K	V	R	P	A
T.Ca_γ	N	E	E	G	R	L	I	E	K	L	L	G	D	-	-	Y	D	K	R	I	I	P	A
T.Ca_δ	N	E	E	E	R	L	I	N	D	L	L	I	V	N	K	Y	N	K	H	V	R	P	V
AChBP	L	D	R	A	D	I	L	Y	N	I	R	Q	T	-	-	S	R	P	D	V	I	P	T
																						*	

								30									40						
T.Ca_α1	E	H	H	T	H	F	V	D	I	T	V	G	L	Q	L	I	Q	L	I	S	V	D	E
T.Ca_β	Q	T	V	G	D	K	V	T	V	R	V	G	L	T	L	T	N	L	L	I	L	N	E
T.Ca_γ	K	T	L	D	H	I	I	D	V	T	L	K	L	T	L	T	N	L	I	S	L	N	E
T.Ca_δ	K	H	N	N	E	V	V	N	I	A	L	S	L	T	L	S	N	L	I	S	L	K	E
AChBP	Q	R	-	D	R	P	V	A	V	S	V	S	L	K	F	I	N	I	L	E	V	N	E
								30									40						
																						*	

Loop D

										50					55		57								
T.Ca_α1	V	N	Q	I	V	E	T	N	V	R	L	R	Q	Q	W	I	D	V	R	L	R	W
T.Ca_β	K	I	E	E	M	T	T	N	V	F	L	N	L	A	W	T	D	Y	R	L	Q	W
T.Ca_γ	K	E	E	A	L	T	T	N	V	W	I	E	I	Q	W	N	D	Y	R	L	S	W
T.Ca_δ	T	D	E	T	L	T	S	N	V	W	M	D	H	A	W	Y	D	H	R	L	T	W
AChBP	I	T	N	E	V	D	V	V	F	W	Q	Q	T	T	W	S	D	R	T	L	A	W
										53													
															*		*					*	

	70												80						86				
T.Ca_α1	N	P	A	D	Y	G	G	I	K	K	I	R	L	P	S	D	D	V	W	L	P	D	L
T.Ca_β	D	P	A	A	Y	E	G	I	K	D	L	R	I	P	S	S	D	V	W	Q	P	D	I
T.Ca_γ	N	T	S	E	Y	E	G	I	D	L	V	R	I	P	S	E	L	L	W	L	P	D	V
T.Ca_δ	N	A	S	E	Y	S	D	I	S	I	L	R	L	P	P	E	L	V	W	I	P	D	I
AChBP	N	-	-	S	S	H	S	P	D	Q	V	S	V	P	I	S	S	L	W	V	P	D	L
																			82				
													*						*		*	*	

Loop A

Loop E

	93								100											110		
T.Ca_α1	V	L	Y	N	N	A	D	G	D	F	A	I	V	H	M	T	K	L	L	L	D	Y
T.Ca_β	V	L	M	N	N	N	D	G	S	F	E	I	T	L	H	V	N	V	L	V	Q	H
T.Ca_γ	V	L	E	N	N	V	D	G	Q	F	E	V	A	Y	Y	A	N	V	L	V	Y	N
T.Ca_δ	V	L	Q	N	N	N	D	G	Q	Y	H	V	A	Y	F	C	N	V	L	V	R	P
AChBP	A	A	Y	N	-	A	I	S	K	P	E	V	L	T	P	Q	L	A	R	V	V	S

	120														128							
T.Ca_α1	T	G	K	I	M	W	T	P	P	A	I	F	K	S	Y	C	E	I	I	V	T	H
T.Ca_β	T	G	A	V	S	W	Q	P	S	A	I	Y	R	S	S	C	T	I	K	V	M	Y
T.Ca_γ	D	G	S	M	Y	W	L	P	P	A	I	Y	R	S	T	C	P	I	A	V	T	Y
T.Ca_δ	N	G	Y	V	T	W	L	P	P	A	I	F	R	S	S	C	P	I	N	V	L	Y
AChBP	D	G	E	V	L	Y	M	P	S	I	R	Q	R	F	S	C	D	V	S	G	V	D
																123						
	*							*								*						

Loop B

	142													149								
T.Ca_α1	F	P	F	D	Q	Q	N	C	T	M	K	L	G	I	W	T	Y	D	G	T	K	V
T.Ca_β	F	P	F	D	W	Q	N	C	T	M	V	F	K	S	Y	T	Y	D	T	S	E	V
T.Ca_γ	F	P	F	D	W	Q	N	C	S	L	V	F	R	S	Q	T	Y	N	A	H	E	V
T.Ca_δ	F	P	F	D	W	Q	N	C	S	L	K	F	T	A	L	N	Y	D	A	N	E	I
AChBP	T	E	S	G	-	A	T	C	R	I	K	I	G	S	W	T	H	H	S	R	E	I
								136							143							
								*														

				160																		
T.Ca_α1	S	I	S	P	E	S	D	R	P	-	-	-	-	-	-	-	-	-	-	-	-	D
T.Ca_β	T	L	Q	H	A	L	D	A	K	G	E	R	-	-	E	V	K	E	I	V	I	N
T.Ca_γ	N	L	Q	L	S	A	E	E	G	E	-	-	-	-	A	V	E	W	I	H	I	D
T.Ca_δ	T	M	D	L	M	T	D	T	I	D	G	K	D	Y	P	I	E	W	I	I	I	D
AChBP	S	V	D	P	T	T	E	N	S	-	-	-	-	-	-	-	-	-	-	-	-	D

				170																		
T.Ca_α1	L	S	T	F	M	E	S	G	E	W	V	M	K	D	Y	R	G	W	K	H	W	V
T.Ca_β	K	D	A	F	T	E	N	G	Q	W	S	I	E	H	K	P	S	R	K	N	W	R
T.Ca_γ	P	E	D	F	T	E	N	G	E	W	T	I	R	H	R	P	A	K	K	N	Y	N
T.Ca_δ	P	E	A	F	T	E	N	G	E	W	E	I	L	H	K	P	A	K	K	N	I	Y
AChBP	S	E	Y	F	S	Q	Y	S	R	F	E	I	L	D	V	T	Q	K	K	N	S	V
				*																		

Loop C

				192	193					198												210
T.Ca_α1	Y	Y	T	C	C	P	D	T	P	Y	L	D	I	T	Y	H	F	I	M	Q	R	I
T.Ca_β	S	D	-	-	-	-	D	P	S	Y	E	D	V	T	F	Y	L	I	I	Q	R	K
T.Ca_γ	W	Q	L	T	K	D	D	T	D	F	Q	E	I	I	F	F	L	I	I	Q	R	K
T.Ca_δ	P	D	K	F	P	N	G	T	N	Y	Q	D	V	T	F	Y	L	I	I	R	R	K
AChBP	T	Y	S	C	C	-	D	D	S	Y	E	D	V	E	V	S	L	N	F	R	K	K
										192												
										*												

T.Ca_α1	P	L	Y	F	V	V
T.Ca_β	P	L	F	Y	I	V
T.Ca_γ	P	L	F	Y	I	I
T.Ca_δ	P	L	F	Y	V	I
AChBP	G	R	S	E	I	L
						210